MASTER OF SCIENCE BY RESEARCH

Investigation of fatigue crack propagation in adhesively bonded joints used in aluminium vehicle structures

Gaur, Piyush

Award date:
2011

Awarding institution:
Coventry University

INVESTIGATION OF FATIGUE CRACK PROPAGATION IN ADHESIVELY BONDED JOINTS USED IN ALUMINIUM VEHICLE STRUCTURES

A thesis submitted in partial fulfillment for award of the degree of

MASTERS BY RESEARCH

BY

PIYUSH GAUR

under the supervision of

Dr. Paul Briskham

Faculty of Engineering and Computing

Coventry University, Priory Street

United Kingdom, CV1 5FB

July 2011

Declaration

This thesis has been completed by me, is only my effort, and nothing is taken in whole or any part from various other sources except where duly acknowledged. In the reference list of the main report the work is recognized for the use of previously published work from websites, books, e-books journals and so on.

Acknowledgement for copyright:

For this project I have given the right for copyright where in future it can be used for any kind of research or any product developed with reference to this project totally belongs to Coventry University.

Signature: Date:

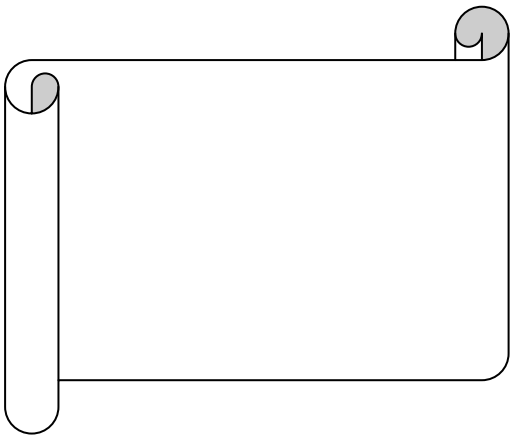

Stamp from Office

ABSTRACT

Adhesive Bonding is an attractive alternative to conventional joining methods, such as welding and mechanical fastening. In applications such as primary aircraft structures or automobiles elements adhesive bonding competes with traditional bolting, riveting or welding. The advantages of adhesive bonding includes high strength/weight ratio, possibility to join any combination of materials, high corrosion resistance and improved fatigue performance. Although, adhesives can be used alone, most of the volume manufacturers can't afford the level of quality control required and have opted to employ hybrid joining methods containing adhesives with spot welds or self piercing rivets because they do not have a reliable software method to analyze and predict the lifetime of bonded or riveted joints. In analysing adhesively bonded joints for design purposes, important properties to consider are strength, stiffness, weight and nature of stress distributions.

In this research, a new mathematical method based on stiffness drop of adhesively bonded joints has been investigated and presented to determine the fatigue crack propagation rates and obtain the crack growth curves for these joints. This method makes use of the raw laboratory fatigue test data and finite element based stiffness data of bonded joints. This concept has been tested and validated for T-peel and single lap shear bonded joint configurations. The bonded joint configurations were prepared using aluminium alloy AA5754 and the adhesive used was Betamate Epoxy adhesive 4601, which is high performance, heat curing, epoxy adhesive. The entire tests were conducted under constant amplitude loading using an R ratio of 0.1 and frequency of 10Hz. The damage models for this work were developed using computational fracture mechanics tools in abaqus.

Various curve fitting models were reviewed and employed in this method to combine the stiffness data obtained from FE damage models and fatigue test data of T peel and single lap shear bonded joints to calculate the fatigue crack propagation rates. The methodology investigated in this work provides a way to obtain the fatigue crack growth curves for adhesively bonded joints by combining the finite element modeling data with fatigue test data of bonded joints.

ACKNOWLEDGEMENT

We all want to live our lives in our own ways but this is not possible of course without the help of others. Since I do not want to risk forgetting to mention anyone, I would first of all like to express my thanks to all of those who know or feel that they in some way have contributed to my research work.

This Master's by Research (M.Res) thesis is a part of TSB Bonded car project that is being carried out by the combination of several automotive OEM's and led by Jaguar Cars along with Coventry University and University of Warwickshire as the academic partners. The project aims in developing a software tool for analyzing and predicting the durability of spot welded joints, rivet joints and bonded joints.

The master research project was carried out between Sep 2010 and Aug 2011 at the Materials Technology Applied Research Group, Faculty of Engineering & Computing Coventry University, United Kingdom.

I would like to express my sincere appreciation and gratitude to *Dr. Paul Briskham* for his teaching, guidance, friendship and support. I admire him as a teacher, as a leader, and above all, as a friend. I have been also grateful to him for his immense support in carrying out all the fatigue test of bonded joints for me.

I also like to thank *Dr. Peter Heyes* for providing me expert advice in the mechanics of adhesives and finite element model updating. The suggestions and help made by *Mr. Andrew Blows*, Technical and Durability specialist at Jaguar Cars and *Mr*. *Tim Mumford*, CAE Engineer at Jaguar cars were of immense help in preparing the T peel and single lap-shear joints damage models and are gratefully acknowledged. I would also like to extend my gratitude to *Dr. G.W. Critchlow* and *Dr. Mark Hooper* for serving on examining committee.

My elder sister for her smile, support, care, and for being always there when I needed her. My infinite gratitude goes to all of my close friends who made my stay in Coventry an unforgettable experience.

Very special thanks to Mayur Mehta to prepare the bonded joints for this research. I learned a great deal and was honoured to work with him.

My gratitude goes forever to Nishant Raj, Prantik Kumar and Bhargav Pathri for their generosity, friendship, and hospitality, for making me feel at home.

This work was supported by Materials Technology Applied Research Group, Coventry University and Jaguar Land-Rover.

Finally, I could not have completed this thesis without the support of my parents and my friends.

July 2011

Piyush Gaur

DEDICATED TO

MY PARENTS AND GRANDFATHER

TABLE OF CONTENTS

LIST OF FIGURES

LIST OF TABLES

ABBREVIATIONS

LEFM	Linear elastic fracture mechanics
VCCT	Virtual crack closure technique
ASTM	American society of testing & Materials
BS	British Standards
DCB	Double cantilever beam
MMB	Mixed mode bending
J	J – Integral
Mode I	Fracture mode 1
Mode II	Fracture mode 2
Mode III	Fracture mode 3
CTOD	Crack tip opening displacement
FEA	Finite Element Analysis
CAA	Chromic Acid Anodizing
PAA	Phosphoric acid anodizing
CGR	Crack growth rate
ΔK	Stress intensity factor
SERR	Strain energy release rate

CHAPTER 1

INTRODUCTION

1.1 BACKGROUND

Since before recorded history; mankind has been joining materials to produce useful items. To increase efficiency and effectiveness, many prehistoric as well as modern devices required the assembly of several components, often involving dissimilar materials (Pocius 2002).

Stone points retained their sharpness and provided mass for arrows, whose wooden shafts provided light weight strength and stiffness, which in turn were outfitted with feathers mounted at the tail to maintain stability in flight (Gettens 1942). Whether lashing with natural fibers, or sealing with resins of gums, mankind has, from the earliest times, been involved in joining of various materials. The sophistication of joining methods available has increased to include a wide variety of mechanical fasteners, welding methods, and the use of adhesives, sealants, mortars, and other binders to bind various materials. Joining offers us the ability to have structures much larger than could be made or transported as single entity. Joining allows us to fabricate efficient, lightweight, open structures with tailored properties and performance matched to the intended use. Scientists continue to be fascinated by the excellent adhesive characteristics of the substance, and the tenacity and durability of the adhesive bonds formed under very unfavourable conditions (Pocius 2002).

In designing modern structures, the decisions whether to use adhesives, mechanical fasteners, some type of welding, or some combination of these methods often fall to the engineers involved in the design process. Adhesives are often the joining method of choice from feasibility point of view where thin, flexible or dissimilar adherends are involved. Adhesives offer certain advantages like reducing stress concentrations, high strength to weight ratio, increased component stiffness and fatigue life, thus providing weight savings that can prove to be quite significant due to snowballing effect weight on lightweight structures (A.J.Kinloch 1997). Continuous beads of adhesives on car body stiffen the vehicle body structure when compared to discrete mechanical fasteners. This

increase in stiffness can reduce the noise, vibration, and harshness (NVH) and leads to quieter, better performing automobiles.

Although, adhesives can be used alone, most of the volume manufacturers cannot afford the level of quality control required and have opted to employ hybrid-joining methods combining adhesives with spot welds or self-piercing rivets. Adhesives help in eliminating the stress concentrations around loaded holes, thereby exhibiting the improved fatigue performance. Adhesives can effectively seal joints by keeping water out of the bond line. This is a very important point from durability point of view. The durability of adhesives in presence of excessive heat, cold, water and organic solvents can have significant limitations. These exposures can degrades the mechanical properties of adhesives and deteriorate the interface (R.D. Adams 2005).

One of the prime requirements in using adhesively bonded joints in automotive bodies is to develop a method by which the failure life of joints for different stress conditions can be easily predicted, ideally, these should also take into account various environment factors mentioned earlier, since exposure to these conditions can degrade the joints. The stress fields within the adhesive layer are quite complex, being highly non-uniform within the adhesive layer involving both peel and shear stresses acting in several directions. An understanding of these complex and non-uniform stress states is important in developing meaningful design criteria, and in designing and analysing bonded structures.

TSB bonded car project is a government and Industrial grant funded project consisting of several industrial partners and led by Jaguar cars .This project mainly aims in developing a methodology for Spot welds, SPR's (Self piercing rivets) and bonded joints used in Jaguar car's body to predict the fatigue life of joints. In this thesis, emphasis has been given in investigating a mathematical method based on stiffness drop approach to calculate the fatigue crack propagation rates and obtaining fatigue crack propagation curves for adhesively bonded joints.

This chapter will give the reader some information about the background of this thesis as well as the aims and objectives of the thesis.

1.2 RESEARCH QUESTION AND HYPOTHESIS FOR THIS THESIS

This M.Res thesis deals with the methods of modeling adhesive bonded joints using finite element method and fracture mechanics based tools in abaqus. Also, this thesis investigate a mathematical method to obtain fatigue crack growth rate curves for bonded joints using fatigue test data and finite element based modeling data.

The motivation beneath this research is the increasing application of adhesives as a joining technique in vehicle structures. The increased use of adhesives was accompanied by the development of numerical and analytical methods, which can be used to analyse the bonded joints but nowadays are still a big problem. Finite Element Method (FEM) is a powerful technique, which can be effectively used to simulate the behavior of adhesive bonded joints in conjunction with computational fracture mechanics based methods.

Thus, the hypothesis for this thesis to prove or disprove a mathematical method to calculate fatigue crack propagation rates and obtaining the crack growth rate curves for adhesively bonded joints by using stiffness data of finite element models and stiffness obtained in fatigue test data of bonded joints. T-peel bonded joints and single lap shear joints are the two configurations investigated in this method. To use this method to obtain the fatigue crack propagation curves, stiffness of the bonded joints is the main parameter. In this method, stiffness can be calculated for finite element models of bonded joints and curves were plotted for stiffness and energy release rates with respect to crack length. The curve fitting methods in finite element models can be used to obtain the relations between stiffness and crack length and also, between energy release rate and crack length. The obtained equations from finite element models thus can be used in fatigue test data of bonded joints to calculate the fatigue crack propagation rates. Fatigue crack propagation curves can then be plotted on log-log scale using calculated crack propagation rates and energy release rates in fatigue test data.

1.3 WORK REQUIRED TO ANSWER RESEARCH HYPOTHESIS

The following objectives need to be achieved in order the answer the research hypothesis-

- The main objective of this project is to investigate the fracture mechanics based modeling method to model the adhesives using finite element method.

- To investigate mathematical methods of combining and correlate stiffness data of FE models with the fracture mechanics based test data of bonded joints to obtain the crack propagation curves for bonded joint configurations.

- To calculate the fatigue crack propagation rates for adhesively bonded joints using fatigue test and CAE stiffness data.

1.4 SCOPE OF WORK AND SOURCE OF FUNDING

The funding for this research based M.Res project is to support the work done by HBM and Jaguar Land Rover in developing a software tool which can be use to predict the fatigue life of bonded joints used in aluminium vehicle bodies.

1.5 STRUCTURE OF THESIS

A brief description of the remaining chapter of the thesis is given below.

Chapter no 2 Adhesive bonding. This chapter deals with the introduction to adhesive bond technology and overview of it. An introduction to the use of adhesive bonding in aluminium vehicle structures, and the surface treatments used in aluminium bonding have also been discussed.

Chapter 3 Literature Review. This chapter provides a review of the literature to identify the previous research in the field of adhesively bonded joints. This chapter deals with the review of the stress analysis methods of bonded joints along with a detailed explanation on the use of two dimensional and three dimensional finite element based solutions, along with closed form solutions. This chapter also explains the fracture mechanics based methods and fatigue crack

propagation methodology used in this thesis for the analysis of bonded joints. There is also a need to find a particular failure criterion for adhesives. A review in this field is presented showing that researchers proposed lots of criteria based on stress, strain or fracture mechanics based methods.

Chapter 4 Experimental Methods and Results. Details of the materials used, joint configurations, experimental plan and methods are provided in this chapter along with the fatigue test results of single lap shear and T-peel bonded joints.

Chapter 5 Finite Element Modelling Methods. This chapter provides the details of finite element modelling methods used in this research. The geometry, boundary conditions, meshing methodology, element choice and modelling of failure locations details are provided.

Chapter 6 Fatigue Crack Growth Analysis. The proposed fatigue crack propagation estimation method has been explained and investigated in this chapter for T- Peel and single lap shear bonded joints. The validation of this method is also presented in this chapter.

Chapter 7 Discussions. This chapter presents a discussion on the experimental results and the modelling methods presented in previous chapters.

Chapter 8 Conclusions and Future Work. The conclusions of the research along with the proposals for future research are presented in this chapter**.**

CHAPTER 2

ADHESIVE BONDING

2.1 INTRODUCTION

Adhesives have been used to join similar and dissimilar materials for many centuries. However, it is only during last century that significant advances have been made in the science of adhesion. The field is further advanced with the development of polymeric and epoxy based adhesives that have replaced animal and plant based glues that were not strong enough for structural application (R.D. Adams 2005).

The joining of any materials using adhesive bonding requires considerable number of steps. Firstly, the surface of any bonded material must be prepared in the correct manner to ensure good adhesion. Care must be taken to select an adhesive that can withstand service conditions, such as high temperature or high humidity. This chapter introduces some important factors such as good adhesion and how this is achieved. Pretreatment and adhesives that are used with aluminium in automotive industry are explained in this chapter.

2.2 STRUCTURAL ADHESIVES

"An adhesive may be defined as a material which when applied to the surfaces of the materials can join them together and resist separation". This definition was first proposed by Kinloch (1987). Structural adhesives are based upon resins compositions that polymerize to give high-modulus, high-strength adhesive so that a load-bearing joint is formed (A.J. Kinloch 1987).

Some generic advantages of using adhesive bonding are listed below:

- Adhesives can join dissimilar materials such as composites, plastics, metal etc.
- Use of adhesives may eliminate certain stress concentrations around loaded holes which can dramatically improve the fatigue life.
- Thin sheet materials can be easily joined by using adhesives.

- Continuous beads of adhesives in vehicle structure can make it stiffer which may improve the noise, vibration and harshness properties of the vehicle.
- Adhesive bonding can improve the appearance of the joint. A smooth blemish surface of bonded joint is more appealing and effective than spot welded structure.

Along with the advantages, adhesive bonding also have some certain disadvantages:

- Adhesives require some certain surface pretreatments in order to sustain performance in certain hostile environments.
- Upper service temperature is often limited in case of adhesives as compared to other joining methods.
- Modern high performance adhesive systems are either epoxy based or solvent based. They can give rise to numerous environmental concerns.
- Adhesives have a limited shelf life.
- Non-destructive test methods for adhesive joints are relatively limited as compared to other joining methods.

2.3 APPLICATIONS OF ADHESIVE BONDING

The biggest advantage of adhesive bonding is the possibility to join many materials without affecting their properties. This allows bonding to be used in almost any application. The industrial sectors which employs structural adhesive bonding include aeronautical, aerospace, automotive, marine and off shore, construction, medical and sports. Out of these, Aerospace and Automotive industries are the largest users of adhesive bonding technology. The application of bonding in these industries is explained below:

AERONAUTICAL AND AEROSPACE APPLICATIONS- Adhesives and aircraft have a long and interesting joint history. Even though flying vehicles have progressed from glorified kites to commercial jet transports, supersonic missiles and space vehicles, adhesively bonded structure has been crucial to virtually every one. Both primary structures, which carries primary flight loads and failure

of which could result in loss of vehicle, and secondary structure are bonded (R.D.Adams 2005). The earliest structural adhesive applications were made during the First World War for bonding the wooden frames aircraft (of biplanes), were strength was adequate but, by today's standards, moisture resistance was poor(Pocius 2002). This practice continues today, primarily with bombers, fighter and attack aircraft where weight is a critical consideration, but also with support craft such as reconnaissance aircraft and freighters (Pocius 2002). Because of this continued emphasis on adhesive bonding technology development over the years, the airframes of modem front-line aircraft such as the B-2 bomber, the F-117, F-22, F-35, or Swedish JAS (Fig.1.1) fighters are largely structurally bonded advanced composites (Pocius 2002).

Figure 2.1: JAS Grippen bonded elements (Budzik 2010)

The use of adhesives also prevents corrosion when different materials to be combined. Due to uniform, plane load transfer through the adhesive, layer notch sensitivity is reduced. The use of bonding also provides high potential for variation in styling due to the possibility of combining different materials (Pocius 2002).

Typical requirements for adhesively bonded structure for space applications vary widely and differ substantially from those for atmospheric vehicles. Because of widespread use of cryogenic rocket fuels, adhesives near tank structure must maintain adequate properties at very low temperatures. At the other extreme,

adhesives have been used to bond ablative or insulative heat shields to the bottom of re-entry vehicles since the advent of manned space flight (Board 1976).

AUTOMOTIVE APPLICATIONS- Adhesives have been employed in the automotive industry since its beginnings, with the use of natural resins to bond wood and fabric bodies (R.D.Adams 2005). The main requirements for the automotive industry are lightweight structures, use of mixed materials, long term performance, crash performance and also styling and design. Since the adhesive can improve the stiffness and strength of a joint the weight can be reduced. Adhesive bonding can furthermore allow the realization of combining different structural materials such as FRP, metals, glasses and ceramics. It is quite clear that many parts of different materials have to be brought together through bonding, sometimes together with rivets (Redux 2002). In many situations this is preferred to welding. Similar to aerospace bonding, adhesives are used in particular when different materials are joined together. Improvement of crash performance is possible by the use of substrates and adhesives with a high potential of energy absorption. Finally, diversity of styling and design are possible due the possibility of combining different materials and components and joining them together by bonding (Pocius 2002).

2.4 THEORIES OF ADHESION

An adhesive must do two things when applied to surfaces which are to be bonded. It must first wet the surface, as manifested by spreading and making a contact angle approaching zero (R.D.Adams 2005). Secondly, it must harden to give a cohesively strong solid. If the adhesive can penetrate the substrate before hardening then mechanical interlocking will contribute to the strength of the joint. Other approaches are also possible. There are number of proposed theories in the literature by which an effective adhesion can be explained. Some of the theories are listed below (R.D.Adams 2005).

2.4.1 Physical adsorption theory

Physical adsorption contributes to all adhesive bonding and it is widely used and applicable theory of adhesion. The basis of this theory is the weal van der wall forces. These forces are mainly generated by attractions between permanent and induced dipoles in atoms and molecules. The potential energies for these type of

attractions are all proportional to r^{-6} , where r is the distance of separation. Such forces within adhesive bond are of very short range and are experienced by only one or two layers molecules in the bond layer.

2.4.2 Chemical bonding theory of adhesion

This theory of adhesion involves the formation of covalent, ionic or hydrogen bond or lewis acid base interaction across the adhesive interface and are stronger then van der waal forces. This theory is based on the reasoning as the physical adsorption theory. The only difference in this case is that primary bonds are formed across the adhesive/substrate interface.

2.4.3 Mechanical interlocking theory

The mechanical interlocking theory is based on the idea that if a substrate has an irregular surface, then the adhesive may enters the irregularities prior to hardening. This idea contributes to adhesive bonds with porous materials such as wood and textiles. An example of this is the use of iron-on patching for clothing. The patches contain a hot melt adhesive which, when molten, invades the textile material.

2.4.4 Diffusion theory of adhesion

This theory suggests that polymers in contact may interdiffuse so that the initial boundary between them is removed. This can only occur if the polymer chains are sufficiently mobile and mutually soluble. One example of this is to swell polystyrene surfaces with an organic solvent and then press them together. The solvent lowers the glass transition temperature below room temperature while interdiffusion occurs and then evaporates (Callister 2007).

2.4.5 Electrostatic theory of adhesion

The basis of electrostatic theory of adhesion is the difference in the electronegativites of adhesing materials. Adhesive force is attributed to the transfer of electrons across the interface creating positive and negative charges that attract one another. For example, when an organic polymer(of conductive nature) is brought into contact with metal, electrons are transferred from metals to polymer, creating an attractive electrical double layer(EDL), which gives rise to

forces of attraction. As polymers are insulators, it seems difficult to apply this theory to adhesives (Callister 2007).

2.5 SURFACE PRETREATMENTS FOR ALUMINIUM BONDING

Surface preparation of the bonded joints is an important step since it directly affects the strength of the adhesive bond that affects the failure mode. By preparing surface correctly, joint strength can be maintained to its full potential, resulting in long term structural integrity (R.D.Adams 2005). Incorrect surface preparation could lead to adhesive bond failure and unpredictable failure. The primary role of surface preparation is to remove surface contaminants, increase the bonding surface area, and improve surface roughness(Minford 1993).

In addition to surface preparation to achieve a satisfactory adhesive bond, it is also necessary to carry out some form of pretreatment. Inadequate surface pretreatment is a common reason why adhesive bonds fail (A.J. Kinloch 1987). Many pretreatments are available ranging from a simple solvent wipe to a use of series complex chemical processes .The main reason for doing surface pretreatment is not to increase the strength of a newly manufactured joint, but to increase the durability of the joint on exposure to high humidity or water(Budzig 2010) .

Pretreatments for metals have been the subject of much research. This is especially true in case of aluminium where particular emphasis has been placed in aerospace applications. This is of course great interest in commercial and military aircraft and much research has been carried out in aircraft industries, adhesive manufacturers and research institutions (R.D Adams 2005). Wide range of mechanical and chemical pretreatments has been used with varying degrees of success to create durable aluminium adhesive bonds. A study by Critchlow and Brewis (Critchlow 1996) had identifed 41 different pretreatments for aluminium. Some of the common chemical pre-treatments includes silica/siloxane preatment, etching with chromic acid and anodizing using either chormic acid or phosphoric acid(R. D. Adams 1997 and Comrie 1998).

To use aluminium pre-treatments in automotive applications, it must cater for high volume production. Also, the pre-treatment must be applied quickly, in seconds rather than in minutes to accommodate high volume automotive manufacture

(Comrie1998). This section reviews some of the methods of pretreatment use to pretreat aluminium.

2.5.1 MECHANICAL PRETREATMENT

A wide range of methods are available for roughening aluminum surfaces; for example grit blasting, mechanical abrasion and scotchbrite pads. Mechanical abrasion could remove weak boundary layers, and increase surface roughness, creating a larger surface area for chemical bonding, and enabling complementary mechanical locking to take place. (Saunders 1994 and Critchlow 1996). The initial joint strength of aluminium bonds can be significantly improved by simply abrading a mill finish surface. (Minford 1993). But unless a further surface treatment is used to increase the stability of natural air formed oxide, then little or no increase in the hot-wet joint durability should be expected (Critchlow 1996 and Minford 1993). A major drawback of abrading operations is the likelihood of removed debris and loose abrasive particles being embedded into the surface. (A.J. Kinloch 1987, Minford 1993 and Saunders 1994). These reduce the area available for strong bonding, and result in areas of none or partial adhesive contact which may reduce the bond durability.

2.5.2 SILICA/SILOXANE PRETREATMENT

This method of chemical pretreatment consists of silica particles with a siloxane based matrix. This method is applied by using roller coating on aluminium coating lines. Once dried, the particular adhesive can be applied on the surface. From environment point of view, it is advantageous to use this treatment because the silica chemistry does not contain any carcinogenic additions (Budzik 2010).

The presence of silica particles enhances the mechanical interlocking between the substrate and adhesives and increases the surface area for bonding. Primary bonding may also exist between the siloxane matrix and the oxidized aluminium surface. Other constituents include surface wetting agents and the corrosion inhibitors. The shelf life of this joint is of the order of many months. The single lap shear bonded joints used in this research were pretreated by using this pretreatment.

2.5.3 ANODISING TREATMENTS

Anodising treatments have been used for enhancing the bond durability by the aerospace industry for more than 40 years. Pretreatment by anodising produces a very thick oxide layer on the surface of aluminium. The porous oxide layer enables adhesive to penetrate the pores readily to form a strong bond (A.J. Kinloch 1987). The anodising treatments that are most commonly used for adhesive bonding purposes are Chromic Acid anodising (CAA Pretreatment) and Phosphoric acid anodising (PAA pretreatment)(A.J.Kinloch 1987).

2.5.3.1 CHROMIC ACID PRETREATMENT

Chromic acid anodising has been used as a preferred method of pretreatment of adhesives for many years by the European aerospace industries. The thickness of the CAA oxide formed by this process is highly dependent on the anodising voltage used (G.W.Critchlow 1997). CAA process also provides good corrosion resistance due to the formation of thick oxide layer (Minford 1993 and Mnich 1993). The CAA oxide layer is generally micro porous. The diameter of the pores is very small, but the pores are usually very deep; which makes it difficult for adhesives to penetrate and fill the pores (Critchlow 1996 and Bishopp 1988).

The drawing of the morphology of the CAA oxide is provided by the Venables as shown in figure. 2.2. Small pores of CAA oxide can be sealed back by immersion in boiling water, which forms a boehmite oxide with a cornflake shape like structure (J.D. Venables 1979). Venable's drawing of CAA oxide after immersion in boiling water is shown in figure. 2.3.

Figure 2.2: Isometric drawing of the morphology of CAA oxide layer (J. D. Venables 1979b)

These images have been removed

Figure 2.3: Isometric drawing of CAA surface after sealing (J. D. Venables 1979b)

2.5.3.2 PHOSPHORIC ACID PRETREATMENT

Phosphoric acid pretreatment was first discovered and patented by Boeing in 1979(Redux 2002). Boeing PAA process is still regarded as the best pretreatment method available for producing durable adhesive bonds (Minford 1993 and Mnich 1993).

In this method, the aluminium substrates are clamped to the anode of a standard anodising bath, at a temperature of 25^0C of the following composition (Redux 2002):

Orthophosphoric Acid [Sg: 1.65]: 1.0 litres

Water : 16.6 litres

The anodising voltage is raised to 10-15V and is held for 20-25 minutes. At the end of this time the adherends are removed and immersed in a bath of water at ambient temperature. This is followed by a spray-rinse with cold water. The anodized adherends can then be air-dried, preferably in an air-circulating oven where the air temperature is no greater than 45^0 C. PAA pretreatment produces a more thinner but an open oxide film extending to about 800nm, with much larger and open pores than that produced by chromic acid anodising. The isometric drawing of the oxide morphology created by PAA is shown in figure.2.4. The anodic oxide contains bound phosphate which imparts the durability of the final adhesive bonded joint. Such a thin and highly porous oxide does not provide good corrosion resistance on surfaces directly exposed to the environment (Albericci 1983, Bishopp 1988 and Minford 1993). Though the mechanical interlocking is very good between the adhesive and substrate.

This image has been removed

Figure 2.4: Isometric schematic of the oxide morphology produced by PAA pretreatment (J. D. Venables 1979b)

2.6 ALUMINIUM VEHICLE AND ADHESIVE BONDING

One of the main reasons why adhesive bonding is used on aluminium vehicles because aluminium is really very well suited to adhesive bonding through proper surface pretreatment creating very stable surfaces for good lo0ng term bond strength retention. Steel is the more difficult to bond due to its worse corrosion resistance making it harder (but not impossible) to produce very stable surface for good long term bond strength retention.

Higher welding currents and forces are required while welding aluminium compared to steel. This can lead to poor electrode life and higher energy consumption. Recent work by Paul Briskham showed that this can be overcome by using regular electrode polishing and has created an opportunity for aluminium spot welding to be widely employed on future vehicles in a similar fashion to the way it is used for steel vehicles (Briskham 2006). In case of aluminium vehicle structure, spot welding or riveting is mainly done to maintain the bonded assembly is position until the adhesive has cured and to provide a back up joint in case the adhesive fails.

Self piercing riveting is widely used now days in conjunction with adhesive bonding, the cold process is well suited to use with adhesives and does not degrade the heat treatment condition of the metal. Rivets also offer superior fatigue life and performance compared to spot welds, allowing less rivets to be used than spot welds. Joining using adhesives produce a continuous bond rather than the point contact of spot welding. This method of joining simultaneously improves the stiffness and fatigue life of structure (Wheeler 1987).

Components made from aluminium can distort when spot welded or when rivets are inserted, adhesive bonding of aluminium does not have this disadvantage and this is the major manufacturing advantage of bonding for aluminium car bodies. The main in service advantage is the increased stiffness and increased fatigue life of the structure due to continuous joints compared to the joints created by spot welds or rivets.

CHAPTER 3

LITERATURE REVIEW

ADHESIVE BONDED JOINTS ANAYSIS - AN OVERVIEW

3.1 INTRODUCTION

Whilst the building and construction industries represent some of the largest users of adhesive materials, few applications currently involve adhesive joints, which are required to sustain large externally applied loads. The sources of these loads and stresses are many and varied. Stress and strain are produced within these joints due to these externally applied loads. Stress is the intensity of loading at any point in a structure and strain is the resultant deformation produced due to these stresses and strains.

However, the development of stronger adhesives and new materials such as composites suggest that adhesives have enormous potential in future construction applications, particularly where the combination of thick bond lines, ambient temperature curing and the need to bond dissimilar materials with a relatively high strength are important. Indeed, adhesive bonding, either alone or in combination with other methods of fastening, represents one of the key enabling technologies for the exploitation of new materials and for the development of novel design concepts and structural applications.

Figure. 3.1 shows some of the typical bonded joints configurations. The single lap joint is one of the most common joint designs employed in industry .They are easy and cheap to manufacture because there is no splice details to make or locate in the bonding fixture. The single lap joints are easy to inspect ultrasonically, because a complete inspection can be made from one side of the joint.

The stress fields within the adhesive layer are quite complex, being highly non-uniform within the adhesive layer involving both peel and shear stresses acting in several directions. An understanding of these complex and non-uniform stress states is important in understanding the behaviour of bonded joints and to develop meaningful design criteria. Hence, this chapter reviews the stress analysis of adhesively bonded joints in a qualitative way.

One of the widely quoted papers in the literature on the stress analysis of bonded joints is Goland and Reissner (Goland 1944) on single lap joints. This paper was important in drawing attention to the effects of adherend bending deflections on the peel and shear stresses in the adhesive layer of single lap joint. Despite the considerable effort of a number of researchers over the last century, unresolved issues still remain. Mainly the failure load of the joints is still very hard to predict and that theories incorrectly show the strength of the joint to increase with increasing adhesive thickness.

Figure 3.1: Typical structural adhesive joints configurations (Andruet 1998)

There are two methods exist for the stress analysis of bonded joints in a qualitative way. Those who predict stresses by using numerical methods and those, which work by, fracture mechanics methods. This overview begins with a description of stress analysis methods followed by fracture mechanics based methods for bonded joints –

- **Numerical solutions** – a detailed description of finite element method (FEM) along with two-dimensional and three-dimensional solutions.

- **Closed form solutions (Single lap joint theories) –** a detail review of closed form theories from Volkerson (1938) to latest proposed theories.
- **Fracture mechanics methods –** a detailed description of fracture mechanics and fatigue crack growth rate approach used in analysis of bonded joints.
- **Failure prediction criteria for adhesive bonded joints**.
- **Summary.**

3.2 AN INTRODUCTION TO NUMERICAL METHODS

The rapid development of computing power has made the use of numerical techniques more feasible and appealing. Numerical methods can be use to analyse various models with arbitrary geometries and loading conditions. They are suitable for the analysis of structures comprised of different materials. Numerical solutions can be used to analyse the complex behavior of adhesively bonded joints. With the increase in computing power, it is feasible to perform a very complicated finite element analysis of various bonded joint configurations and there is much work published in this area. Such modeling work has shown to be capable of including the effect of material discontinuities, plasticity and complex joint geometry. Numerical methods can be applied to solve differential equations, which represent structural behavior. Bigwood and Crocombe (1989) used the finite difference method to solve the differential equation that represents the peel and shear stresses in an adhesive layer. Bigwood and Crocombe (1989) included nonlinear effect in their previous work and performed an elastic plastic analysis of adhesively bonded joints using the same approach.

Another discretization procedure is to divide the given structure into small parts and then to formulate the model to each one of these parts and then to reassemble those small parts to model the whole structure. This method is widely used in engineering. This finite element method and its application to the determination of stresses in adhesive bonded joints are discussed in next section.

3.3 NUMERICAL METHOD SOLUTIONS

This method has been used in many scientific and engineering fields including fluid dynamics, heat conduction, and structural analysis. This section review is confined to the finite element analyses of adhesively bonded joints. Zienkiwicz and Taylor (Taylor 2002), in their book, “The Finite Element Method”, give a very comprehensive review of formulation and use of finite element models. Cook et al. (Cook 1995) defined finite element method as a, “Piecewise approximation in which the approximation function ϕ by considering simple functions, each defined over a small region”. There are two important features of finite element method: discretization of domain and the approximation of the solution using the nodal values of the solution of the element boundary. The nodes are the point at which the elements are assumed to be interconnected.

The main features of FE method are:

- The entire solution domain is divided into small finite segments (hence the name finite elements).
- Over each element, the behavior is described by the displacements of the element and material law.
- All the elements are assembled together and the requirements of continuity and equilibrium are satisfied between neighbouring elements.
- Provided that the boundary conditions of the actual problem are satisfied, a unique solution can be obtained to the overall system of linear algebraic equations.
- The solution matrix is sparsely populated (i.e. with relatively few non-zero coefficients).
- The FE method is very suitable for practical engineering problems of complex geometries. To obtain a good accuracy in regions of rapidly changing variables, a large number of small elements must be used.

The finite element method gives an approximate solution. The accuracy of the solution depends mainly on the type of element used and the fineness of finite element mesh.

3.3.1 TWO DIMENSIONAL FINITE ELEMENT SOLUTIONS

Due to increasing computing power, use of finite element method has become a common tool in studying the behavior of adhesive joints. To use FEA on bonded joints, each adherend must be treated as continuum and the geometry can be represented as continuum and the geometry can either be treated represented as two-dimensional or three dimensional identities. Complex material models are readily incorporated into the finite element method, and large displacements, such as those seen in the single lap joint can be simulated as well as thermal behavior.

A large number of two and three dimensional finite element analyses of adhesively bonded joints have been performed. Some of the analyses produce accurate results and requires less modelling effort then three-dimensional analyses. Plane stress or plane strain elements were often used in the finite element analyses of adhesively bonded joints. When this approach is used, very thin meshes are required in the adhesive bond line in order to obtain a reasonable accuracy. One of the first people to use FEA in bonded joints was Adams and Peppiat (R. D. Adams, 1973) who showed in their work that there are significant stress concentrations at the end of adhesive layer, adjacent to the corner of the adherend and within the spew fillet. Stresses at the spew fillet appear to be singular in nature and the presence of these theoretical singularities has been a subject of consequent studies.

Adams and Harris (Harris,1987) in their analyses proposed a detailed model of stresses at the corners of the adherends and was the first one to include material nonlinearity in their model. A quadrilateral plane stress element was used for the analysis. They performed the analyses of a single lap joint and of a joint with fillets at the edges of the joint. They also concluded that stress and strain distributions were singular for the elastic analysis and the inclusion of plasticity in their model will result in a singular stress field. The degree of rounding at these corners was found to have a significant influence on the predicted stress strain distribution within this joint. Harris and Adams used Von Mises yield criteria to define the failure conditions for the adherends and modified Von Mises criterion

for the adhesives. Their results agreed with those obtained by Goland and Reissner (Goland 1944) for the standard single lap joints.

Adams et al. (Adams 1978) performed a detailed axis symmetric analysis of the butt tension joint and considered the effect of detailed geometry at the edges of the joint on the stress distribution in the adhesive layer. Crocombe and Adams (A. D. Crocombe 1981) also analysed the single lap joint using finite element method and they also included the effect of spew fillet, which decreases the stresses at the end of adhesive layer. Crocombe and Adams (R. D. Adams 1981) studied the mechanics of the peel test and included the non-linear deformations and plasticity effects in their work. Harris and Adams (Harris1984) extended this work and accounted for non-linear behavior of single lap joint.

In all of the aforementioned studies, it was noted that the presence of stress singularities makes the predictions of stresses and strains highly dependent on the size of the finite element mesh used in the vicinity of the singularity. Theoretically, infinite stress or strain is predicted as the size of finite element tends to zero and evidently, it is not possible practically. Adams (1990) states, that, practically, sharp corners do not exist and there is always some degree of rounding present at the embedded corner. Zhao (Zhao 1991) showed that at a certain distance from the corner of the order of degree present, the stress-strain distributions reverted to those predicted by a model that did not include any degree of rounding. Richardson (Richardson 1993) used finite elements of the order of nanometers to produce a detailed description of stresses within an adhesively bonded cleavage joint. He also observed that the influence of any stress singularities present within an adhesive layer are highly localized. It was suggested, however, that it is imperative that the presence of these singularities be accounted for in any detailed analysis of adhesive bonded joints.

Carpenter and Barosoum (Barsoum 1989) formulated a specific finite element to simulate various proposed closed form solutions to the stress and strain fields with a single lap joint. It was shown that the theoretical singularities within such a joint could be removed through the use of strain-displacement equations. Beer (Beer 1985) gave the formulation of a simplified finite element chiefly concerned

with correct representation of the mechanical properties of an adhesive with a structural model rather than the prediction of detailed stresses within an adhesive. In order to validate the application of finite element methods to the analyses of single lap joints, Tsai(M. M. Tsai 1995) compared predictions from a two dimensional finite element model with the results from a photo-elastic study of single lap joint with quasi-isotropic composite adherends performed using Moire's interferometry. Moire's interferometry is an optical method of measuring surface strains. Tsai and all noted a good correlation between practical and theoretical results. It was noticed that at the edges there was some difference between prediction and practical results at the edges of the joint. This was attributed to free edge effects and because the coupling between bending, shearing and tension of a quasi-isotropic composite was not accounted for in their two-dimensional model.

Joints with mismatch and anisotropic adherends were considered by Adams et al (1978), including material and geometric non-linearity and with particular interest in the interlaminar stresses induced in the adherends made up of composite materials. Good correlations were noted between their predictions of failure load and those seen practically. This was attributed to the fact that the joints with composite adherends invariable failed via interlaminar failure which was remote from the influence of these singularities in the model and the values of the stresses predicted were less sensitive to the details of the finite element mesh used. It was also noted in these papers that the addition of a spew fillet of 45^0 to the joint with composite adherends had the effect of considerably increasing the strength of the joint. This was shown to be due to the spew fillet smoothing the path of load transfer across the joint and therefore reducing the stress concentration within the composite adherends. As the interlaminar strength of composite adherends is relatively low then any means by which the through thickness stress can be reduced will evidently result in a higher strength of the joint.

3.3.2 THREE DIMENSIONAL FINITE ELEMENT SOLUTIONS

Stresses in adhesive joints are sometimes obtained with reasonable accuracy from one or two dimensional analysis. There are many cases where a two dimensional analysis is not applicable or doesn't produce any acceptable accuracy. Even for the single lap joint, a three dimensional analysis may be required if accurate determination of stress variations across the width is desired.

The three dimensional nature of the stress distribution within the single lap joint was noted by Adams and Peppiat (Adams R. D.,1973) who used an approximate method to predict the influence of Poisson's ratio effects on the stress across the width of the joint. They also analysed the distribution of shear stresses along the width and length of single lap joint. They found that the distribution of shear stresses is not uniform across the width of the joint and these shear stresses are higher at the edges of the joint. A plane-strain analysis gives smaller shear stresses than plane-stress analyses. In single lap joints, the points that are the edges of the joint behave as if they were under plane strain condition, while the points at the center of the specimen exhibit a behavior close to plane strain. Therefore, the application of two dimensional analyses doesn't exactly represent what happens at any point in the structure.

In cases where a three dimensional analysis is required, finite element models are the best tool available. The main advantage of using this method is that no special assumption is needed. The principal disadvantage is the increase of data preparation and computational time. Tsai and Morton (M. M. Tsai 1993) extended their earlier two dimensional analyses into three dimensional analyses and again compared the results using Moire's interferometry. It was demonstrated that the peel stresses were higher at the edges of the joints and this is attributed to the influence of anticlastic bending. The remainder of the stress components are shown to be less sensitive to position across the width of the joint and compared well with predictions from a plane-strain two dimensional analyses.

Analyses in three dimensions were also undertaken by Zhao (Zhao 1991), who performed a simplified analysis in which the boundary conditions to three dimensional model of the joint overlap length were derived from a closed form solution. Zhao noted that the highest shear stresses were predicted towards the

outer edges of the joint. Lyrner (Lyrner 1984) used three dimensional finite element analyses to quantify the stress distribution in the adhesive adjacent to small button shaped voids and compared the results from two and three dimensional analyses. It was demonstrated that the plane strain condition imposed in the two-dimensional work was reproduced at the middle of the three-dimensional analyses.

Karachalios (Karachalios 1999) considered the relationship between the three dimensional stress distributions and failure observed in single lap joint with a spew fillet and included both material and geometric nonlinearity in finite element models. He also observed that the failure was seen to initiate at the centre of the joint where the highest peel stresses, and the maximum principal stresses, were predicted to occur. Adams and Davies (Davies 1996) investigated the variation in stress distribution, using three dimensional finite element analyses, within the single lap joint with composite adherends. It was also noted that the transverse shrinkage arising from the Poisson's ratio effects was responsible for the increase in adhesive shear stress towards the free edges of the adhesive layer. This was due to the nature transfer in the joint whereby there was the difference transverse deformation between the upper adherend and lower adherend at the joints ends, resulting in imposed shear strain across the adhesive layer.

Taylor (1996) developed a simplified three dimensional model of adhesively bonded joint. The adherend were modelled by nine node Mindlin plate elements and the adhesive was modeled by special brick elements with eighteen offset nodes. Analogous to the two dimensional model, the adhesive and the adherends share nodes, reducing the number of degrees of freedom of the joint.

Thus, in order to gain a full understanding of the detailed stress distribution of the single lap joint, the finite element method can be used to great effect. However, care must be taken to account for the nicety of application of finite element to this geometry in that the presence of singularities must be accounted for, linear and non-linear geometric and material effects must be included. It has been shown that the nature of stress distribution within the single lap joint is three dimensional and care must be taken in the interpretation of two-dimensional results if an understanding of overall behavior is to be achieved.

3.4 CLOSED FORM ALGEBRAIC SOLUTIONS

The finite element solutions explained in the previous section for the analyses of bonded joints requires considerable expertise in using FEA to produce meaningful results and it is also subject to the requirement for relatively large amount of computing power. The result is that finite element method does not always hold favour over the often more straight/forward implementation of the closed form solutions proposed for bonded joints during the last century. In this section a comprehensive review of closed form solutions have been presented. These solution sometimes provide reasonable accurate behavioral and strength predictions.

Volkerson (Volkerson 1938) presented a continuum mechanics approach to analyse the shear lag configuration of the single lap joint. However, there were limitations to this analysis, most significant of which was its failure to account for the effect of the bending moments induced by the eccentricity of the applied load. Nor did it account for the adherend shearing, and it predicted the maximum shear stress to occur at the free surface at the end of the joint overlap. As this is a free surface, the shear stress should, in practice, be zero. The major drawback of the Volkerson analysis is that it neglects the peel stresses which arise in the adhesive layer due to the bending arm between the applied forces. This factor should be taken into consideration as adhesives are very sensitive to peel stresses.

Goland and Reissner (Goland 1944) further modified and improved the Volkerson analysis and proposed a two stage methodology of analysis in which they have calculated the bending moments first due to the externally applied forces and then applied the boundary conditions to a model of the overlap layer. They considered two different configuration of joint with and without adhesive layer flexibility. The former approach was found to be more applicable to joints with metallic or stiff adherends and was the most relevant analysis for the current study. In their theory, the shearing and normal stresses within the adherends were neglected but it was the first significant theory to include the influence of bending moment's upto the stress distribution especially the peel stresses within

the adhesive layer. The graphical representation of peel and shear stresses obtained by Goland and Reissner is shown in figure.3.2.

This image has been removed

Figure 3.2: Shear and Peel stress distribution across the bondline of single lap shear joint (Spaggiari, 2003).

Hart and Smith (Hart-Smith 1973) in 1973 further modified the proposed model of Goland and Reissner. They proposed a method to model the deformation of upper and lower substrates in the overlap region separately and not as a whole composite sandwich. Their approach involves the solution of the adhesive stresses and bending moments at the same time and proposed a bending moment factor k. In the subsequent years, other researchers carried on studies on the accuracy of the solutions proposed by Goland and Reissner and Hart-Smith model. Sneddon (Sneddon 1961) and Adams and Peppiat (Adams R. D.,1974) found an error in the initial formulation of Goland and Reissner's theory and presented a correction which derived an alternative bending moment factor (Goland 1944).

Chen and Cheng (D. C. Chen 1991) had shown a development of their earlier work (D. Chen 1983) in which they extend their own proposal theory of single lap joint behavior to include non-identical adherends. They both allowed the resulting system of equations to be solved using closed form methods in which they assumed uniform shear stresses across the bondline thickness. This theory was also proposed by Wu et al. (Wu 1997), who also show that it decomposes to Goland and Reissner's solution if further simplifying assumptions were made.

Unbalanced joints with dissimilar adherends have been analysed by Yang and Pang (Yang 1996) who derived the expressions similar to the expressions proposed by Chen and Cheng but solved by using a Fourier series method. A state of uniform shear stress through the adhesive thickness was assumed. Good correlation was obtained between the results from complimentary finite element analysis. Coppendale (Coppendale 1997) and Weitsman (Weitsman 1981) have studied the influence of the thermal expansion of the adhesive and have shown that it has a significant effect at the ends of the overlap.

Non-linearity in adhesively bonded joints was first accounted by Hart-Smith (Hart-Smith 1973) using an approach similar to Goland and Reissner but solving iteratively to account for the plasticity. The influence of the peel stresses on the yield behavior of the adhesive was not accounted for and it was the shear stress component alone that was used to control the plasticity. An improvement of Goland and Reissner's solution was also presented in which better account was made on the flexibility of the adhesive layer.

A similar method was also proposed and presented by Adams and Mallick (R. D. Adams 1984), who proposed the use of effective modulus, calculated using the strain energy from integrating the adhesive stress-strain curve that could then be input into a linear elastic solution. This was seen to give strength predictions which were close to the solutions predicted by much lengthier calculations including full adhesive non-linearity.

The main lack of closed form solutions is in accounting realistically for adhesive and adhesive non-linearity. Even elastic formulations produce complex equations which are difficult to solve. With the increased computing power today, it is now possible to set up these equations on computers and to get an almost instantaneous approximate solution which gives a good indication of the stresses acting in a lap joint configuration under tensile loading.

3.5 FRACTURE MECHANICS METHODS

Designing for engineering structures have been done in the past by using strength of materials approach. Under strength of materials approach, stresses developed in the material are often compared with the maximum allowable strength of the material. Although this approach have been widely used and

successfully applied, problems have arisen in a number of infamous structural failures, in which preexisting or service induced flaws have propagated catastrophically. Stress and local strains are greatly increased at the tip of these defects, which often serve as initiation sites for structural failures. Fracture Mechanics thus provides an alternative set of criteria for evaluating the integrity of structures that contain flaws or preexisting cracks, and is implemented successfully in designing such structures.

Essentially fracture mechanics is the study of strength of a structure which contains a flaw or a crack, usually elliptical in shape. It is generally more suited to failure load prediction then joint optimization studies**.** Fracture mechanics has been applied extensively in studying adhesively bonded joints. Instead of looking at the local values of peak stresses, which are infinite at the crack tip, fracture mechanics method assess if the conditions in the structure are suitable for failure or not. This principle was first set by Griffith in 1920. He suggested that any brittle material containing flaws will fail when energy the structure can supply to crack tip under loading (the strain energy release rate G) is equal to the energy required to propagate (the critical energy release rate Gc). A several number of other criteria have also been proposed for the prediction of crack propagation including stress intensity factor (K), crack tip opening displacement (CTOD) and J-Integral (Jc). The main problem of using fracture mechanics approach is related to the dependencies of fracture energy to the adhesive thickness and to the absence of flaws in the adhesive.

3.5.1 AN ENERGY CRITERIA FOR FAILURE

Application of strength base criteria break down when sharp cracks are present, because mathematically the stresses are predicted to become singular (infinite) at the crack tip. Inspite of singular stresses and strains, the energy concentrated in the vicinity of the crack tip must remain finite, suggesting that an energy based failure criteria would only involve bounded quantities. We know that a force moving through a distance produce work, thus a stress moving through a separation distance during a failure is equal to the energy per unit area, which is basic fundamental unit of fracture mechanics. Fracture mechanics thus offer an alternative approach for designing engineering components and structures.

Mathematically, the stresses at a crack tip are predicted to be infinite for a linear elastic material, in real material the high stresses usually exceeds the yield point, resulting in the plastic deformation on a local scale. When this is the case, linear elastic fracture mechanics (LEFM) can be used effectively for the analysis and designing of such structures. There are two basic approaches to linear elastic fracture mechanics, the stress intensity factor approach and the energy release rate approach, both of which are widely employed for analyzing cracked structures. Both approaches are explained in details in subsequent topics.

3.5.2 THE STRESS INTENSITY FACTOR APPROACH

The concept of stress intensity factor was developed by Irwin (1958) and is based on the fact that the stresses ahead of the crack tip are proportional to the $r^{0.5,}$ where r is the distance from the crack tip. Inspite of the infinite stresses predicted by this model, the stress intensity factor, K, remains finite, allowing the severity of a given crack and loading condition to be characterized with this fracture mechanics based parameter. This approach has been widely used to determine the stress intensity factor for a wide range of crack configurations.

In simplest form, the relevant failure criterion could state that the failure in a material will occur when the applied stress intensity factor, K, reaches the critical stress intensity factor, K_c, a material property. Fracture may occur in three different loading modes: Mode I (opening mode), Mode II (forward shear) and Mode III (antiplane or out of place shear or tearing) as shown in figure.3.3 . Just as the strength based criteria become more involved for multiaxial fields, the fracture criterion for mixed loading may include contribution from each mode in some appropriate manner.

Figure 3.3: Schematic diagrams of failure modes (Gunawardana Dec 2005)

3.5.3 THE STRAIN ENERGY RELEASE APPROACH

The energy release rate is viable approach but often equivalent approach to fracture mechanics. Griffith laid the foundations for this approach in 1921. The applied energy release rate, G, is the amount of energy per unit crack area available to a growing crack by the applied loading conditions, a relationship that is often expressed as:

$$G = \frac{\partial(W - U)}{\partial A}$$

Here W is the external work, U is the stored elastic energy, and A is the crack area. Thus, this failure criteria states that crack will propagate when this applied energy release rate reaches the critical value, Gc, also known as the fracture energy of the bonded system. The concept of energy required per unit area to propagate a crack has found widespread applications, including to bonded systems. Nonetheless, the stress intensity factor approach and the energy release rate approach can be shown to be equivalent for homogenous materials using relationships proposed by Broek (1978):

$$G = \frac{Ki^2}{E}$$

Where E = young's modulus of the material and Ki = critical stress intensity factor.

3.5.4 THE J-INTEGRAL APPROACH

The J-Integral, also known, as contour integral in computational fracture mechanics represents another way of calculating the strain energy release rate. It can be an effective measure to calculate the energy release rate of the adhesives using finite element methods. The concept of J integral was firstly developed by James Rice and Cherapanov in 1968. They independently showed that an contour integral (J) was independent of the path around the crack tip.

The J integral is widely accepted as a fracture mechanics parameter for both linear and non-linear material response. It is also related to energy release rate associated with crack growth, especially for nonlinear materials. If the material response in linear (response of 2D damage bonded coupons is also linear), it can also be expressed in terms of stress intensity factors. Because of its importance

in the assessment of flaws, its accurate numerical approximation is very important to the practical application of fracture mechanics in design calculations. The J-Integral is based on the virtual crack extension/domain integral methods (Parks 1977 and Shih 1986). This method is particularly attractive because of its simplicity to use, adds little to the cost of analysis, and provides excellent accuracy, even with rather coarse meshes in finite element models.

Consider a 2-d body of linear or nonlinear elastic materials free of body forces and subjected to a 2-d deformation field (plane stress and plane strain) so that all the stresses developed depends only on two coordinates X_1 and X_2.(figure.3.4) (Abaqus HTML Documentation Oct, 2009)

This image has been removed

Figure 3.4: Contour for the evaluation of J-Integral along the crack tip (Abaqus HTML Documentation Oct, 2009).

In the context of the linear and non-linear analysis, the J-Integral is defined in two dimensions as

$$J = \lim_{\Gamma \to 0} \int_{\Gamma} \mathbf{n} \cdot \mathbf{H} \cdot \mathbf{q} \, d\Gamma,$$

Where Γ is a contour beginning of the bottom crack surface and the ending of the top surface as shown in figure 4 above. The limit $\Gamma \to 0$ indicates that the Γ shrink onto the crack tip; q is the unit vector in the virtual crack extension direction and n is the outward normal. H is given by:

$$H = WI - \sigma \, \partial u / \partial x$$

For linear and elastic material behaviour W is the elastic strain energy, thus representing the strain energy in an “equivalent elastic material”. For linear elastic materials, the J-Integral is in fact the strain energy release rate, G, and can be related to the stress intensity factor K by using the following relations:

$$J = G = \frac{K^2}{E} \text{(For plane stress)}$$

$$J = G = \frac{K^2}{E}(1 - V^2) \text{ (for plane strain)}$$

Here v is the Poission ratio.

Due to its robust nature, excellent numerical approximation, path independent nature, ease of calculation and seamless integration with finite element theory, it has been used to calculate the strain energy release rates for the bonded joints coupons. For the ease of discussion the two dimensional J-Integral theory was considered, nevertheless the two dimensional theory can be easily extended to three dimensional cases.

3.5.5 TWO DIMENSIONAL CRACK ANALYSIS USING FINITE ELEMENT METHODS

The computation of stress intensity factors and strain energy rates is very important, although not an easy task when a complex geometry is considered; in these cases finite element method can be a effective approach upto some certain success to calculate fracture mechanics parameters.

Using fracture mechanics in conjunction with finite element methods involves several steps. The first very step consists of modelling the stress singularity using finite elements. This can be done using ordinary finite element with a very fine mesh in the area of stress singularity. Although the use of higher order finite elements may improve the accuracy of the results obtained from linear order elements. As mentioned by Owens and Fawkes (Owens 2001), the first approach was made by Tracey (Tracey 1971) who developed a triangular element with polynomial representation of the displacements. Tracey and Cook (Cook 1977) extended the model to quadrilateral representation of finite elements. They modelled a singularity of order r^{-p} using the potential function of order p for the

displacements. A breakthrough was introduced independently by Henshell and Shaw (Henshell 1989) and Barosoum (Barosoum 1976) who developed a method to model a singularity of the order $r^{-0.5}$ for the stresses at the crack tip. Their proposed method consists of displacing the mid side node of rectangular plane elements to the quarter positions next to the crack tip.

This element in finite element methodology is known as quarter point element or singular element (figure.3.5). This singular element gives a stress singularity of $r^{-0.5}$ for the stresses but only along the two sides containing the displaced nodes. If the crack is approached along any other direction, it will not be necessarily give the same singularity. Barosoum solved this problem by collapsing a quadrilateral element into a triangular element. This approach effectively produces a stress singularity of $r^{-0.5}$. If the middle joint is moved away from the quarter position, the singularity moves too. If the point is exactly at the midpoint of the element's side, the singularity moves to a point indefinitely distant, effectively resulting in singular in a non singular element (figure.3.6).

Figure 3.5: Quarter-point two dimensional continuum finite element (Andruet 1998)

These images have been removed

Figure 3.6: Collapsed quarter-point two dimensional continuum finite element (Andruet 1998)

Another effective approach to model the crack field in adhesives is the use of available analytical solutions. In this method, only one finite element model the whole crack region and the position of the crack then can be modelled during the crack extension procedure. Byskov (Byskov 1970) discovered this approach for the first time by modelling the stresses using very special complex functions developed by Muskhelishvilli (Mushkhelishvili 1963). Rao et al. (Rao 1971) used analytical solutions to model the presence of cracks in a continuum. In their study, the regions with stress concentrations were modelled with primary finite element which includes stress singularities, and the remaining domain was modelled by using secondary elements, commonly known as plane finite elements. Such a case is depicted in figure.3.7. Davidson et al. (Davidson 1995) developed an analytical crack tip element to predict strain energy release rate for interfacial problems.

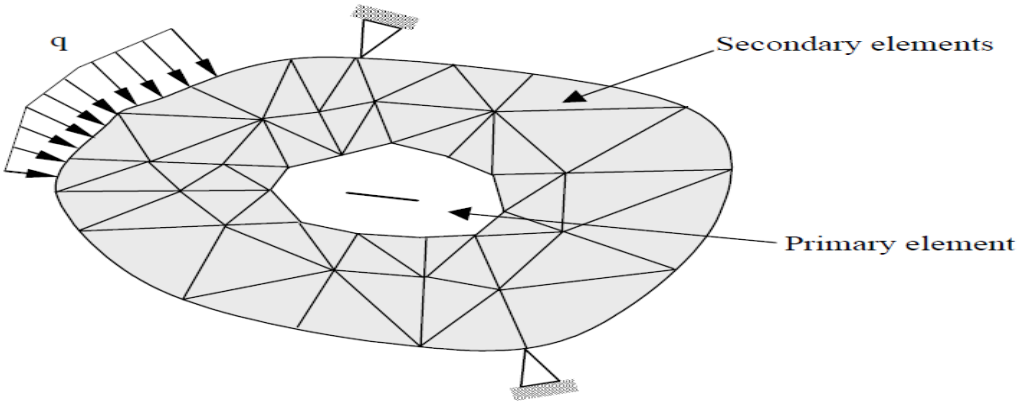

Figure 3.7: Arbitrary body with a region of stress concentration.

The citied formulations do satisfy internal equilibrium and compatibility conditions but do not satisfy compatibility of displacements between singular elements and the elements surrounding them. To solve this problem, the displacements of the boundary between ordinary and finite singular elements are forced to be equal by using Lagrange multipliers in the energy formulation. The finite elements derived using this method are special elements known as Hybrid elements. Tong et al. (Tong 1973) used these special elements to handle crack analysis of plane structures. This method yielded the compatibility between the displacements of the cracked super elements and the finite elements surrounding it. Aminopour and Holsapple (Aminopour 1991) developed hybrid displacements finite elements to analyse a propagating crack at the interface of two materials. This analysis included anisotropic materials and remeshing of the structure to simulate the propagating crack.

Once a good representation of stresses is achieved, the next step is to compute the fracture mechanics parameters, particularly stress intensity factors or strain energy release rates. There are numerous ways of calculating the stress intensity factors or strain energy release rates using finite element methods.

- **Stress Intensity Approach**: In this approach, the obtained stress expressions are correlated with the stresses from the finite element analysis. Thus, stress intensity factors can be obtained using the equation given below

$$Ki = \sqrt{2\pi r}\,\frac{\sigma ij}{fij(\theta)}$$

  Where σij are the stresses of a node with coordinates r and θ.

- **Strain Energy Release Method** : From the definition of strain energy release rate for displacement control

$$G = -\frac{dU}{da}$$

  The following approximation can be:

$$G = -\frac{(U2 - U1)}{\Delta a}$$

Where,

U_1 = Strain energy of the original crack configuration

U_2 = Strain energy of the extended crack configuration

To use this method, two finite element meshes must be analysed: the original one and another one with the crack extended by the distance Δa.

- **Virtual crack closure Method**: The method was first used by Ronald Krueger of NASA Inc. The main objective of using this method is to avoid two step finite element analysis of the complete structure to obtain strain energy release rates. This method consists of doing a finite element analysis of the whole structure for the original crack configuration and then finding the values of stiffness matrix (ΔK) for crack length Δa and storing these values so that these values can be used in subsequent crack extension analysis. Hellen (Hellen,1975***)*** provided a simple expression for computing $\Delta k/\Delta a$ as a summation of scalar terms derived from the reduction of the system of equations by gauss elimination method. Haber and Koch (Haber 1985) formulated an explicit expression for energy changes due to virtual crack extensions. The crack singularity was modelled using quarter point elements and the remaining structure by iso-parametric elements. This method gives accurate results with relatively coarse meshes.

Hellen (Hellen,1989) expanded by the application of virtual crack extension method for non-linear elastic materials. Using time incremental theory (Implicit Finite Element Scheme), elastoplastic material conditions can be effectively modelled.

Barbero and Reddy (Barbero 1992) proposed the Jacobian method to obtain displacements from stress intensity factors. This method needs a single finite element analysis and doesn't require the virtual crack extension. All these analysis was based on the delamination problem in composites laminates. The basic idea of this method is that potential depends upon the displacement and the nodal coordinates. This is true in case of iso-parametric elements because

displacements and coordinates are interpolated using the same functions. They applied the same method to two and three dimensional problems.

3.5.6 THREE DIMENSIONAL CRACK ANALYSIS USING FINITE ELEMENT METHODS

Fracture mechanics computations become more complex when the crack changes from two dimensions to three dimensions, which cannot be neglected. Some of the cases for 3-D include configuration with through, part through, or embedded cracks. Cracks in thick solids and cracked structures with arbitrary shapes generally present important three dimensional effects. Therefore, the effect of cracks in such geometries cannot be predicted by analytical expressions or two dimensional finite elements; thus three dimensional finite elements are required.

The need for computations of fracture mechanics parameters for three dimensional cases was already addressed in the early 1970's. Hellen (Hellen, 1989) gave values of stress intensity factors for a cracked plate using virtual crack closure technique. This method requires two finite element analyses for any cracked configurations. A further variation of the virtual extension method was developed and proposed by Nikishkov and Atluri (Nikishkov 1987). The equivalent domain integral method was aimed at finding values of the J-integral for a general three dimensional case. In this method, the J-integral and strain energy release rates for Mode III fracture are redefined as follows:

$$\mathrm{Jk} = -\int_{\mathrm{A}} (\mathrm{Wnk} - \sigma\mathrm{ij}\frac{\partial \mathrm{u}}{\partial \mathrm{x}}\,\mathrm{nj})\,\mathrm{sdA}$$

$$\mathrm{Giii} = -\int_{\mathrm{A}} \left(\mathrm{Wiii}\,\mathrm{ni} - \sigma 3\mathrm{j}\frac{\partial \mathrm{u3}}{\partial \mathrm{x}}\,\mathrm{nj}\right)\mathrm{sdA}$$

Where,

s = arbitrary continuous function which is zero on outer boundary of A

f = area under s

A = Integration surface: It is divided into A_o and A_e.

Figure.3.8 shows a possible s function.

Figure 3.8: Virtual crack extension method (Nikishkov and Atluri 1987)

Barbero and Reddy (Barbero 1992) used the Jacobian derivative method for the computation of strain energy release rates for three dimensional cracked bodies. This method is very generic and effective because of its computational simplicity. The authors presented an analysis of the cylinder with a circular track on the surface. Good agreement was obtained between their results and analytical solutions.

Badari Narayana et al. (Badari Narayana 1994) showed that the modified crack closure integral method can be used for the three dimensional analysis. They developed a method for the derivation of the modified crack closure integral using eight noded brick elements. They presented the derivation on the basis of virtual crack closing over the full elemental area in the plane of the crack. They also proposed the concept of subarea integration in which the crack front inside the finite element is divided into a number of segments. By using the same approach, one can calculate the strain energy release rate at several points inside the element without refining the finite element mesh. The authors presented two standard examples to explain this method: a thick center-cracked tension specimen and a semi-elliptical crack surface in the thick slab. This method can also be applied to linear and non-linear cases, and no special finite elements are required. The main advantage of this method is its computational simplicity.

Some other researchers also worked in the area of modified crack closure integral method to three dimensional problems. For example, Shiva Kumar et al. (Shivakumar 1988) obtained crack closure integral expressions for eight noded and twenty noded brick elements as shown in figure 3.9 and 3.10.

Figure 3.9: Eight Noded Brick Element (Krueger 2002)

Figure 3.10: Twenty noded brick element (Krueger 2002)

3.6 INTRODUCTION TO FATIGUE LIFE APPROACH

Fatigue in engineering structures is the loss of structural integrity over time due to the repeated or continuous application of stress. The response of structure to constant stress is called ‘static fatigue’; however the term fatigue is more generally associated with cyclic stressing. The fatigue phenomenon is common to most of the engineering materials and it has been estimated that 80% of all the

engineering failures occur due to fatigue. The studies of fatigue was started in earnest in the 1850's with the wide spread use of steel in the railways and received added impetus with the introduction of steel ships and aluminum alloy aircraft. The majority of the published data is on the fatigue concerning metals; there is a growing interest and literature on the subject of fatigue in polymer adhesives and composite structures.

The mechanism of fatigue failure in polymers differs from those of metals as polymers are more susceptible to environmental factors such as moisture and temperature. Also, the visco-elastic behavior of polymers at moderate temperature will affect their responses to cyclic stresses. The study of fatigue in bonded composites joints is further complicated by the fact that the whole system works as a heterogeneous system in which the adhesive is itself composite materials. Adhesive bonded joints are generally considered to have a good fatigue resistance as compared with alternative mechanical joining methods such as bolting, self piercing rivets or spot welding. This has been attributed to the reductions in stress concentrations, which affect the fatigue life of metals. The adhesive layer also prevents fretting fatigue, which may be problem in mechanical joints (R.D. Adams 2005).

A most common distinction in fatigue is between the high cycle fatigue (HCF) and low cycle fatigue (LCF). HCF considers events that may occur million of times in the life of any engineering structure, with a predominantly elastic response. Low cycle fatigue may involve thousands of events before failure but it is associated with more widespread plasticity. There are three main approaches which are commonly used to analyse fatigue life in engineering structure. These are fatigue life approach (SN approach), the strain life approach and the fatigue crack growth approach (FCG approach). The stress life and the strain life approaches are associated with the safe-design philosophy, in which a component is considered to be flaw free and is thus designed for a fixed service life after which the part should be replaced. In the fatigue crack growth rate approach, an initial flaw distribution is assumed (since it is based on fracture mechanics principle) and knowledge of the conditions and rate at which these cracks grow. Fatigue crack growth approach is been used in this thesis for the analysis of bonded joints.

3.6.1 FATIGUE LIFE PREDICTION OF ADHESIVELY BONDED JOINTS USING FCG APPROACH

Engineering structures subjected to cyclic loads are more prone to failure under loads smaller than the predicated critical static loads. This fatigue process produces slow crack growth at stress intensity factors lower than the critical value. Fracture mechanics parameters, such as J-Integral and critical stress intensity factors can be related to fatigue crack growth. It was experimentally found that for cracked specimens subjected to cyclic loads, the stress mean value has an important impact on the crack growth rate per cycle.

Lin and Liechti (Lin 1987) stated that for adhesively bonded joints, the correlation between debond growth rates and the changes in stress intensity factors has the same sigmoidal shape as the fatigue crack propagation in metals. Meguid (Meguid 1989) showed that the relation between fatigue crack propagation rate, da/dN, and the stress intensity factor range, $\Delta K = K_{max} - K_{min}$ for the Paris-Ergodan equation. A typical Paris law curve is shown in figure 3.11.

Figure 3.11: Typical Fatigue Crack Growth Rate Curve (Bahram 2008)

The curve is divided into three regions. In region I there is an existence of a threshold value below which there is no crack growth or no fatigue failure, in region II the relation between log(ΔK) and log (da/dN) is practically linear. Finally, in region III there is a fast crack growth rate which may ultimately lead to failure.

In other words, $K_{max} > K_c$. The shape of the curve is called the crack growth rate curve and is valid for most of the materials, and it is obtained by fitting measured crack growth rate.

There have been many attempts to model a relation between the fatigue crack propagation rate, da/dN, and the stress intensity factor range. The relation which is most commonly found in literature was given by Paris and Ergodan in 1963:

$$\frac{da}{dN} = C(\,Kmax - Kmin)\hat{}m$$

Where m and c are material dependent constants. This equation is valid only in region II of the crack growth rate curve and doesn't take into account the effect of the mean stress. Forman et al. improves the model to account for the effect of the mean stress:

$$\frac{da}{dN} = C\frac{(\Delta K)^m}{(1-R)Kc - \Delta K}$$

Where

$R = \sigma max / \sigma min.$

K_c = Critical stress intensity factor.

Fatigue in adhesively bonded joints was first studied by Mostovoy and Ripling (Mostovoy 1975) and Brussat and Chiu (Brussat 1977). They concluded that linear elastic fracture mechanics gives reasonable accuracy in the description of the crack growth rate due to fatigue. Dataguru et al. (Dattaguru 1984) showed that non-linearities played an important role in various bonded joint configurations.

Lin and Liechti (Lin 1987) correlated crack debond growth rates to obtain the strain energy release rates for four specimens. They found that geometrically non linear analysis was needed for the computations of energy rates. Similarly was found in debond growth rate curves of the specimen studied. The fourth specimen presented a different shape for the debond growth rate curve.

Kinloch and Osiyemi (A. J. Kinloch 1993) used a double cantilever beam specimen to correlate experimentally crack growth rates with analytically obtained strain energy release rates. A fatigue crack growth curves was determined with this data and used for fatigue life prediction of single lap joint geometries. Good agreement between the predicted and experimental results was found.

Some work has been done on the composite crack patch configurations. Nabousli and Mall (Nabousli 1997) studied the thermal effects of a cracked composite plate which was adhesively bonded. Due to mismatch in stiffness matrices and thermal expansion coefficients of the three components, large stresses were developed within the adhesive layer. Also, due to the small thickness of the adhesive film, a conventional finite element analysis required a large number of elements across the thickness of adhesive. For this reason, some authors called the above approach as three layer model. Three layer model techniques consist of modelling the adherends. The cracked plate and the composite patch, and the adhesive layer with Mindlin plate elements with transverse shear deformation. Constraints equations were use to enforce compatibility at the adhesive/adherend interfaces. Two configurations were studied: a single sided repair, and a double sided repair. Three patch materials, boron/epoxy and glare were used to study the influence of stiffness and thermal coefficients mismatch among the different structural components. Strain energy rates were computed using the modified crack closure integral method extended to three dimensional configurations. The three layer model method was validated with previous results and conclusions were obtained from different analysis.

This image has been removed

Figure 3.12: Crack Patch Repair Configuration (Andruet 1998)

3.7 FAILURE PREDICTION OF ADHESIVE BONDED JOINTS

Several failure criteria are discussed here in the context of the finite element method of adhesively bonded joints. Some of the proposed failure criteria are also applicable to closed form predictions of stress/strain levels.

On considering how to best predict failure, the method which appears most obvious is simply a stress or strain at which particular materials will fail. As adhesive perform well in shear it would appear best to specify a maximum shear limit to give some idea of joint strength. Greenwood et al. (Greenwood 1969) performed such an analysis for single lap joints using closed form solutions, and found that the maximum shear stress occurred at the adhesive at 45 degrees to the loading direction. The use of principal stress is preferred because the tendency is for adhesives to fail through tensile loading, even if it is loaded in shear because this shear gives rise to tensile and compressive principal stresses.

Alternatively, the maximum peel stress can be used as a criterion for failure and it was shown that reasonable predictions of strength could be achieved. However, it was noted that the predictions were highly inaccurate for joints in which adherend yielding was present. Harris and Adams (Harris1984) showed that using the maximum principal stress can give reasonable success when combined with non-linear finite element methods and their predictions were within 10% of experimental values. The choice of using maximum principal stress or strain criteria for failure of the adhesive was seen to depend upon the specific joint configuration. Maximum principal stress was successfully applied to highly ductile adhesive where one may expect the application of maximum strain criteria.

Adams and Harris subsequently showed that it presence of any stress singularity, maximum principal stress at a distance was specified, because they have defined the failure criteria at Gauss point. Gauss points in finite element theory are those points in which finite element method evaluates stress and strains with greatest accuracy.

Ikegami (Ikegami 1969) employed maximum Von Mises stress criterion as a measure of stress in the adhesive layer. This proposed criterion was of limited success because the behavior of adhesively bonded joints is highly dependent on the hydrostatic stresses, and this was not accounted in the analysis proposed by Ikegami. A criterion of critical stress or strain was also proposed by Lee and Lee (Lee 1987) for the failure analysis of tubular single lap joints. They used the combination of criteria and it depends upon the adhesive bondline thickness. The application of the above defined criteria to experimental data was firstly investigated by Chai (Chai 1993) through observing failure in notched flexure specimens and measuring the strain field in the specimen. It was also shown by Chai that critical shear strain decreased with increasing adhesive thickness. It was also noted that the failure of the adhesive can be expressed in terms of critical fracture energy, which too also varies with thickness.

Crocombe and Adams (R. D. Adams 1981) also defined an alternative failure criterion by including plasticity in the adhesive characteristics using the effective uniaxial plastic strain. They noticed that the effective uniaxial plastic strain were dependent on the density of finite element mesh and in reality was a critical strain at a distance location. Adams and Crocombe have done all these studies on peel joints. An alternative criterion in which plasticity in the adhesive can be studied is by using the critical plastic energy density.

Crocombe at al. (A. D. Crocombe 1990) used cleavage and compression specimen for the evaluation of failure criteria, and avoided the problem of stress singularities by using the semi-closed form solutions for the analysis of stress and strain distribution. They found that the maximum principal stress criterion gave reasonable success in the failure predictions of untoughened epoxies under Mode I and Mode II loading.

Zhao et al. (Zhao 1991) used a criterion whereby if the average stresses over a certain distance within single lap joint reached a critical value, then the joint was deemed to have failed. The distance picked was a line progressing into the adhesive from the point of singularity. A criterion of critical average stress over the distance was applied to joints with sharp adherend corner, or a small radius, whereas a criterion of maximum stress over the distance was used for larger radius. Unfortunately, no reason was given for the choice of such critical distance. Clarke and McGregor (Clark 1992) further extended this idea by predicting the failure if the maximum principal stress exceeded the maximum principal stresses. It was also noted in their analysis that the sensitivity to changes in local joint geometry, such as radius of the adherend corner, was reasonably low for this criterion.

Crocombe et al. (A. D. Crocombe 1995) studied the failure of cracked and uncracked specimens subjected to various loading conditions and used a critical peel stresses at a distance from the singularity with some success. Kinloch and Williams (A. J. Kinloch 1980) also considered some cracked specimens, and applied failure criteria at some critical distances with some success, but their work was not extended to consider the un-cracked specimens. Crocombe applied a method of failure prediction where the adhesive was deemed to have failed if the whole of the adhesive layer was seen to yield under the applied load but this was only applicable for highly ductile adhesives. Schmit and Fraise (Schmit 1992) used a similar criterion for the prediction of the strength of the stepped adhesive joints with some success, but again this was only really of use in predicting the behavior of highly ductile adhesives.

Fracture Mechanics is the study of the strength of structures which includes flaws such as voids and cracks where stresses are said to be singular. As stated earlier, fracture mechanics applies criteria to assess whether the conditions are such that failure will occur at these points, one such criteria being the strain energy release rate, denoted by G. Other fracture mechanics based criteria which can be used in adhesive bonding are the crack tip opening displacement measurements, the J Integral, and the stress intensity factor measurements. The strain energy release rate, G, has a strong physical meaning and is the easiest of

the mentioned fracture mechanics parameters to obtain for adhesives specially if the crack in the adhesive is near to the interface between the adherend and the adhesive. This point is supported by Toya (Toya 1990). It is also possible to include the effects of the rate of the load application and temperature with these failure loads.

The adhesive joints are often subjected to mixed mode loading. It was always noted that in the observations that crack will generally run perpendicular to the direction of maximum tensile stress under tensile loading. The above mentioned criterion was not true in case of mixed mode loading. Kinloch and Shaw (A. J. Kinloch 1981) derived formulae which account for fracture under such loads. They also noted that the parameters such as stress intensity factors, K_{ic} will vary with the geometry of the joint. Adhesive bondline thickness is seen to control Gc and, for a thin bond line, the induced tensile stresses will be increased and this will in turn increase the size of the plastic zone. However, for the thicker bond thickness the plastic size will be reduced, and Gc will decrease. It was shown that G_{ic} and K_{ic} have their maximum values when the size of the plastic zone is equal to the thickness of the adhesive bondline.

Trantina (Trantina 1972) applied fracture mechanics to adhesive joints with some success and applied the failure criteria to the finite element model to find out the adhesive fracture energies. The influence of the bondline thickness was not accounted for. Hu (Hu 1992) used a shear lag analysis and applied failure criteria in terms of J-Integral ad it was shown that this gives a good prediction of failure and was not able to account for adhesive thickness. This is considerably a good method of predicting failure for adhesive materials loaded in shear.

Fracture Mechanics based approach can also be applied to continuous materials which do not contain cracks as various authors have studied the stress intensity at the bi-material interface which are present in adhesive joints. Gradin and Groth(Gradin 1984) applied fracture mechanics method to a non-cracked specimen in cleavage tests and finite element methods were used to find a factor of stress intensity at the onset of fracture and were then used to predict failure with an accuracy of 10%. Groth applied the same method to single lap joints without fillets and the stress intensity factors was shown to be independent of the

bondline thickness and the overlap length. This work was again extended by Groth to model the joints including fillets and he noted that the criterion was only accurate in predicting the strength of the joints with long overlap lengths. All the above work done was elastic analyses.

Crocombe et al. (A. D. Crocombe 1990) used a combination of fracture mechanics and finite element method to predict failure in cleavage under Mode I loading to within 7% of the actual joint strength. This work was only applied to a narrow range of joints, however, and further work is needed in order to assess whether a more generally applicable theory can be developed.

An alternative method was developed by Fernlund et al. (Fernlund 1994) whereby a fracture envelope is generated for a particular adhesive system of energy release rate versus mode of loading. This method accounts for materials and geometric parameters, such as adherends and adhesive thickness. The envelope was found by loading a double cantilever beam specimen with a specially designed test rig. Various joints configurations were testes and analysed using closed form solutions to give a joint's mode ratio, between Mode I and Mode II loading, and the energy release rate. This prediction is then compared with the fracture envelope to ascertain whether failure will take place via propagation of crack in the adhesive bondline.

Another recently used approach the study of failure mechanism in adhesive bonded joints is the damage modelling. Damage mechanics is the mean of including the decrease in mechanical properties which occur on the failure of adhesives and can be achieved by including softening of the material which initiates at some critical stress. This approach was firstly used by Crocombe et al (A. D. Crocombe 1990) by modelling the softening(damage and crack initiation) with spring elements within the finite element mesh which are activated when the stress in the surrounding material is high enough. This gives predictions which can be related to the fracture mechanics based method. To date this method of simulating damage has not been applied to simulating material, and plasticity has also not been included.

Ashcroft and Critchlow et al. (Ashcroft 2010) proposed a unified model to predict the fatigue behavior of adhesively bonded joints. Their proposed model is based

on the damage mechanics approach, wherein the evolution of fatigue damage in the adhesive boned joint is defined by a power law function of plastic micro strain. They have simulated the three dimensional damage evolution and crack propagation using the above proposed method. It has been shown that a damage progression law governed by equivalent localized plastic strain can be used as a unified method to predict all the major parameters associated with fatigue in bonded joints. In this unified method, as the damage is controlled by localized equivalent plastic strain induced in the adhesive layer as a function of loading, there is no need to specify an initial flaw or the crack path through the adhesive. Hence, this method is versatile and potentially can be used to predict the variable amplitude fatigue and combined creep fatigue with little modifications.

3.8 CHAPTER SUMMARY

It is clear from the above literature review that most of the design rules and assumptions used in theoretical models for adhesive joints are drawn from single lap joint analyses that have received so much attention over the last century. The understanding of the mechanical properties of the adhesives is very important considering its widespread use throughout industries. The following points can be drawn from the above review:

- Finite Element Method (FEM) provides the most detailed method of analysing bonded joints. The only main disadvantage of this method is how to treat the stress singularity at bi-material interfaces.
- The various features omitted in analytical analysis to enable closed form solutions to be obtained have a little effect on the final accuracy of the solution.
- The only advantage of closed form solution is the avoidance of stress singularities across the crack tip.
- Also, there is abundance of literature pertaining to the absolute fatigue life of bonded joints.
- Damage mechanics is seen to be a promising area in which accurate methods of failure predictions may be developed, but to date only little work has been published in its application to bonded joints.

- Fracture mechanics offers a powerful tool to characterise failure of both monolithic materials and bonded systems.
- Fracture mechanics can be also be used to predict the crack propagation in monolithic materials and also, can be applied to adhesively bonded joints with reasonably good success for characterising the critical and subcritical debonding.
- This approach can also be used effectively to calculate the fatigue crack propagation rates in bonded joints and also in obtaining the crack propagation curves for the same in conjunction with finite element damage models of bonded joints. This would be contributing towards the development of a methodology to obtain the fatigue crack propagation curves by combine the fatigue test results with the results of finite element models of bonded joints.

CHAPTER 4

FATIGUE TESTING AND RESULTS OF SINGLE LAP SHEAR AND T-PEEL BONDED JOINTS

4.1 INTRODUCTION

The initial aim of the project was concerned with the investigation of a mathematical method to calculate the fatigue crack propagation rates for adhesively bonded joints. This aim was achieved by testing pretreated single lap shear and T-peel bonded joint configurations followed by developing finite element based two dimensional models of the same tested joint configurations. This chapter describes the method, equipment and procedures used during the experimental testing of bonded joints carried out in the materials testing lab.

The testing was conducted in two stages. The first step was to manufacture the adhesive bonded coupons for testing. It was decided to prepare the bonded joints with known crack lengths (precracks) so that they could be correlated and combine with the results of finite element models. The precracks were introduced in the pretreated joints by using PTFE film.

The second stage was to test the adhesively bonded joints on an Instron fatigue frame fitted with a 10kN load cell. The stiffness results obtained from the fatigue test data was then combined with the stiffness results of the finite element models to calculate the fatigue crack propagation rates and obtain the crack growth curves for single lap shear and T-peel bonded joints. As the testing proceeded, the experimental plan underwent some alterations like changing to more stiffer testing grips and displacement measurement using a strain gauge across the width of the specimens for better stiffness correlation.

4.2 ADHESIVE JOINT PREPARATION

This section addresses the bonded joint preparation required to test and obtain the fatigue test data to calculate the fatigue crack propagation rates**.** The bonded joint preparation involves material selection for adhesives and adherends, geometry of the adherends employed, method of pretreatment used and curing of the joints. Surface cleaning and pretreatment is the most important step since it

directly effects the results. Some of the key factors in the adhesive joints preparation are listed below:

- Adherend properties (material, alloying elements, sheet thickness, etc)
- Adhesive properties (adhesive type, bulk adhesive properties, etc)
- Adherend preparation (surface preparation, pretreatment, etc)
- Bonding method (bondline thickness control, environmental conditions, etc)
- Cure cycle (curing technique, pressure, etc)

The basic process of manufacturing bonded joints involves the following steps:

- Cleaning of the pretreated coupons.
- Applying PTFE tape.
- Applying adhesive and
- Curing of the adhesive in an oven.

4.2.1 MATERIAL CHARACTERIZATION

ADHESIVE USED: The structural adhesive, Betamate Epoxy 4601, from Dow Automotive was used to manufacture the adhesive joint samples with material aluminium alloy 5754 (AA 5754) and were used to manufacture single lap shear and T-peel bonded joints. This adhesive is widely employed in automotive industry due to its high strength, good moisture resistance and good degradation resistance and Oil absorption for use on oily surfaces. It is a one part, high performance, heat curing epoxy adhesive, which has a manufacturer recommended curing temperature of 108 to 150^0C @ 5 minutes wet out and 170 to 200^0C@ 15 minutes wet out. Betamate 4601 is resistant to degradation and substrate corrosion on environment aging. It also has high sag resistance, high wash-off resistance and exceptionally high peel strength (8750N/mm). The nominal thickness of the adhesive film employed is 0.25mm and shelf life of this adhesive is dependent upon the storage temperature of the material. Shelf stability is assured for 180 days from the date of shipment when stored according to storage requirements (***Dow Automotive 2008***).

Table 4.1 summarizes the features of epoxy adhesive 4601.

Table 4-1: Mechanical Properties of Epoxy 4601

Properties	Value
Peel Strength	8750 (N/mm)
Solid Content, WT%	>99
VOC, Wt %	<1
Flash Point	>300 (150)
Nominal Cure	180^0 C / 30 min
Tensile Strength	60 MPa
Young's Modulus	3500 MPa
Lap Shear Strength	23.9 MPa
Elongation at Break	5%
Poisson's Ratio	0.45

ADHERENDS USED: Single lap joints and T-peel bonded joints were used to investigate the methodology in this research. Single lap joint and T-peel joint configuration closely represents many joints found in industry and is economical to manufacture and test. The adherends used to manufacture T-peel and single lap shear bonded joints were aluminium alloy 5754 (AA5754). This alloy comes under the category of Al 5xxx alloys. Magnesium is the major alloying element of this alloy. Manganese (Mn), chromium (Cr), titanium (Ti), vanadium (V), beryllium (Be) and gallium (Ga) may be added to the alloys of 5xxx series as minor alloying elements. Aluminium magnesium alloys are non heat treatable and may be strengthened by the strain hardening. Effectiveness of strain work hardening increases when magnesium content is increased. Alloys of this series have moderate to high mechanical strength combined with high ductility and good corrosion resistance (***Callister 2007).***

The typical composition of AA5754 is summarized in table 4.2.

Table 4-2: Typical composition (in weight percent) of AA5754 Aluminium Alloy (Callister 2007)

Magnesium	Manganese	Iron	Copper	Silicon	Aluminium
3.2%	0.25%	0.20%	0.10%	0.10%	Balance

4.2.2 ADHERENDS GEOMETRY

Once the material is selected, the next step is to determine the joint geometry according to the configuration and adherend thickness required. The aluminium sheet thicknesses employed in T-peel and single lap shear bonded joints were 2mm and 3mm. The guidelines for preparation of the single lap joints and T-peel bonded joints is given in BS ISO 4587:2003 (BIS 2003) and ISO 8510-1:1990 (ISO 1990). The geometry of single lap shear and T-peel bonded joints employed is shown in figure.4.1 and 4.2 . 23mm panel overlap size was used in these joints because this size is typically employed for aluminium car body design featuring self piercing rivet joints.

Figure 4.1: Geometry of T-peel joint (All dimensions are in mm) (MTARG 2010)

These images have been removed

Figure 4.2: Geometry of single lap joint (All dimensions are in mm) (MTARG 2010)

4.2.3 BONDED JOINTS FABRICATION

It was decided to obtain the fatigue test data of pre-cracked T-peel and single lap shear bonded joints to calculate the fatigue crack propagation rates and obtain the crack growth curves. Aluminium sheets were available in both PT2 silica pretreated and phosphoric acid anodized pretreated sheets. It was also decided to see the effect of pretreatment methods on the failure of the joint, hence adherends used for single lap shear joints were PT2 silica pretreated and T-peel joints used were Phosphoric acid pretreated (PAA) (**The theory behind both of these pretreatment used is described in section 2.5 of chapter no 2**).

To correlate and combine the fatigue testing results with finite element modelling results of bonded joints, it was decided to prepare the bonded coupons with different cracks lengths by using PTFE (Poly-Tetra Fluoro-Ethylene) tape of known converge . The precrack lengths employed in these joints were are 3.0mm, 5.0mm, 7.0mm and 9.5mm measure from the edge of PTFE tape on a normal joint with 1.0mm of PTFE. The aluminium sheet thicknesses employed in these joints were 2.0mm and 3.0mm. The overlap length used in these joints was 23 mm (See figure 4.1 and 4.2).

4.2.3.1 PREPARATION OF T-PEEL BONDED JOINT

The aluminium sheets to prepare T-peel bonded joints were PAA pretreated. Hence, there was no need for cleaning the surface of the sheets. The process of making T-peel bonded joints starts with setting the proper fixture at the edge of the table as shown in figure.4.3.

Figure 4.3: Fixture used for T- peel joints (P.Briskham 2010)

Two holes were drilled 10mm to 10.2mm from the end of each edge (27mm max from each edge) of each sheet. To hold the sheets firmly, a metallic strip was inserted on to the sheets that works as a spacer. The sheets were clamped by using G-clamps which ensured that the front face of the fixture remains parallel to the sheets (figure. 4.5). PTFE tape was then applied across the fillet of the sheets as shown in figure.4.4.

These images have been removed

Figure 4.4: Applying PTFE tape across the fillet of T-peel bonded joint (P.Briskham 2010)

Figure 4.5: Clamping the aluminium sheets with G-clamps (P.Briskham 2010)

The next step is then to put the bead on the adhesive on the sheets. The epoxy adhesive is very sticky and viscous in nature. Like other fluids, the adhesive becomes less sticky, if it is heated and hence, it was necessary to heat the high pressure glue gun with the help of the blower as shown in figure.4.6. After heating the glue gun, the adhesive was then put on the sheets by keeping the sheets in one line. To induce precracks in these joints, the adhesive bead was not put on to the PTFE tape starting from its edge equal to the precrack length, i.e. to have a 3.0mm precrack, the adhesive was only put in 20mm overlap length of the joint (23 - 3 = 3.0mm). The similar procedure was followed while introducing other precracks, i.e. 5.0mm, 7.0mm and 10.0mm.

These images have been removed

Figure 4.6: Heating of the glue gun before applying adhesive on the sheets (P.Briskham 2010).

After applying the adhesive, the sheet was clamped on a flat aluminium sheet with the help of clips. The short ends of the joints were then clamped with G-

clamps which provide an extra pressure on adhesive to flow uniformly in each direction. However, care must be taken in putting too much pressure which can dislocate the sheets and PTFE tape resulting into poor quality of the joint. The final assembly of T-peel bonded joints for curing is shown in figure.4.7.

(a) (b)

Figure 4.7: Final assembly of T-peel bonded joints for curing (P.Briskham 2010).

4.2.3.2 PREPARATION OF SINGLE LAP SHEAR BONDED JOINTS

As the name suggests, lap shear bonded joints is made by lapping one sheet on other. The fixture used for lap shear bonded joints is made up of a plate and a couple of spacers attached with it (see figure. 4.8). The aluminium sheets used to prepare these joints were pretreated by PT2 silica pretreatment.

This image has been removed

Figure 4.8: Fixtures used for lap-shear bonded joints (P.Briskham 2010)

Two holes were drilled 10mm to 10.2mm from the end of each edge (27mm max from each edge) and then the two holes of the sheet were aligned in such a way so that are lined up and no rotational loads were induced while testing the same joints. The next step is to apply the PTFE tape. For applying PTFE tape, the other fixture is used which is made up of a flat plate and a strip as shown in figure.4.9. The strip is 21.5mm wide (20mm bond-width + 1.5mm overlap).The PTFE tape can be put on the sheet by inserting it under the strip. In lap shear joint, the PTFE tape should be applied on both of the sheets to maintain the bondline thickness. PTFE tape is used to ensure that the excessive adhesive coming out of the joint does not stick with fixture while curing.

Before applying the adhesive, one of the sheets was joined with a fixture using M10 bolt, a washer and a nut. The epoxy resin 4601 was then squeezed out of a tube using a high pressure glue gun along the overlap region on one of the sheets. The other sheet was then placed on the top with the drilled holes aligned. The extended slot on the other side of the fixture is to attach the upper sheet and is useful to move the upper sheet for adjusting the overlap length while joining (figure.4.10). The sheets can then be fasten with the help of bolt, washer and nut. Bull dog clips were placed to apply a downward pressure on the sheets, which squeezes the adhesive out through the edges of the overlap region as shown in figure.4.11. The excessive adhesive, which was outside of the overlap region,

was then removed and the adherends were then held together by clips for the duration of curing. The final assembly for curing is shown in figure.4.12.

Figure 4.9: Applying PTFE tape on single lap shear adherends (P.Briskham 2010).

These images have been removed

Figure 4.10: Coupons fastened with fixtures and adhesive is applied after putting PTFE tape (P.Briskham 2010).

Figure 4.11: Applying clips and G-clamps to put extra pressure on bonded sheets (P.Briskham 2010)

These images have been removed

Figure 4.12: Final assembly of lap-shear bonded joint for curing (P.Briskham 2010)

4.2.4 CURING OF THE JOINTS

After joining the sheets of single lap shear and T-peel bonded joints, the joints were then cured in an oven as shown in figure.4.13. A preheating was required at a curing temperature for about 20 minutes. Curing was carried out by heating the

joints at 180^0C for 2 hours. The joints were then stored until the testing was carried out. The bondline thickness formed in adhesive bonds was 0.25mm.

Figure 4.13: Oven unit showing controls (P.Briskham 2010).

4.3 FATIGUE TESTING OF T-PEEL AND SINGLE LAP SHEAR BONDED JOINTS

This section describes the testing work conducted on T-peel and single lap shear bonded joints to obtain the fatigue test data. As mentioned earlier the testing was carried in two stages.

The first stage was to prepare bonded coupons (T peel and lap shear) with predefined crack lengths. The main reason of including pre-cracks in bonded joints was to record the crack propagation in the adhesive. The predefined crack lengths employed were 3.0mm, 5.0mm, 7.0mm and 9.5mm and was introduced in these joints by using PTFE film coverage.

The second stage was to test these joints on an Instron fatigue frame fitted with a 10kN load cell. The machine used for the fatigue tests was a servo-hydraulic dynamic testing machine having a load capacity of 10kN interfaced to a computer for machine control and data acquisition.The testing was conducted under ambient conditions of 23^0 C and a schematic of the testing arrangement is shown in figure.4.14. All the tests on T-peel and single lap shear was run at a frequency of 10Hz using an R-ratio of 0.1 (*where* $R=P_{min}/P_{max}$ *and* P_{min} *and* P_{max} *are the*

minimum and maximum loads applied over the fatigue cycle respectively) and fatigue test data was generated for T-peel and single lap shear joints. A small load was applied to all of the bonded coupons to ensure that adhesive doesn't crack during stiffness measurement. The load used during the test was chosen in such a way that it lies below the threshold of adhesive. As soon as the load reaches the adhesive level, the crack starts growing into the adhesive and the joint finally separated out. A minimum of three crack lengths were used in the test in order to get a good curve fit. Each crack propagation was recorded using a 4 megapixel USB microscope at a rate of 15 frames per second. The experimental results of bonded joints were used to analyse and combine with the stiffness results of damage models to calculate the fatigue crack propagation rates and fatigue propagation curves.

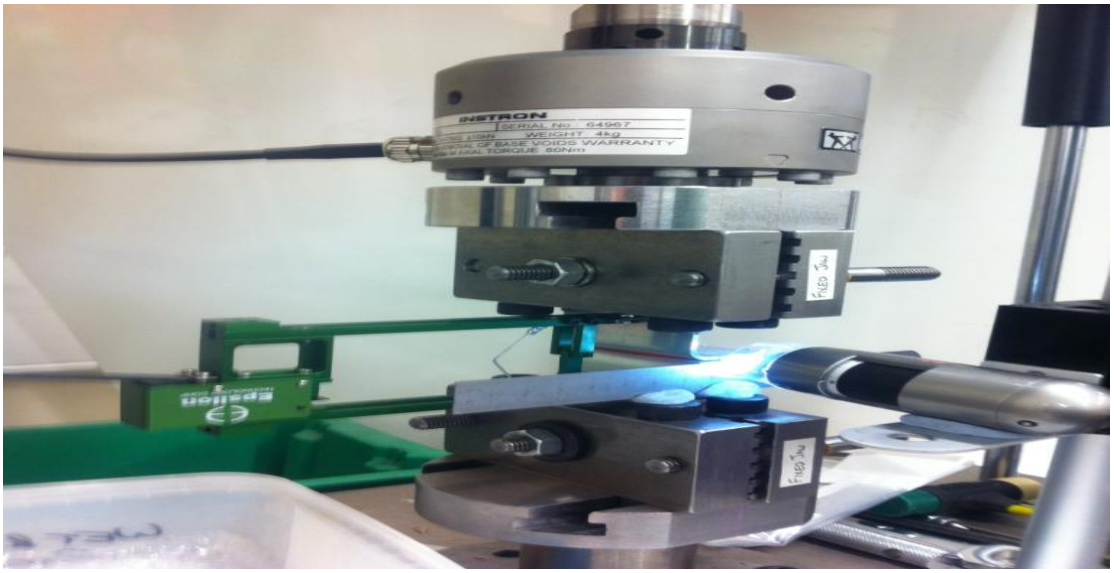

Figure 4.14: Schematic diagram of the fatigue load frame used to test adhesive joints

4.3.1 FATIGUE TESTING AND RESULTS OF T-PEEL BONDED JOINTS

The following section provides details about the fatigue test conducted in material lab for T-peel bonded joints. Peel joints with different sheet thickness were employed and tested to obtain the fatigue test data. The sheet thicknesses employed in these joints are 2.0mm and 3.0mm. These joints were designated as T22B, T33B and T23B joints. The testing of each joint with the results is described below.

4.3.1.1 FATIGUE TESTING AND RESULTS OF T22B JOINTS

The tests of these joints were started by finding a load level which is just below the threshold needed to grow the crack into the adhesive, in order to determine a load level that is just enough to grow the crack**.** The precracks employed in these joints are 3.0mm, 5.0mm, 7.0mm and 10.0mm.

Some precracked samples of T22B joints were ran for about 3000 to 5000 cycles at the same load level without growing the crack into the adhesive. The load displacement data recorded for these test were useful for obtaining the stiffness values for each crack length. These joints were regarded as no run to failure joints (NRTF) under the obtained curves.

The same joints tested above were run at a higher load above the threshold level to achieve crack propagation and fails the joint. On these tests, the crack started growing as soon as the higher load was applied; even the load applied was 0.1kN higher. The joints tested under these loading conditions were marked as run to failure (RTF). This data was useful in calculating the stiffness values from the points where displacement starts to change and crack starts growing the adhesive. The surfaces failed under these tests are all cohesive. Figure.4.15 and 4.16 shows displacement cycles curve of T22B joint recorded in an Instron fatigue testing machine for 10.0mm and 3.0mm pre crack.

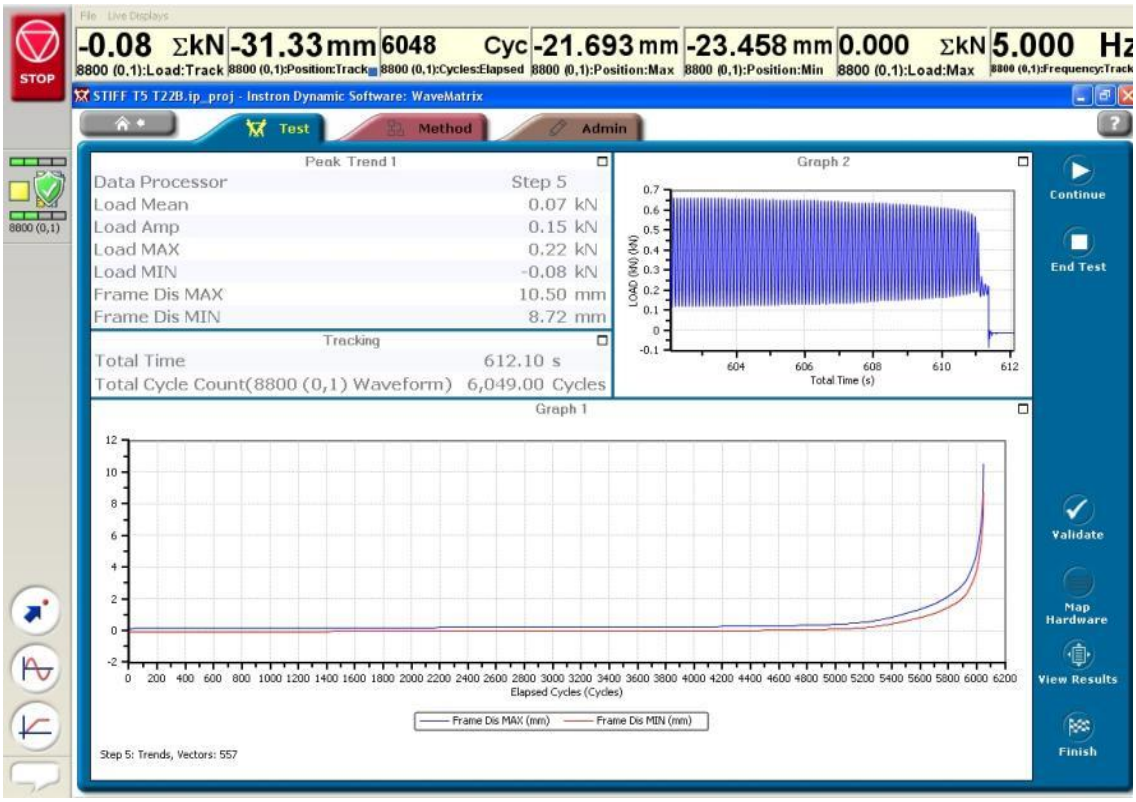

Figure 4.15: Displacement cycles curve of T22B joint with 3.0mm pre-crack

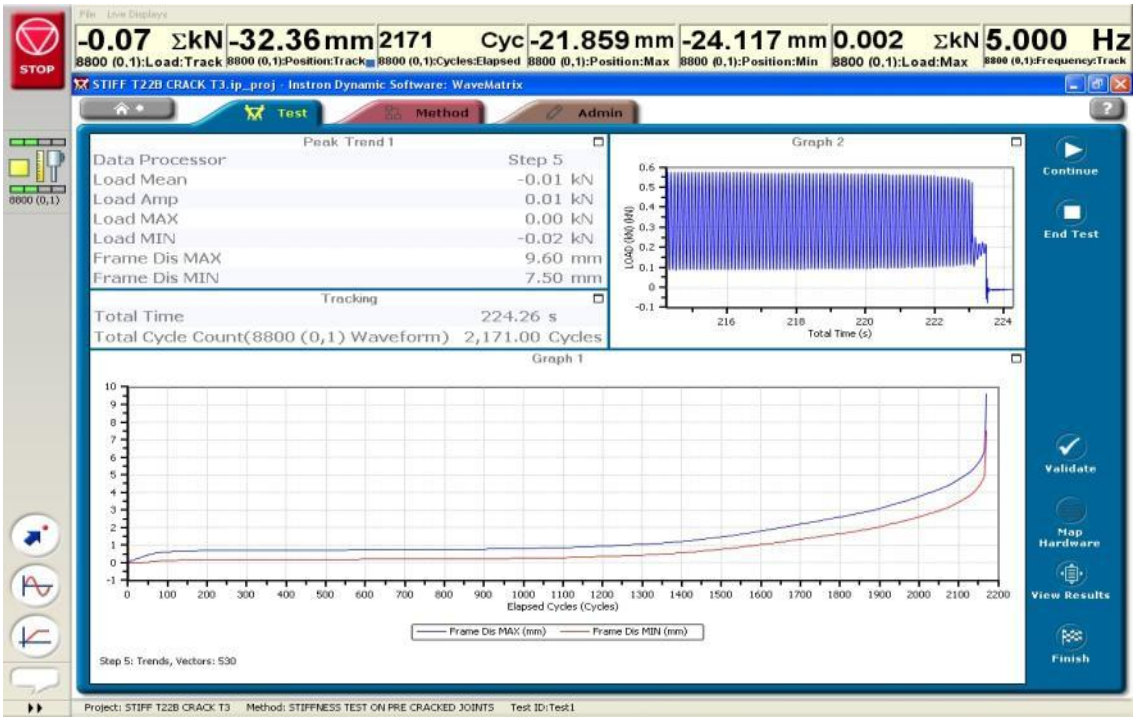

Figure 4.16: Displacement cycle curve of T22B joint with 10.0m pre-crack

The fatigue test results of T22B joints are given in table 4.3.

Table 4-3: Fatigue test results of T22B joints

S No	Joint Configuration	Precrack Length(mm)	Load Applied(kN)	Cycles to Failure(N)
1	T22B	3mm Precrack	0.6 to 0.7kN	6, 049 cycles
2	T22B	5.5 mm Precrack	0.6 to 0.7kN	6,000 cycles
3	T22B	7mm Precrack	0.6 to 0.7kN	5,568 cycles
4	T22B	10mm Precrack	0.6 to 0.7kN	2,171 cycles

4.3.1.2 FATIGUE TESTING AND RESULTS OF T33B JOINTS

T33 joints were tested in this research work using 3.0mm, 5.0mm, 7.0mm precracks length and joint with no pre-crack length in it. These joints were tested at different load levels for the crack propagation inside the adhesive film.

4.3.1.2.1 T33B JOINT WITH NO PRE-CRACK LENGTH

T33B joint with no pre-crack length was fatigue tested at the load level of 1.1kN and failed in a pure cohesive mode as shown in figure.4.17. This image shown is the scanned image of the failed joint. The cycles to failure for this joint were recorded at 666,738 cycles.

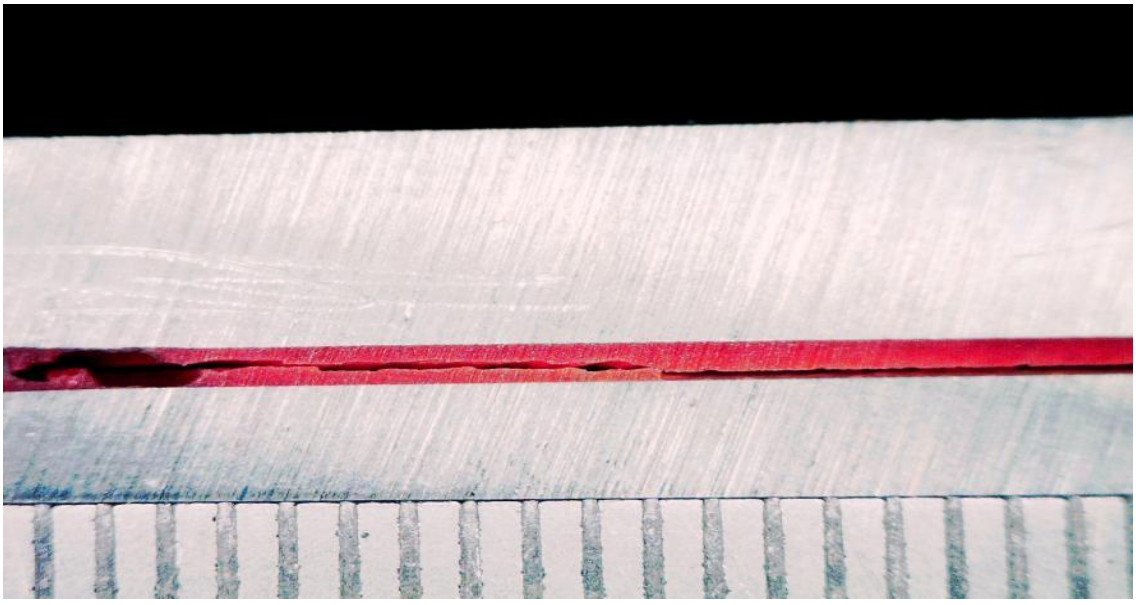

Figure 4.17: Cohesive failure of the adhesive observed in T33B joint with no precrack.

4.3.1.2.2 T33B JOINT WITH 3.0mm PRE-CRACK LENGTH

This joint was tested in two stages. In first stage, the joints were tested at load levels of 0.51kN and 0.6kN for two days and no crack propagation was recorded in the videos under these loads. In the second stage, the load level was increased to 1.2kN and at this load, the crack begins to propagate and finally the joint get separated at 750,255 cycles. The failure observed in this joint was cohesive failure of the adhesive bond.

4.3.1.2.3 T33B JOINT WITH 5.0mm PRE-CRACK LENGTH

This joint was tested at a load level of 1.1kN. The failure observed was cohesive and the cycles to failure for this joint were recorded at 43,059 cycles.

4.3.1.2.4 T33B JOINT WITH 7.0mm PRE-CRACK LENGTH

The joint with 7mm pre-crack was tested at a load of 1.1kN and failed at 46k cycles. The joint failed by cohesive mode within the bondline region.

The displacement cycles curve recorded during fatigue testing of 5.0mm precrack and 7.0mm precrack T33B joints are given in figure.4.18 and 4.19.

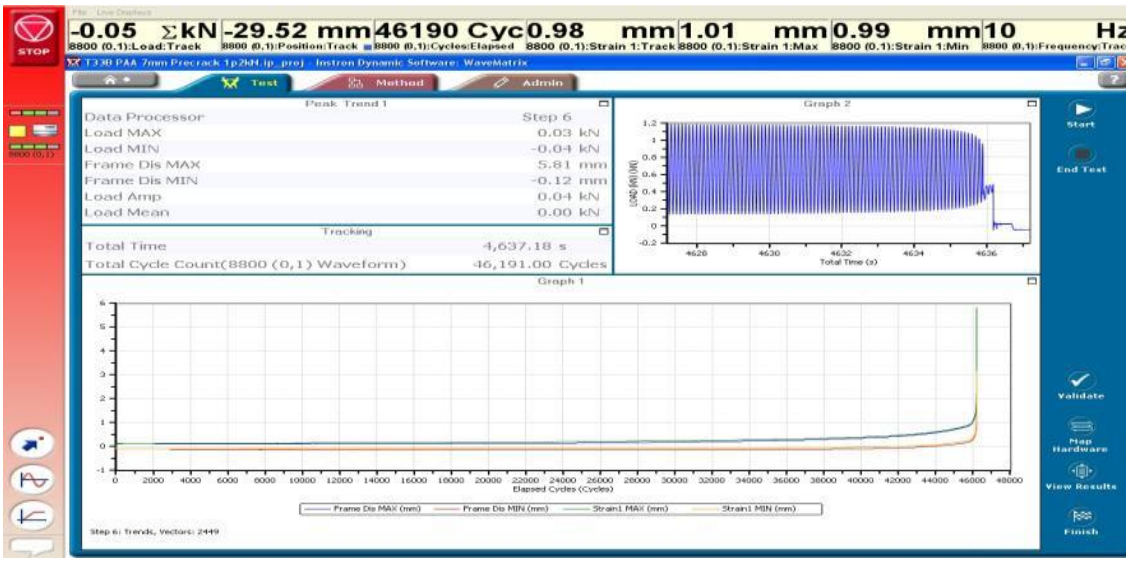

Figure 4.18: Displacement cycle curve recorded for T33B joint with 7.0mm precrack

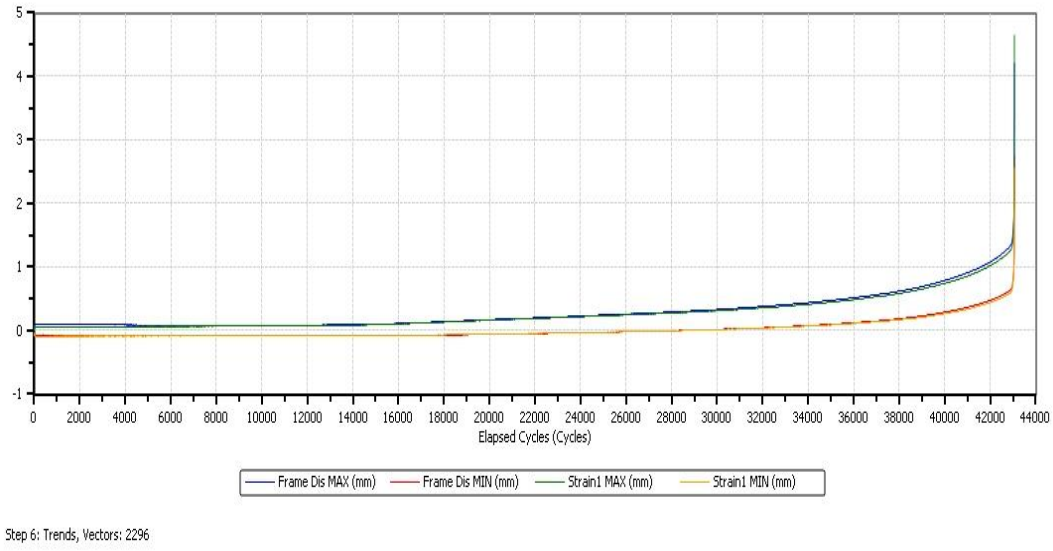

Figure 4.19: Displacement cycles curve recorded for T33B joint with 5.0mm precrack (Y axis denotes displacement and X axis denotes cycles).

The fatigue test result of T33B joints is shown in table 4.4.

Table 4-4: Fatigue test results of T33B joints

S No	Joint Type	Precrack Length(mm)	Load Applied (kN)	Cycles to Failure(N)
1	T33B	3mm Precrack	1.0 kN	750,255 Cycles
2	T33B	5mm Precrack	0.5kN	43,059 cycles
3	T33B	7mm Precrack	0.5 kN	146, 917 cycles
4	T33B	No precrack	1.1kN	666,738 cycles

4.3.1.3 FATIGUE TESTING AND RESULTS OF T23B JOINTS

Fatigue tests on these joints were conducted using precrack lengths of 3.0mm, 5.0mm and 7.0mm respectively. Crack propagation for 5.0mm joint was recorded at subsequent time intervals by using a high resolution USB microscope.

To get more accurate and detailed fatigue test data, these joints were tested at low load level of 0.51kN to 0.6kN to find a load level which lies below the threshold of the adhesive, i.e. the level was noted between 50k and 100k cycles for these joints. The fatigue tests of different precracked T23B joints are described below.

4.3.1.3.1 T23B JOINT WITH 3.0mm PRE-CRACK LENGTH

This joint was tested at a load level of 0.51kN. The joint failed under pure cohesive mode. The cycles to failure for this joint were noted at 284,720 cycles. Figure.4.20 shown the displacement cycles curve recorded during fatigue testing of this joint.

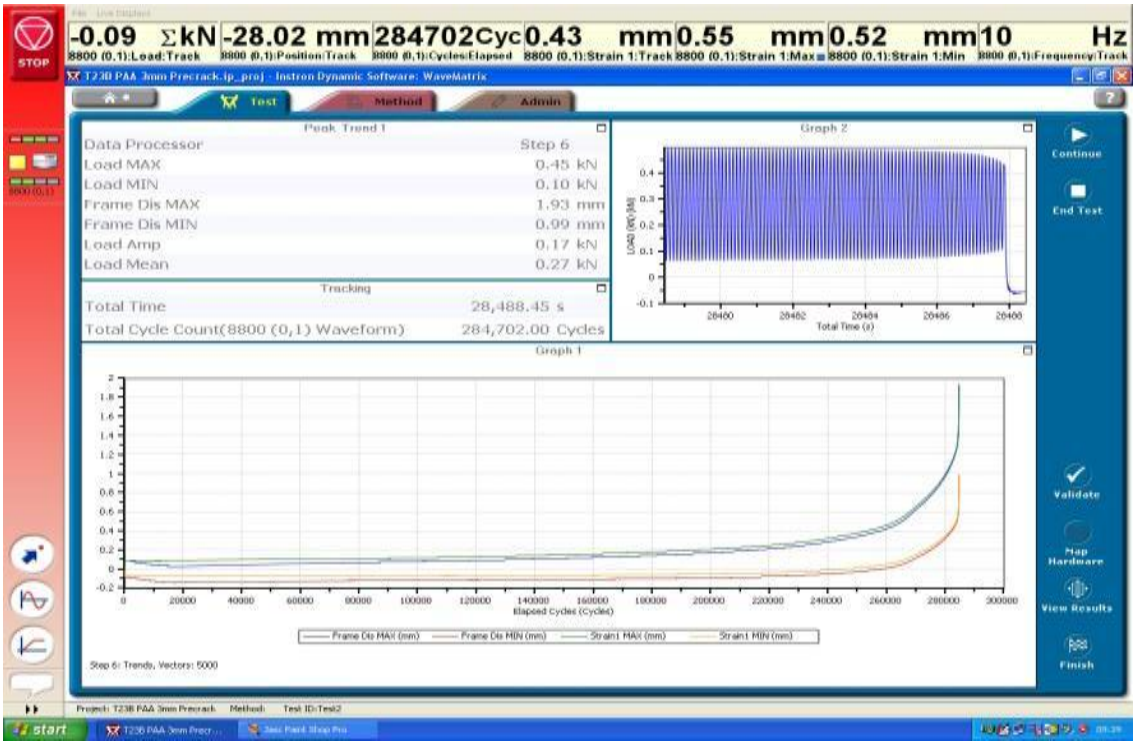

Figure 4.20: Displacement cycle curve of T23B 3.0mm precrack bonded joint

4.3.1.3.2 T23B JOINT WITH 5.0mm PRE-CRACK LENGTH

This joint was tested at load levels of 0.5kN and 0.6kN. The failure observed in this joint was interfacial as shown in figure.4.21. The image shown is the scanned image of the failed joint. The cycles to failure for this joint were noted at 874,721 cycles. Also, the crack propagation was recorded and measured at subsequent time intervals and was validated against the calculated test data.

Figure 4.21: Interfacial failure observed in T23B joint in 5.0mm precrack (scanned image)

4.3.1.3.3 T23B JOINT WITH 7.0mm PRE-CRACK LENGTH

This joint was tested by applying an axial fatigue load of 0.6kN. The joint fails by cohesive mode and cycles to failure was recorded at 146,000 cycles.

The fatigue test results of T23B joints is given in table no 4.5.

Table 4-5: Fatigue test results of T23B joints

S No	Joint Type	Precrack Length(mm)	Load Applied(kN)	Cycles to Failure(N)
1	T23B	3mm Precrack	0.51kN	284, 702 cycles
2	T23B	5mm Precrack	0.51kN	874,721 cycles
3	T23B	7mm Precrack	0.61kN	146, 917 Cycles

4.3.2 FATIGUE TESTING AND RESULTS OF LAP SHEAR JOINTS

Single lap shear bonded joints are the other configuration tested in this research work. The aluminium substrates (AA5754) used to prepare these joints was pretreated by using PT2 silica pretreatment and was cured at a temperature of 180^0 C for two hours.

Previously, due to the availability of recording the crack propagation in bonded joints, single lap shear bonded joints were tested without introducing any precracks. The aluminium sheet thickness employed in these joints was 2.0mm and 3.0mm. These joints were classified as LS22B and LS33B joints.

4.3.2.1 FATIGUE TESTING AND RESULTS OF LS22B JOINT

The first test on these joints was conducted was using LS22B joints. Two tests were conducted on LS22B joint to obtain the detailed fatigue test data. The load applied in both of these tests was 8kN. Crack propagation was recorded for both tests by using USB microscope. During fatigue testing, it was noted that the lap shear joints were subjected to shear loading across the bondline thickness, due to which opening of crack was mixed mode (Mode I + Mode II). Hence, due to this mode mixity, the failure of these joints was interfacial failure across the top sheet.

In the first joint, the crack propagated from the front side which was quite easy to record and measure. In other LS22B2 joint, the crack instead of propagating from the front propagates from the rear side of the joint as a result of which we were unable to record the crack propagation as the USB microscope was positioned in the front of the joint.

The cycles to failure from both of the fatigue test data were recorded at 55,000 cycles and 80,000 cycles respectively. Figure.4.22 shows the displacement cycle curve of LS22B joint testing (**Y axis denotes displacement and X axis denotes cycles**).

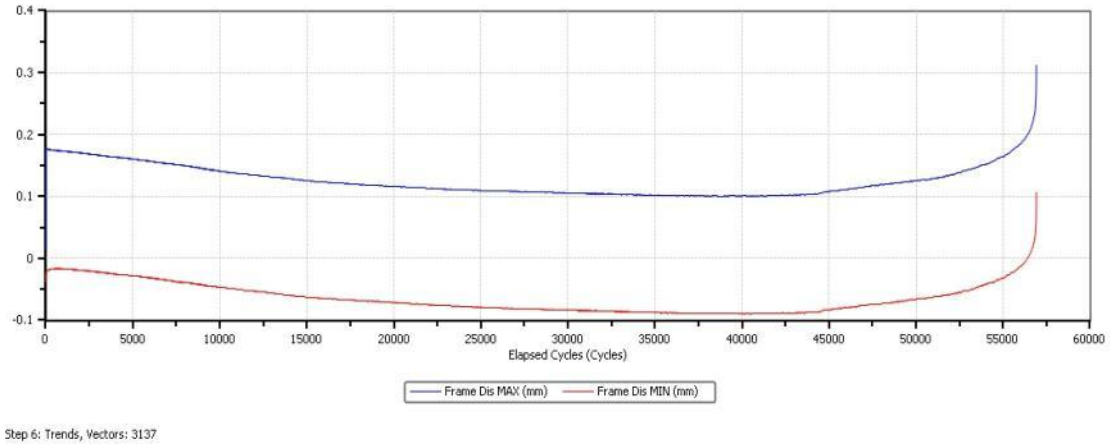

Figure 4.22: Displacement cycle curve recorded during fatigue test of LS22B joint

4.3.2.2 FATIGUE TESTING AND RESULTS OF LS33B JOINT

This is another configuration tested in this research. The joint was tested by applying a load of 9kN. The failure observed in this joint was interfacial failure across the top sheet of the joint. The cycles to failure was recorded at 37,000 cycles.

The fatigue test results for single lap shear joints are shown in table 4.6.

Table 4-6: Fatigue test results of single lap shear bonded joints

S No	Joint Configuration	Load Applied(kN)	Cycles to Failure(N)
1	LS22B	8kN	55,000 Cycles
2	LS22B	8kN	80,000 Cycles
3	LS33B	9kN	37,357 Cycles

4.4 CHAPTER SUMMARY

The fatigue tests was performed on precracked T-peel bonded joints and single lap shear bonded joints to obtain the fatigue test data, which was used to calculate the fatigue crack propagation rates in conjunction with stiffness data of FE models of bonded joints. The fatigue test performed during this research project was divided into two phases. The first phase was to prepare T-peel and single lap shear bonded joints configurations with different precrack lengths. The precracks were introduced in the joints to record the crack propagation and to get a good curve fit with at least three crack lengths. The precracks were introduced

in these joints by using PTFE film. The T-Peel adherends were PAA pretreated and lap shear adherends were pretreated by silica pretreatment. The adherends are then drilled and holes are lined up and the adhesive film was applied on the surface of the adherends and the joints are held together by bull dog clips. The joints were cured in an oven at 180^0 C for two hours and then keep it for further testing.

The second phase consists of putting the prepared joints on an Instron fatigue testing machine to obtain fatigue test data. Single lap shear joints and T-peel bonded joints are made in different fixtures and are gripped with the jaws in different alignments on the Instron fatigue testing machine. The jaws are aligned in same direction for T-peel bonded joints and in opposite direction for single lap shear joints. All the joints were tested under different loading levels and the load levels were chosen in such a way that it lies below the threshold level of adhesive. The cycle to failure for each joint were recorded from the test data and is presented in this chapter in tabular form.

The crack propagation were monitored and recorded for T33B, T23B and lap shear joints by using USB microscope during the test. The recording of the crack propagation in some of the joints were quite useful in seeing the effect of PAA pretreatment and also, the type of failure associated with particular bonded joint. It was noted from fatigue test results of the above joints that joints with small precrack length are subjected to high cycle fatigue failure (greater than 10^5 cycles) and with larger precrack length are subjected to low cycle fatigue failure.

CHAPTER 5

FINITE ELEMENT MODELLING OF ADHESIVELY BONDED JOINTS

5.1 INTRODUCTION

In order to investigate a method to obtain fatigue crack propagation rates and crack propagation curves using the finite element models and fatigue test data of bonded joint configurations, this project has developed 2D based damage models within the elastic range of the bonded coupons using standard finite element procedures in combination with fracture mechanics based computational tools. This chapter presents the FE work conducted at Jaguar Land Rover premises to enable the investigation of crack propagation methods to be carried out.

Numerical modelling of adhesive bonded joints for this project was carried out by using finite element method. The effectiveness of using finite element method has been explained in Chapter 3 of this thesis. This chapter provides several details about the modelling approaches used to develop T-peel and single lap shear bonded joints. The commercially available FE code abaqus, licensed to Jaguar Land Rover has been used at its premises to develop these models. The geometric model development, problem set up and meshing of the two dimensional models was carried out by using Altair Hypermesh as a preprocessor.

A consistent system of units based on Newton (N), millimeters (mm) and time in seconds (sec) was used. A nomenclature for using single lap joints and T peel bonded joints has been explained subsequently in this chapter. The model geometry is discretised into finite elements and the selection of finite element and meshing approaches is discussed.

5.2 GEOMETRY AND BOUNDARY CONDITIONS

The geometry and configuration of the single lap joints and T-peel joints used in this research is shown in figure 4.1 and 4.2 of Chapter 4 of this thesis and the nomenclature use to refer single lap joint geometry is shown in figure.5.1.

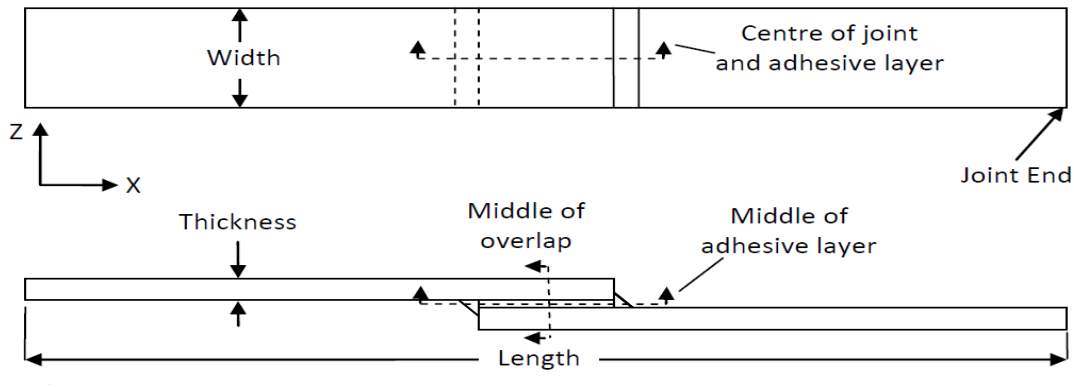

Figure 5.1: Nomenclature for different joint dimensions and geometric locations

All of the joints were based on a 23mm flange (panel overlap) size because this size is typically employed for aluminium car body designs featuring self piercing rivet joints. Symmetry in the joint geometry and loading was employed in order to minimise the computational cost of the analysis. The geometric and loading symmetries allowed for modelling of only half of the joint in 2D, which substantially reduces the analysis time. The results of two dimensional damage models of lap shear and T peel joints were post processed using Abaqus/CAE and viewer at Jaguar Land Rover.

For static loading, the boundary conditions were applied in the form of fixed displacements at the adherend edge. The boundary conditions employed in FE models is shown in figure.5.2. To ensure that the free edges of the bonded coupons remain free to strain the left hand corner of the joint is held in x and y directions and the subsequent nodes are held in y direction only. Free straining is however allowed in X direction.

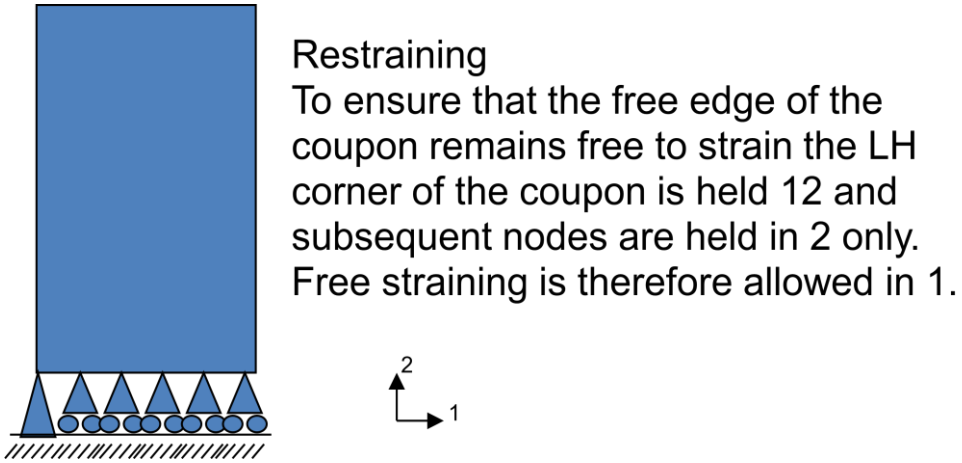

Figure 5.2: Boundary condition employed in bonded joint models (1 and 2 represent X and Y axis)

5.3 MESHING METHODOLOGY

Meshing of single lap shear and T peel joints is a challenging task due to the presence of a very thin adhesive layer compared to the overall dimensions of these joints. The addition of fillets at the end of the overlap of these joints further complicates the meshing of these joints. There are numerical singularities in the geometry of single lap shear and T peel bonded joints due to the presence of rectangular adherends and fillet corners. The selected mesh should be adequately represents the deformed as well as undeformed shape of the bonded joints.

In abaqus online documentation (Abaqus HTML Documentation Oct, 2009), two meshing approaches have been given and defined for adhesive bonded joints.

The first method is to use a continuous mesh, which may transition from the fine mesh in the adhesive bonded region to coarse mesh in the adherends region while maintaining the continuity by sharing equal number of nodes between the elements. The method of meshing the adhesives requires some partitioning of the geometry and thus each region can be meshed very easily by varying the element size in the FEA software. In the adhesive bond region, elements were placed by using *ELSET technique (keyword in .INP file) by sharing equal number of nodes in abaqus. The elements in the bonded region represent the crack length upto 9.5mm and are deleted at each and every incremental time step (Implicit FE time scheme) in the analysis. To reduce complexity in the models, the adhesive fillets were not modelled in these joints.

The second method of meshing is to use dissimilar meshes in the adhesive layer and the adherends and then to join together by using tie constraints. Tie constraints make the translational and rotational motion with all active degrees of freedom. Thus a coarse mesh can be used in the adherends and a fine mesh can be used in the adhesive layer.

The first method of meshing requires more preprocessing time than the second method. However, the use of tie constraint increased the computational time and resource requirement for an analysis as it required the enforcement of additional constraints. The first method of meshing was used to develop the damage models of single lap shear and T peel bonded joints for different sheet thickness.

5.4 CHOICE OF ELEMENTS AND MATERIAL PROPERTIES USED

The selection of the element type was based upon the response of single lap shear and T peel joint under static loading. The adherends of the single lap joint and T-Peel bonded joint experiences bending during static loading.

In abaqus for 2D analysis of damage models, plane stress and plane strain element formulation are available. Continuum quadrilaterals 2D elements were used for meshing the adherends. The main reason of using quads element is the better convergence rate as compared to triangular shell elements. Since all the damage models were modelled under plane strain conditions, the plane strain two-dimensional element, known in CPS4 element in abaqus element library has been used in meshing the adhesive bond region. The meshing of the T-peel joints and single lap shear joint was done in Hypermesh and element size of 2.0mm was used to mesh the adherends. In the adhesive bond region, very fine meshes (0.25mm) were used and are congruent meshes (matching meshes) in both of the adherends. Nominally the elements in the glue layer are 2.5 e-2 focusing down to eight collapsed quads required for these analyses of 5.4e-4 longest edge length. The plane strain elements used in damage models predicted the Von Mises stresses across in the bond line region and displacements were then calculated along Y axis to calculate the stiffness of the joints. The mesh pattern used for T peel and single lap shear bonded joints is shown in figure.5.3 and 5.4.

Owing to the bending of the joints in the adherends, conventional 2D shell elements may suffer some shear locking that generates some shear stress in the elements, resulting in a stiffer response under bending conditions than the actual stiffness of the structure. Thus, the incompatible mode elements in abaqus library were used to avoid this shear interlocking in shell elements. In addition to the standard displacement degrees of freedom, incompatible mode elements have incompatible deformation modes added internally to the elements (Abaqus HTML Documentation Oct, 2009). This reduces the computational time of the analysis.

The material properties used in FE models are given as follows:

Adhesive Properties used*:*

Adhesive Type: Betamate Epoxy 4601

Elastic Modulus: 3500 MPa

Poisson's ratio: 0.45

Adherends properties used:

Adherends Material: Aluminium

Elastic Modulus: 70000 MPa

Poisson's ratio: 0.33

Total load applied is 21.818kN per unit width; hence the total load applied in FE models was 1.2kN.

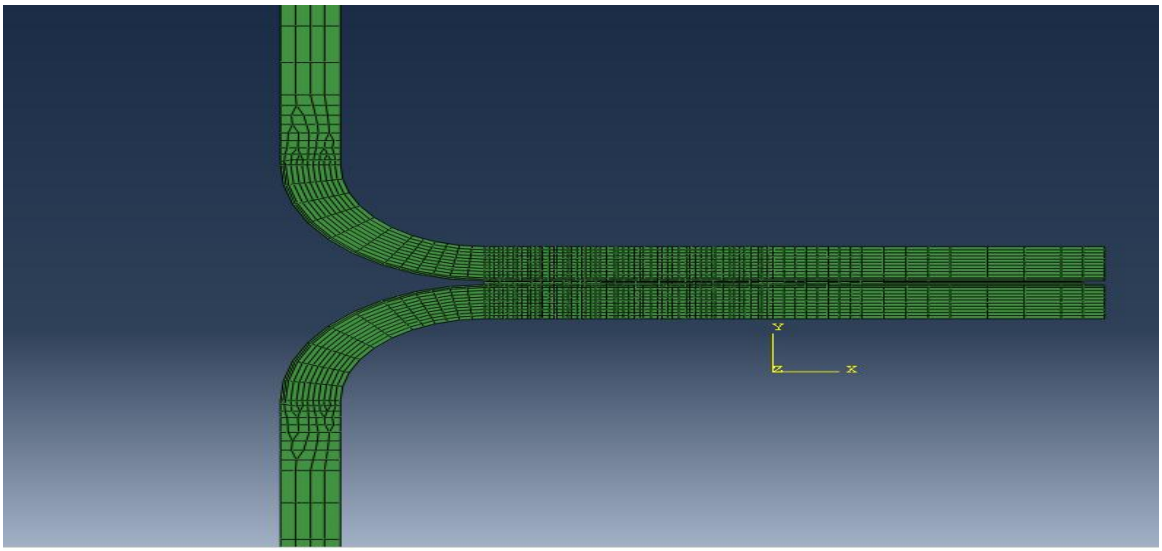

Figure 5.3: Overall detailed mesh of T peel bonded joint

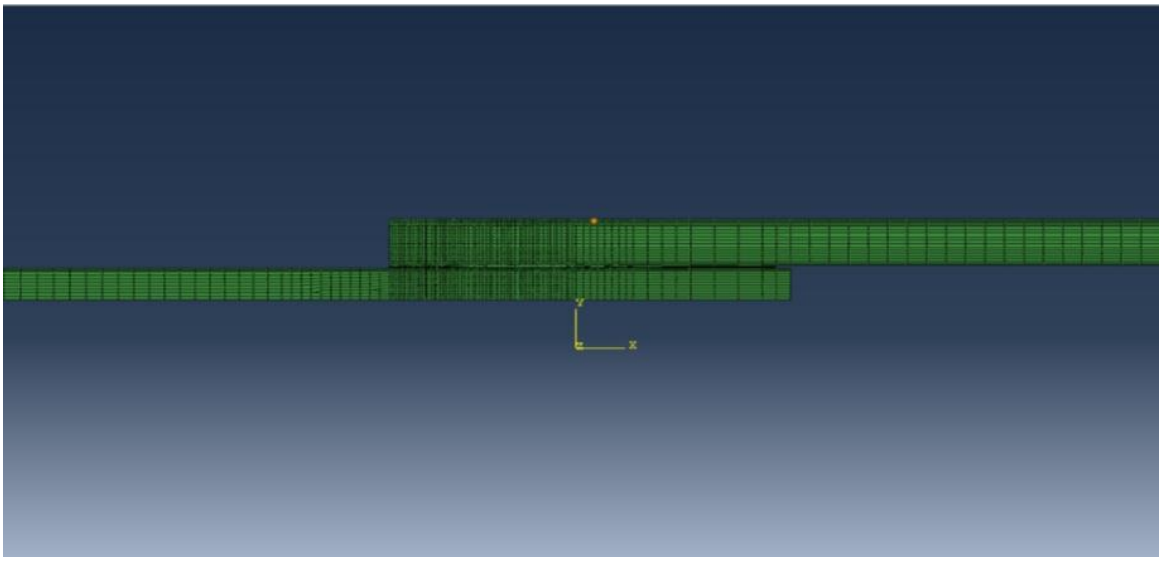

Figure 5.4: Detailed mesh of single lap shear bonded joint

5.5 FAILURE LOCATIONS MODELLED IN BONDED JOINTS

There are three possible failure locations in any adhesive bonded joints and each location were modelled separately in damage models. This possible failure includes:

- Interfacial failure at the adhesive/metal interface.
- Cohesive failure of the adhesive.
- Cohesive failure of the adherends.

Interfacial failure in bonded joints occurs at adhesive/adherend interface. This failure mode can result from either due to improper surface mismatch or by using inadequate surface pretreatment. Cohesive failure of the adhesive occurs if the crack propagates inside the adhesive layer. The crack may propagate in the centre of the adhesive film or near to the adherend interface. This type of failure is mainly a localised effect and occurs near to the ends of the joint.

For each damage models, there are three possible failure modes modelled, failure at interface 1, and failure at interface 2 or through the adhesive layer as shown in figure.5.5. There is a requirement to run the model with different crack lengths and aluminium combinations with 2 global geometry conditions, T-peel and single lap shear bonded joints.

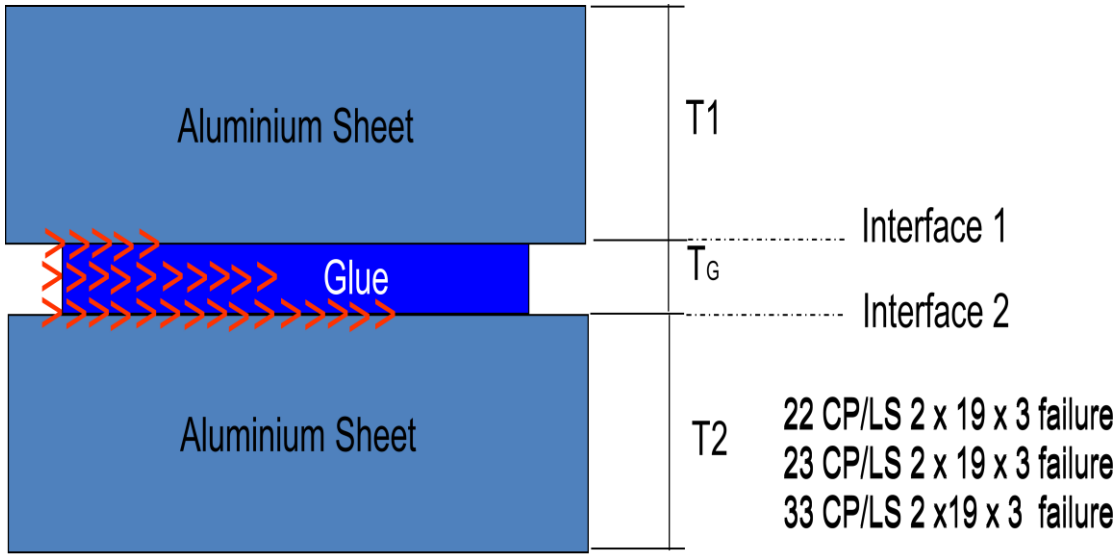

Figure 5.5: Failure locations modelled in 2D adhesively bonded damage models

5.6 MODELLING CRACKS IN BONDED JOINTS

All the damage models developed were run by using node displacement method in the adhesive region. All the models were developed as global and sub models. Element deletion technique is used in the bonded region to represent the opening and propagation of cracks. At every time step of the analysis, each element set were deleted by offsetting the nodes associated with deleted elements representing the opening and closing of cracks.

Linear elastic fracture mechanics approach is also used to extract out the energy release rates associated with each crack length. The energy release rates were extracted in form of J Integral due to its path independent nature and ease of its calculation through sub user routine program. A sub user routine program was developed by using PERL scripting language at Jaguar Land Rover premises to extract the energy release rate associated with each crack length. The Perl script developed for this process is given in appendix 1 of this thesis.

Each global model used in this research consists of 19 global steps. Each step simulates a crack growth of 0.5mm. Thus the minimum crack length used in bonded joint models is 0.5mm and the maximum crack length modelled is 9.5mm. This means that the model stops simulating the crack growth at just under half the total bond line width of 20mm. A typical global model is shown in figure.5.6.

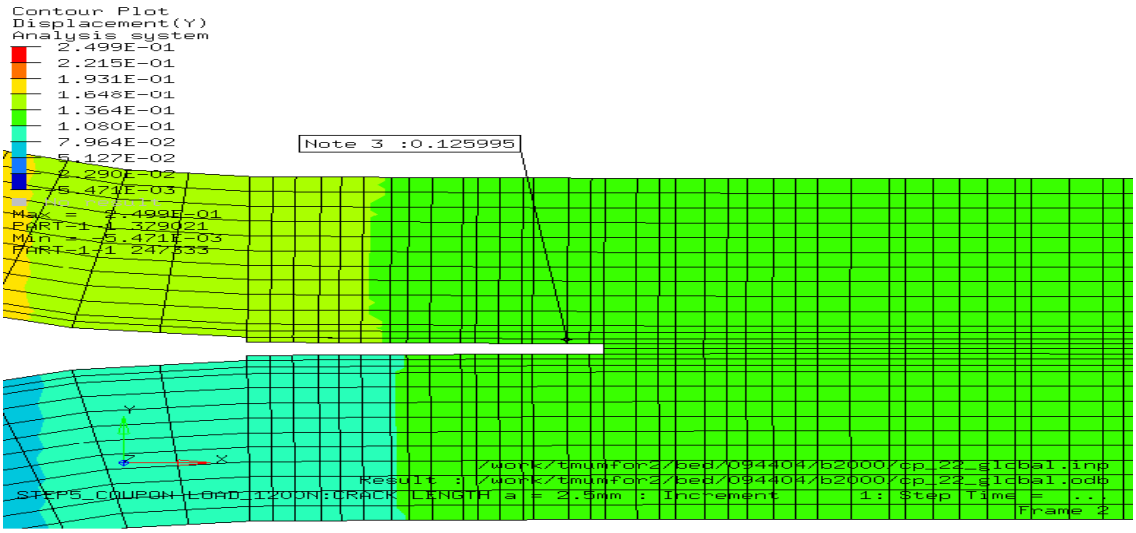

Figure 5.6: Crack modelling of bonded joints using *ELSET technique in abaqus (global model)

To extract out the strain energy release rates, submodelling approach has used to model the single lap shear and T peel bonded joints. The displacements obtained from the global model are use to drive the boundary nodes of the sub model as shown in figure.5.7. The sub model must occupy the same global physical space as the un-deformed global model. This allows abaqus to find the global nodes that can befriend those in the edges of the sub model.

From the works of Wu and Crocombe (A. D. Crocombe 1994) we can sae that some parts of the joint model are critical so cannot be modelled by simple meshing. For example, the areas close to the lap ends in the case of a lap joint. Bogdanovich and Kizhakethara (Bogdanovich 1999) suggest that these areas requires more complex meshing like a non-uniform element mesh. The newer versions of abaqus have got this procedure of sub-modelling. This is a multistep procedure where the displacement and the stresses for a successively reduced local region is calculated in several steps. The nodal displacement values in the previous step are applied as external boundary conditions for the next step so the new step should get a more accurate answer than the previous step. Sub-modelling in abaqus is used mainly for mesh modifications only; it does not affect the analysis strategy. The re-meshed local submodelling can be inserted back into the global model and the stress analysis can be performed for the full

combined model. The submodel can be redefined at any step of crack propagation analysis.

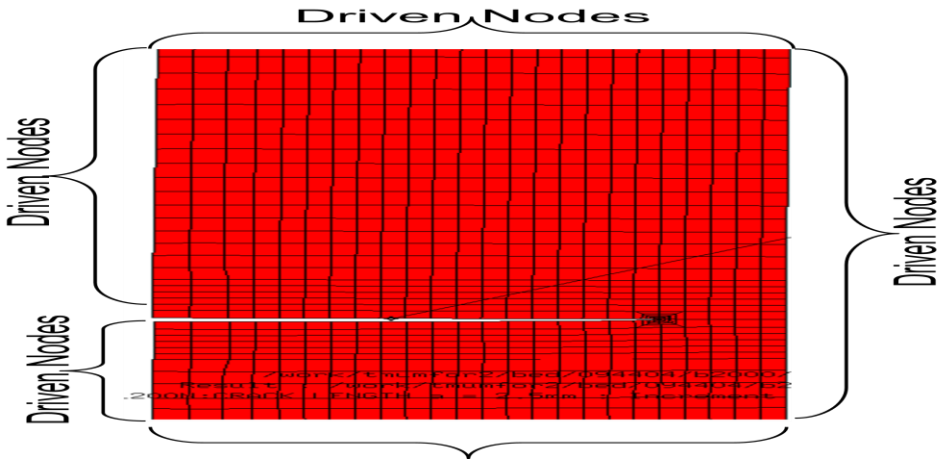

Figure 5.7: Sub-modelling approach used in local model of bonded joints

From the above explanations, the modelling methodology adopted for bonded joints can be represented in a form of a semiautomatic way of growing cracks in global model and submodel as shown in figure.5.8. This semiautomatic method also shows the method of calculating J Integrals and Stress Intensity factors. The main advantage of using this method is that many bonded joint models with many crack lengths can be run in a single submission to abaqus solver.

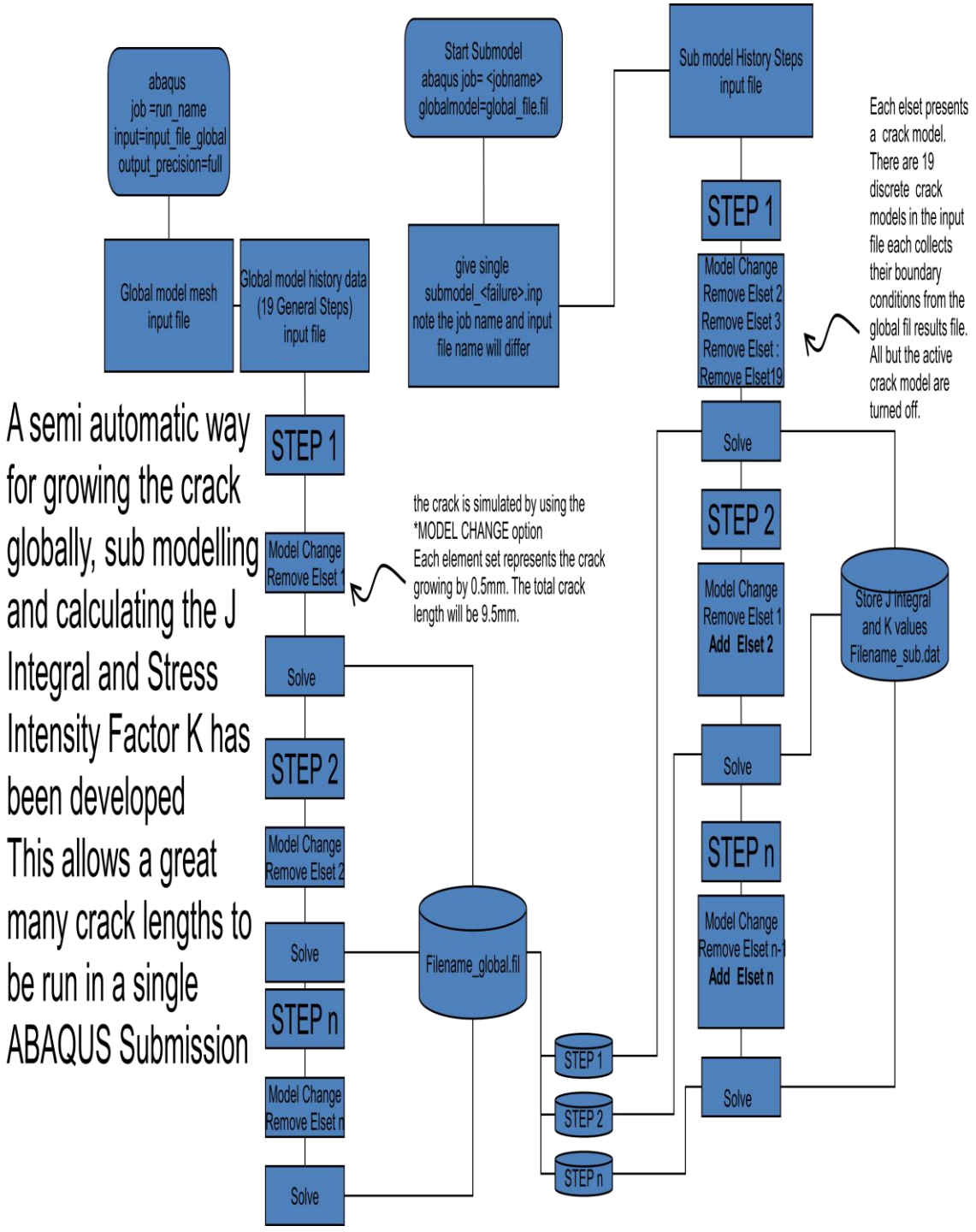

Figure 5.8: Modelling approach used to create damage models of bonded joints (developed by Tim Mumford, CAE Engineer, Jaguar Land Rover)

5.7 CHAPTER SUMMARY

This chapter explained and presented the finite element based modelling methods used to model adhesives. Since the damage models developed at Jaguar Land Rover premises were based on fracture mechanics based method,

the work presented in this chapter has shown that stress prediction is not sufficient for predicting the strength of bonded joints, but is a valid benchmark for the proposed statistical method for the predicting fatigue crack propagation in adhesively bonded joints.

CHAPTER 6

FATIGUE CRACK PROPAGATION ANALYSIS OF BONDED JOINTS

6.1 INTRODUCTION

Using the finite element modelling techniques and procedures for bonded joints described in chapter no 5 and the experimental methods with fatigue test results presented in chapter 4, the fatigue crack propagation rates were calculated and crack growth curves were obtained by using the methodology presented and explained in this chapter. The validation of the above methodology against the recorded crack propagation measurements is also presented in this chapter.

Single lap shear and T-peel bonded joints are the configurations investigated in this analysis. This chapter presents a methodology by combining the stiffness results of finite elements models with the stiffness results of fatigue test data of bonded joints to calculate the fatigue crack propagation rates.

6.2 METHODOLOGY USED

The methodology used to calculate the fatigue crack propagation rates and obtain the fatigue crack propagation curves is presented and explained in this section. Since all the damage models are modelled upto the elastic limit, hence, it was assumed that the response of the damage models is linear within the elastic limit *(within the elastic limit, stress is directly proportional to strain)*. Practically, the stiffness of any structure decreases with the crack propagation because most of the stored strain energy (stored potential energy) is used to create the new surfaces while the crack propagates.

Since stiffness is the main parameter in this method, the stiffness drops were calculated for finite element models and fatigue test data of T-peel and single lap shear bonded joints against the applied load range and the displacement range. Then the method makes the use of standard curve fitting techniques and moving averages method to reduce the scatter in fatigue test data and obtain the relation of stiffness and energy drop curves with respect to crack length in finite element models. These mathematical equations were used in fatigue test data to obtain smooth crack propagation curves for T-peel and single lap shear bonded joints.

The method of calculating fatigue crack propagation rates and to obtain the fatigue crack propagation curves includes the following step by step procedure as given below.

- Using the finite elements results of 2D damage models, calculate the stiffness of each joint by using the displacements obtained and the load applied in FE models. Using subroutine program developed my PERL scripting at Jaguar Land Rover premises, the energy release rates were extracted out in form of stress intensity factors and J-Integrals. Plot the curves of stiffness and energy release rates vs. crack length. The curves obtained for one of the joints is shown in figure.6.1 and 6.2 for illustration.

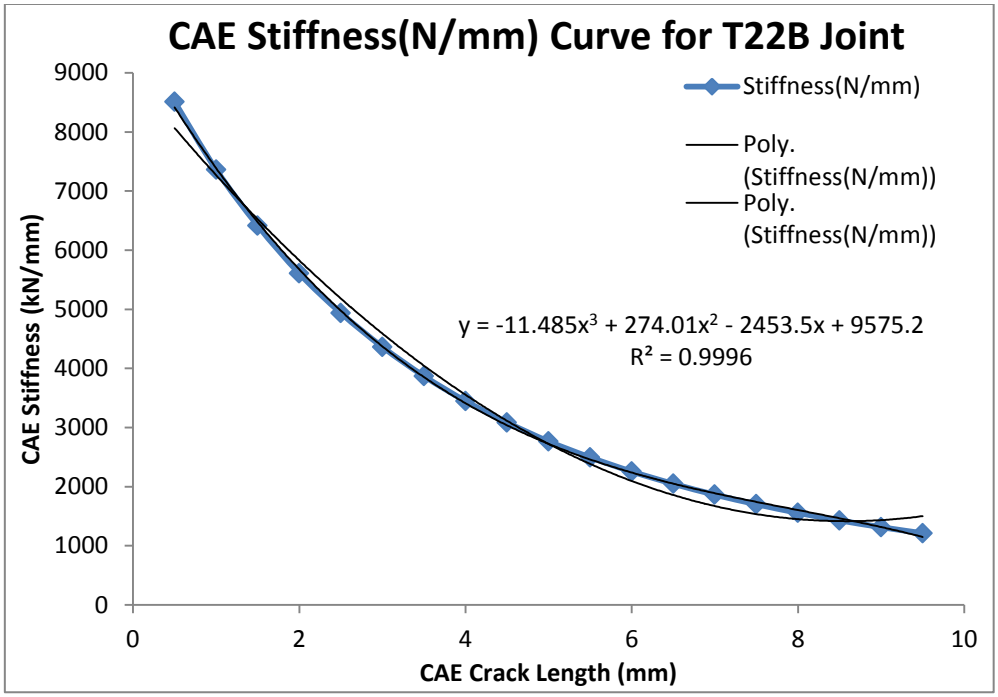

Figure 6.1: Stiffness vs. Crack length curve of T22B FE model (For illustration)

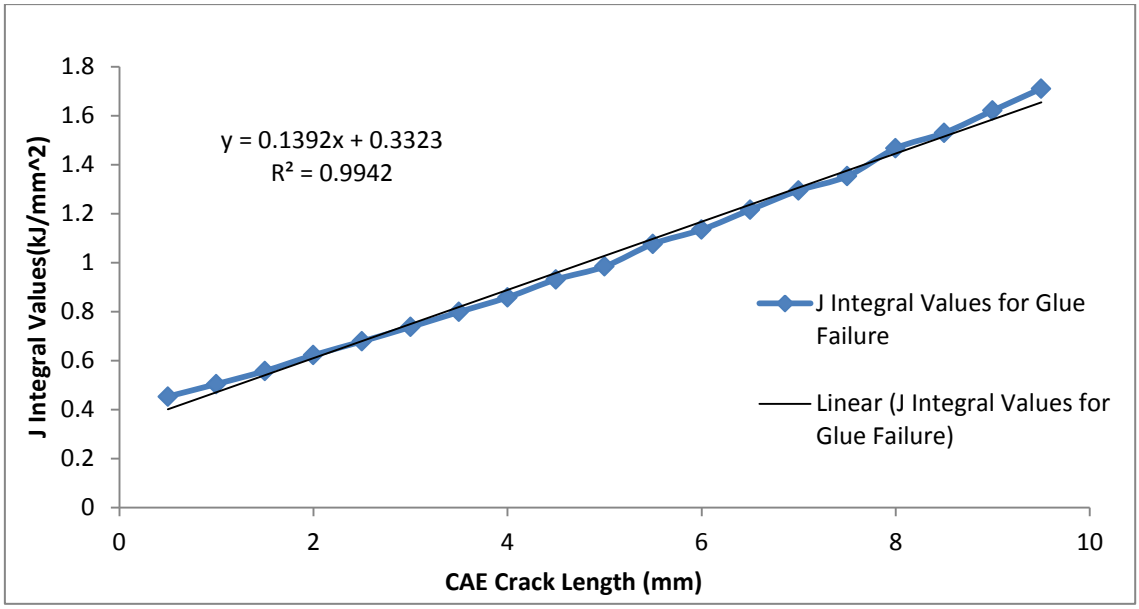

Figure 6.2: Energy release rate curve for T22B FE model

- Fit a suitable curve, i.e. power law fit (used in fatigue S-N curves) or polynomial fit in case stiffness drop curves (K. B. Davies 1973) in both of the curves (from FE models) to obtain a relationship of stiffness and energy release rate as a function of crack length. The suitability of curve fitting methods is discussed in chapter no 7 of this thesis.
- Using the fatigue test data of bonded joints, calculate the stiffness of each joint using the load range and the displacement range data. After calculating the stiffness, obtain the curve between the stiffness and the cycles to failure (N). Such a curve is shown in figure.6.3 for T33B joint.

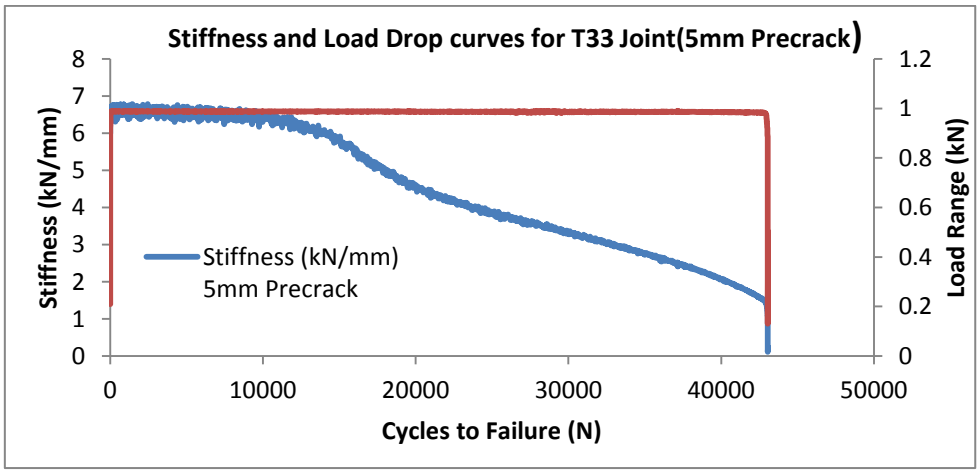

Figure 6.3: Stiffness Drop curve of T33B Peel joint from fatigue test data

- Use the equations obtained by curve fitting in FE models of bonded joints in fatigue test data and calculate the crack lengths and energy release rates for each stiffness values in test data. Take the successive differences of the crack length and cycles to failure (N) in fatigue test data and then dividing the change of crack length with change in cycles gives us the fatigue crack propagation rates on bonded joints in the fatigue test data as given below.

$$\textit{Change in crack length (da)} = a_j - a_i$$

$$\textit{Changes in cycles (dN)} = N_j - Ni$$

Where, a_i and a_j = crack length in *i*th step and *j*th step in 'mm' respectively

*N*i and *N*j = No. of cycles in *i*th step and *j*th step respectively

i = No. of experimental steps, and *j* = *i+1.*

$$\textit{Fatigue crack growth rate (da/dN)} = (a_j - a_i)/(N_j - Ni).$$

- Using the calculated fatigue crack propagation rates and cycles to failure, the curves of crack length (a in mm) vs. cycles to failure (N) and energy release rates(J) vs. cycles to failure (N) can be plotted for every fatigue test data of bonded joint. One of the obtained plots are shown in figure.6.4 and 6.5 below.

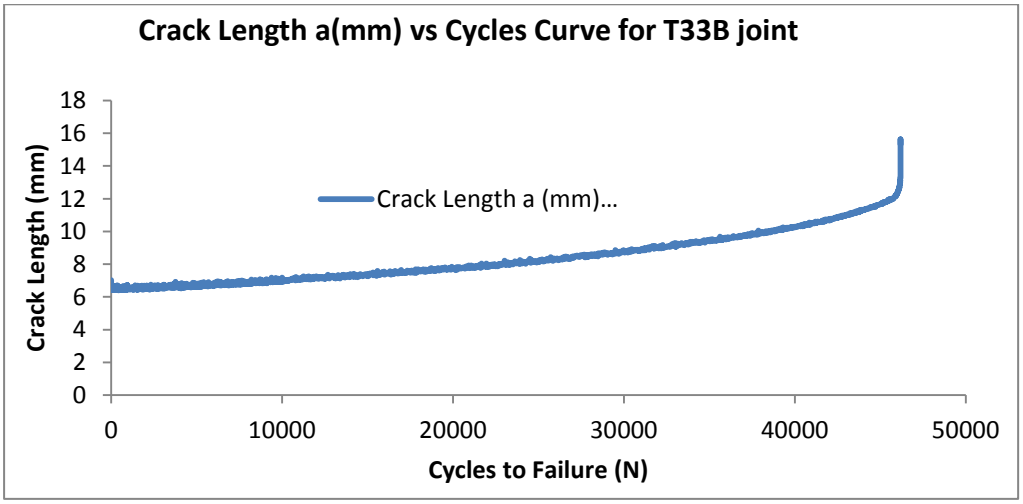

Figure 6.4: Crack length (a) vs. cycles curve obtained for T23B joint with 5.0mm precrack

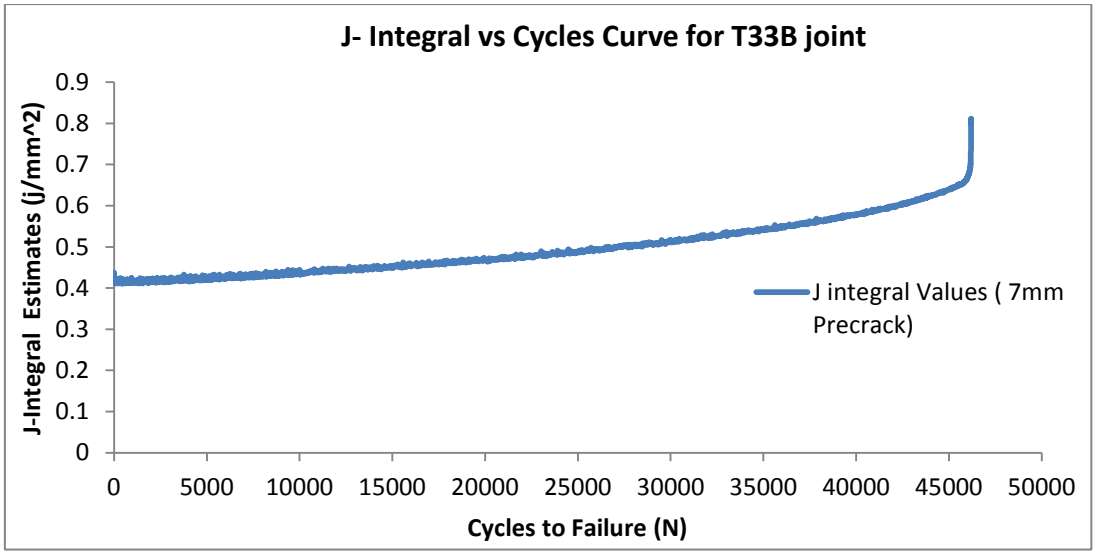

Figure 6.5: Energy release rate curve for T33B joint with 7.0mm precrack

- Due to large scatter in fatigue test data, moving averages and logical operations have been performed in excel to smooth the data and decrease down the number of data points. After calculating all the values, the fatigue crack propagation curves can be obtained for bonded joints by plotting the crack growth rates and energy release rates on double log-log scale. One of the curves obtained by this method is shown in figure.6.6.

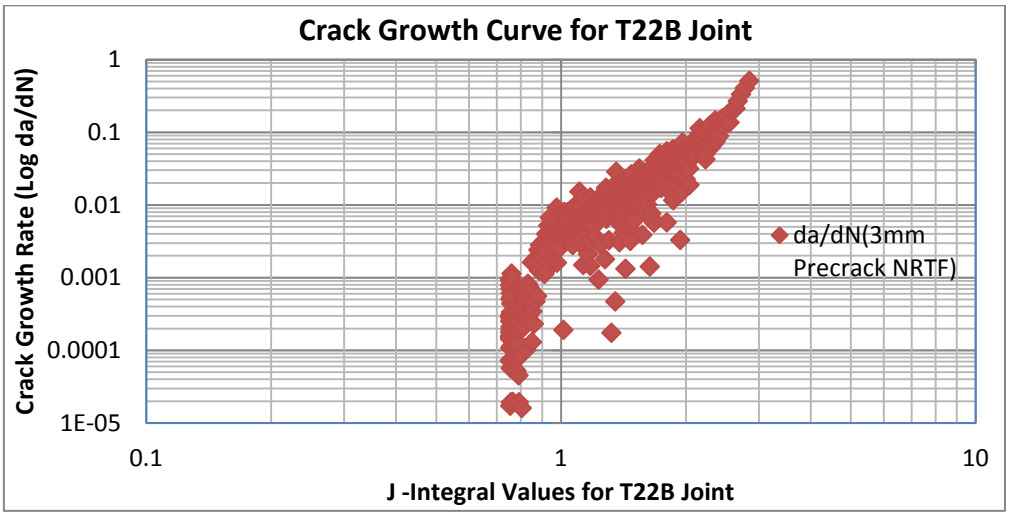

Figure 6.6: Crack growth curve obtained by stiffness method for T22B joint with 3.0mm precrack.

The tests conducted on bonded joints for this methodology were all constant amplitude tests which reveal that there is an increase in crack length with the number of loading cycles. The use of proper curve fitting techniques in FE models and fatigue test data enables us to work out and present this mentioned

methodology to determine the fatigue crack growth rates and obtain the crack growth curves for adhesively bonded joints. A discussion on curve fitting techniques for fatigue test data is presented and discussed in next chapter of this thesis.

6.3 T PEEL JOINT ANALYSIS USING THE STIFFNESS METHOD

6.3.1 TEST DESCRIPTION

The T peel bonded joints analysed were prepared with different precrack lengths and are tested in this work. The precrack length employed in these joints were 3.0mm, 5.0mm, 7.0mm and 10.0mm and sheet thickness used were 2.0mm and 3.0mm. The joints were made up of aluminium alloy (AA 5754) and were pretreated by using Phosphoric Acid Anodising (PAA Pretreatment). The adhesive used in these joints was Betamate Epoxy 4601 adhesive.

These specimens were tested at different load levels of 0.5 kN, 0.75kN for T22B joint, 1.1kN to 1.2kN for T33B joints and 0.51kN to 0.6kN for T23B joints. All the loads have been chosen in such a manner that the load level remains below the threshold level of the adhesive, i.e. without growing the precrack into the adhesive. Axial fatigue loading was applied to all of these joints. The crack propagation was recorded by using a high resolution USB microscope. All cracks in these joints were grown within the adhesive layer and were failed by pure cohesive mode.

6.3.2 FINITE ELEMENT MODELLING OF T PEEL BONDED JOINTS

Only the two dimensional damage models were modelled for T peel joints neglecting the plasticity effects into it. Because of the symmetry in the model, only half of the joint area needs to be modelled in Abaqus. Stress and strain components were used to calculate the stiffness of these models.

To ensure that the free edge of the coupon remains free to strain, the left hand side corner of the coupon is held in 1 and 2 directions and subsequent nodes are held in 2 only. However, free straining is allowed in 1 only. 1, 2 and 3 are the translational degrees of freedom and 4, 5 and 6 are the rotational degrees of freedom used in the finite element models. A load of about 1.2kN is applied on

the other free hand of the joint. The constant plastic strain element CPS4 from the Abaqus library has been used in peel damage models.

6.3.3 ANALYSIS OF T22B JOINT

The first step of the analysis of T22B joint using the method explained above is to post process the FE results of T22B damage model. Hyperview was used to calculate the respective stiffness at each and every time step of the linear static analysis, i.e. as the crack propagates by every 0.5mm. The stiffness was evaluated using the displacement values obtained in FE models. Since all the models modelled are linear, thus it was quite evident that the FEA stiffness will drop with the increase in crack length. Stiffness drop curves are thus plotted for T22B joint. The stiffness drop curve and energy release rate curve for T22B FE model is shown in figure.6.1 and 6.2.

In the same manner, using the fatigue test data the stiffness values for T22B joints were obtained by calculating the load range and displacement range in the T22B joints test data. Using the calculated data, the stiffness drop curves and the load range curves were plotted for different crack lengths against the number of cycles for every precracked joint. The respective stiffness and load range curves in accordance with the joint configurations is given in appendix 2 of the thesis.

6.3.3.1 CURVE FITTING IN T22B TEST DATA

The main idea of obtaining the fatigue crack propagation rates and curves using the test stiffness were developed using the test data of T22B joints (see figure. 6.7).

The curve (figure.6.7) was obtained by plotting the cycles-to-failure on the y axis and stiffness values on the x axis by taking all the precracked joints stiffness data within one curve. FE Stiffness results of T22B joint was also combined and included with these test results. FE crack length was plotted on secondary vertical axis with respect to the stiffness values. Then, taking the initial precrack lengths and their initial stiffness values from the test data, these four crack lengths were plotted against the stiffness as denoted in the figure by orange line. Then a power law curve has been fit to it having coefficient of regression value of 0.9994(*power law gives the maximum coefficient of regression value in this case*).

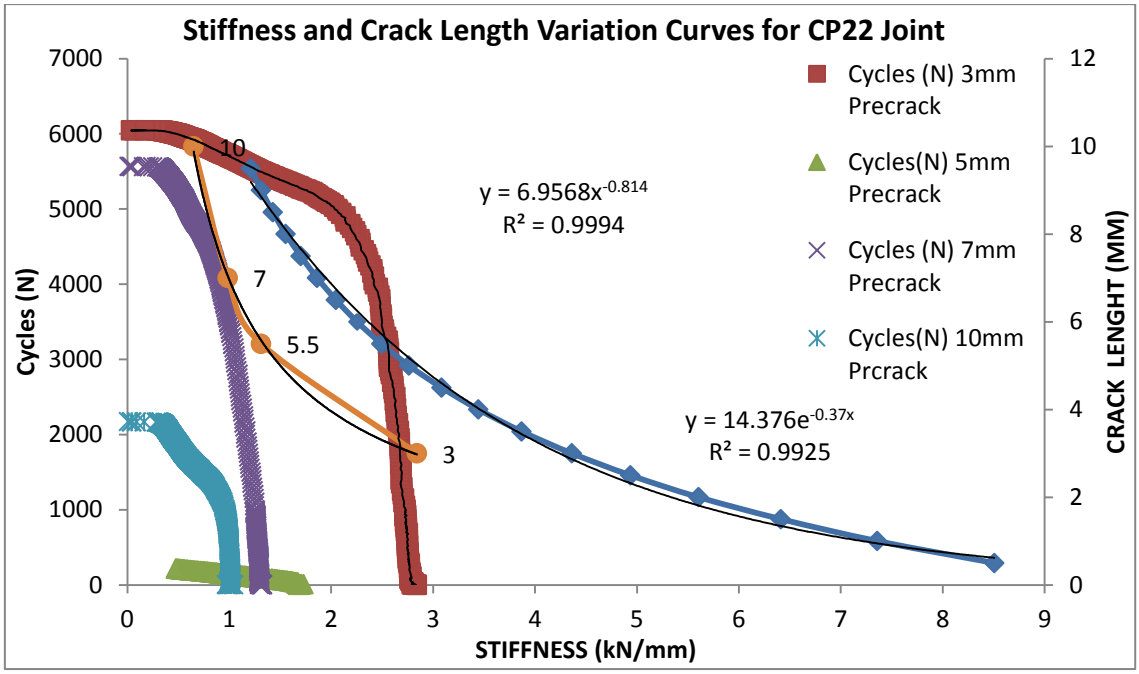

Figure 6.7: Stiffness and Crack length variation curve of T22B Joint

6.3.3.2 CALCULATION OF FATIGUE CRACK GROWTH RATES

Using the initial precrack lengths along with their stiffness values and fitting a line of best fit in the above curve gives a relation between the crack length and stiffness. From the above curve (figure 6.7), the equation obtained by curve fitting is given below:

$$y = 6.9568\, x^{-0.814}$$

Where y = crack length in mm and x= stiffness (kN/mm).

In the same manner, fitting a line of best fit in the energy release rate vs. crack length curve as shown in figure 6.2. The equation obtained is given below-

$$y = 0.0042x^2 + 0.0969x + 0.4063$$

Where y= energy release rate (j/mm^2) and x= crack length (mm).

The equations obtained above were used to calculate the crack lengths and energy rates associated with these crack lengths in the test data of precracked T22B Joints. The variation of crack length and energy release rate with cycles to failure was also plotted for every precracked T22B joint and is given in appendix 2 of this thesis. The crack propagation rates thus can be calculated by using the crack length and cycles data from these tests.

6.3.3.3 FATIGUE CRACK GROWTH RATE CURVES FOR T22B JOINTS

After calculating fatigue crack propagation rates for every precracked joint, the fatigue crack propagation rates for every precrack length were plotted against the J-integral values on **log-log scale** as shown in figure.6.8.

From the test data of T22B joints, it was noted that there were negative terms ***(inflexion points)*** in the crack growth rates and the points plotted were scattered which required the smoothing of fatigue test data. To achieve this, the negative terms was removed from the fatigue test data of every precrack length and a moving average was performed by taking the average of every ten points of energy release rates and fatigue crack propagation rates.

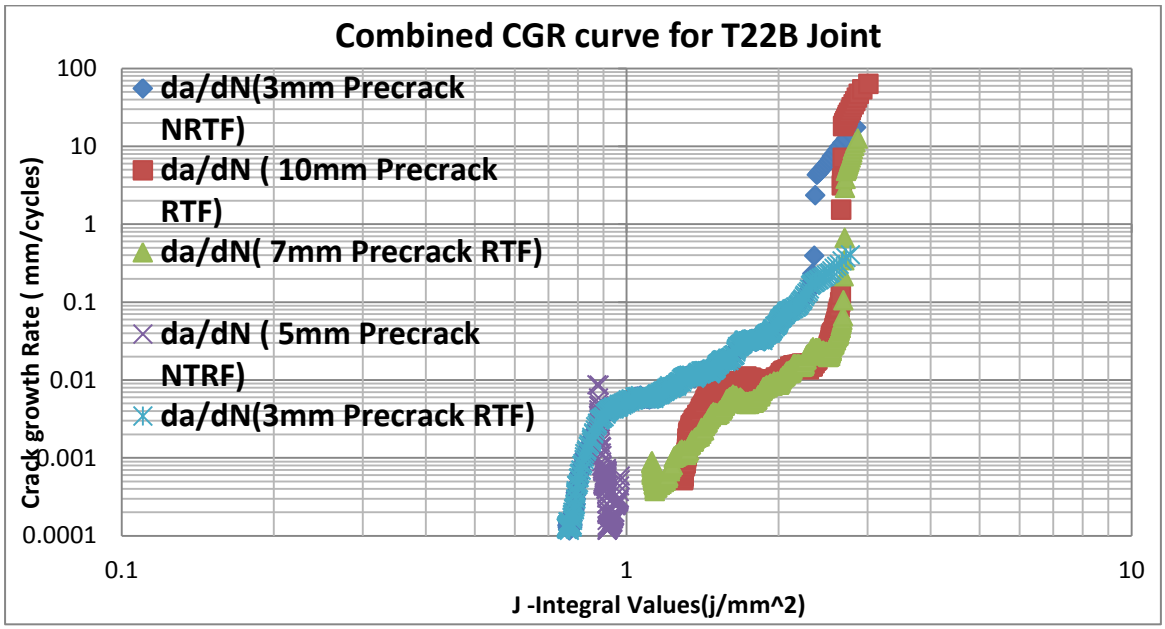

Figure 6.8: Crack growth rate curve of T22B joints

Summary: The fatigue crack curves of T22B joints for various precracks were obtained by combining the fatigue test data of bonded joints and FE stiffness data of damage models. Although, the method makes use of standard curve fitting models and moving averages, the nature of the curves obtained by combining these two data's for T22B joint resembles the nature and shape of Paris-Ergodan law defined in chapter 2 of the thesis. The method relies in selecting a suitable curve fit in the stiffness data by which the accurate values of crack lengths, energy release rates and fatigue crack propagation rates can be calculated.

6.3.4 ANALYSIS OF T23B JOINT

The fatigue crack propagation rates and fatigue crack curves for T23B joints was calculated and obtained in the same manner as done for T22B Joints. The precracks employed for these joints were 3.0mm, 5.0mm and 7.0mm. The displacements of these joints were measured across the specimen width by using a strain gauge instead of measuring displacement across the frame of the machine. The analysis consists of the following steps:

6.3.4.1 STIFFNESS CALCULATIONS AND CURVE FITTING IN FE MODEL OF T23B JOINT

The finite element modelling of T23B peel joints has already been explained in sec 6.3.2 of this chapter. The FE results of T23B joint was post processed by using Hyperview and stiffness drop and energy release rate curves was obtained for this joint as shown in figure.6.9 and 6.10. A line was fit in both of the curves to obtain a relation of stiffness and energy release rate as a function of crack length.

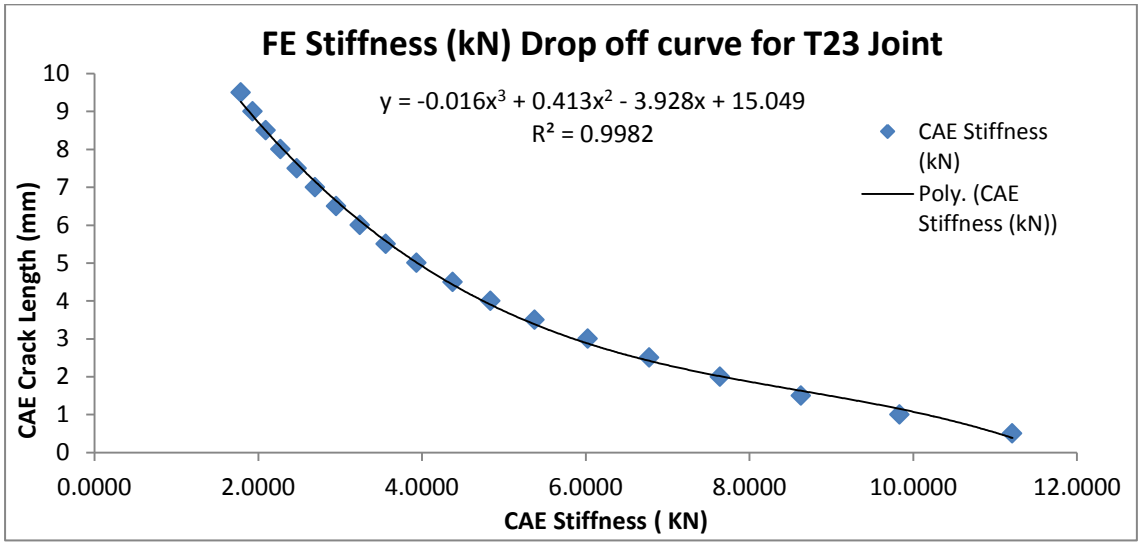

Figure 6.9: Stiffness drop Curve of finite element model of T23B joint

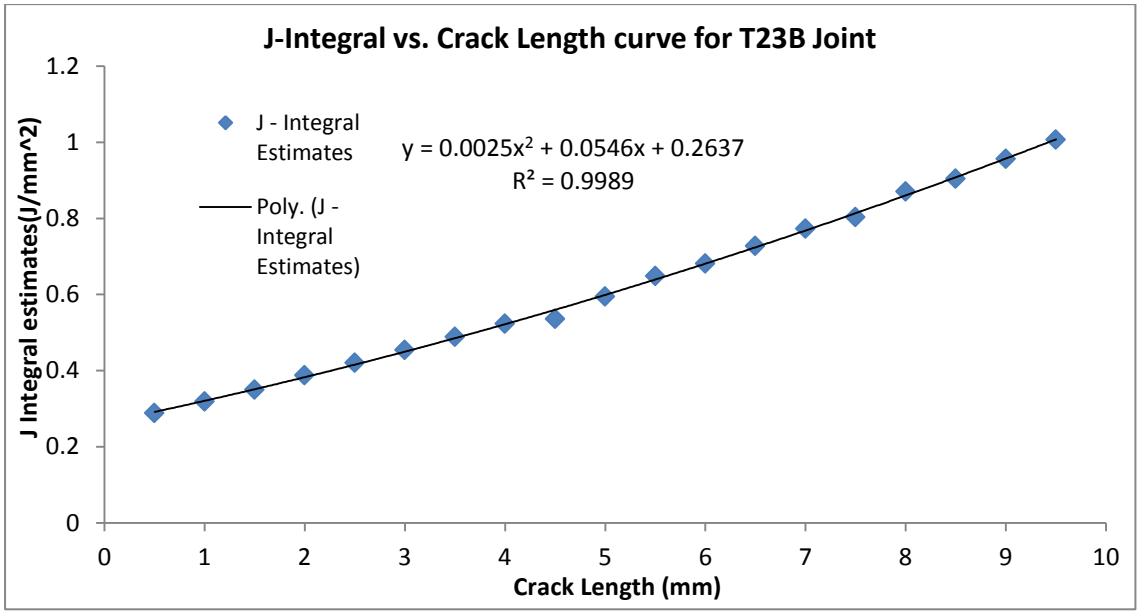

Figure 6.10: Energy release rate curve of finite element model of T23B joint

Using the test data of T23B precrack joints, the stiffness values was calculated and plotted against cycles to failure. The stiffness drop curve for each precracked joint is given in appendix 2 of the thesis.

6.3.4.2 CALCULATION OF FATIGUE CRACK PROPAGATION RATES FOR T23B JOINT

The following equation was obtained by fitting a cubic polynomial curve (K. B. Davies 1973) in the above curve. The equation obtained was

$$Y = -0.016x^3 + 0.413x^2 - 3.928x + 15.049$$

Where, y = Crack Length (mm), x= Stiffness (kN/mm).

In the same manner, the following equation was obtained by fitting a polynomial curve in the energy release rate curve.

$$y = 0.0025x^2 + 0.0546x + 0.2637$$

Where, y = Energy release rate (j/mm^2), x= Crack Length (mm).

The above equations were used to calculate the crack lengths and energy release rates in fatigue test data. Taking the successive difference of calculated crack lengths and number of cycles in test data of each precracked T23B joints, the fatigue crack growth rates were calculated. The variation of crack rates and

energy release rates with cycles to failure were also plotted for every precrack and is given in appendix 2.

6.3.4.3 CRACK PROPAGATION CURVES FOR T23B JOINT

After calculating the fatigue crack propagation rates and energy release rates in terms of J-Integral values by using standard curve fitting technique for every precrack joint, moving average was applied in crack growth rates and energy release rates columns of test data of T23B joint. The moving average in T23B test data was done by taking average of first fifty points instead of taking average of first ten points of each precrack test data to make the crack growth curve smoother in the test data of T23B joints.

The following curve was obtained for each precrack length as shown in figure.6.11.

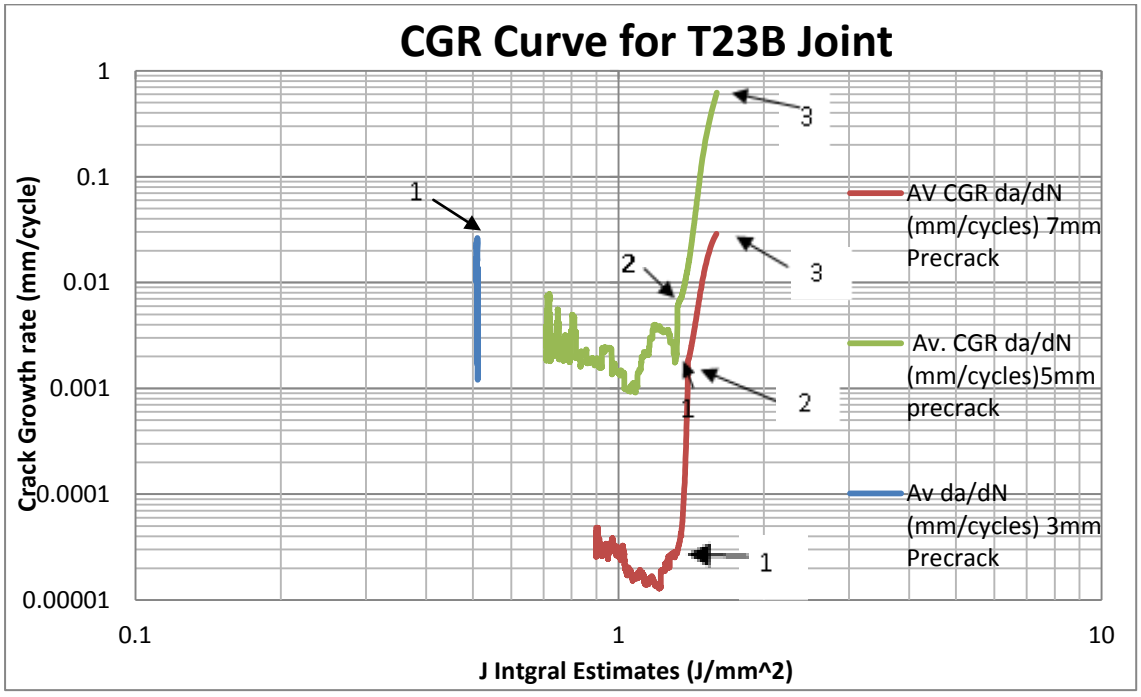

Figure 6.11: CGR curve of T23B joints

Summary: From the CGR curve of T23B joints, the behavior and shape of the curve gives the expected sigmoidal shape. From 3mm precrack T23B joint, there is a slow crack growth uptill point 1 and finally the joint get separated after crossing point 1.

Similarly for 5mm precrack joint, the crack growth first decreases upto point 1. It was also noted in the test that after certain number of cycles, i.e. after 3050

cycles, due to the excess vibration, the strain gauge was detached from the test rig. As a result the data upto those cycles was removed from the test data. Due to this excess vibration of strain gauge there were some peaks in crack growth curves of 5mm precrack joint. After crossing point no 1, there is steady crack growth upto point 2. From point 2 there is a fast crack growth and finally the joint separates at point 3.

The same trend was noted in CGR curve of 7mm precrack joint. There crack growth decreases upto point 1 and then the crack growth stabilizes and follows a linear pattern up to point 2. There is fast crack growth after point 2 and the joint failed at point 3.

6.3.5 ANALYSIS OF T33B JOINTS

The fatigue crack growth analysis of T33B joint was also done in the same manner as done for T22B and T23B joints. Joints with no precrack, 3.0mm precrack, 5.0mm precrack and 7.0mm precrack were used in the analysis. For curve fitting purposes, only precracked joints were considered in this analysis. The steps of the analysis are given below:

6.3.5.1 STIFFNESS CALCULATION OF FINITE ELEMENT MODELS AND FATIGUE TEST DATA

The FE results of T33B joints were post processed by using Hyperview. Stiffness values and energy release rate curves were plotted as shown in figure.6.12 and 6.13. A relations of stiffness and energy release rate as a function of crack length was obtained by using a line of best fit in these curves.

In the same manner, the stiffness values were calculated by using the displacement range and load range in the fatigue test data of each precracked joint. The stiffness and load range curve were plotted against number of cycles for every precrack employed. (See appendix 2).

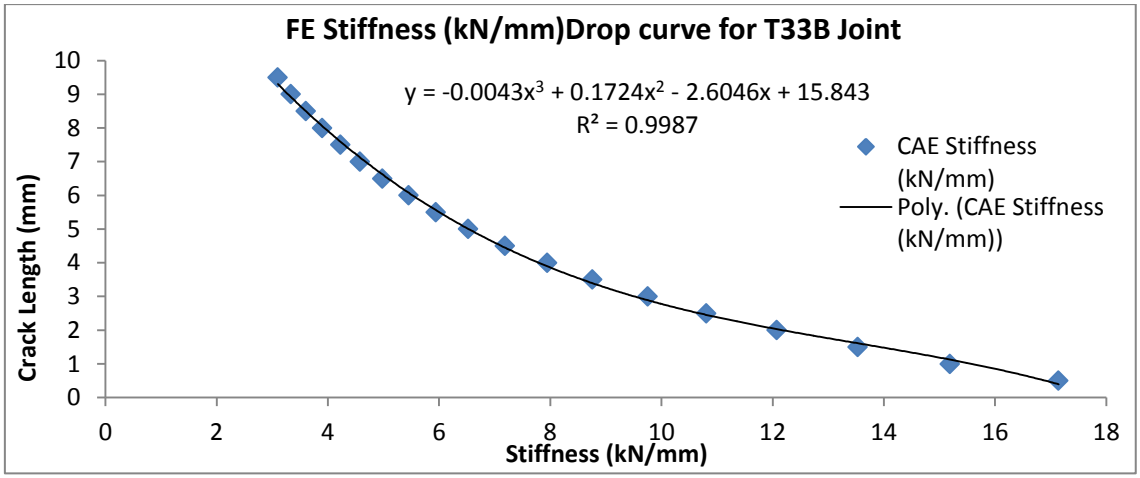

Figure 6.12: Stiffness drop curve for FE model of T33B joint

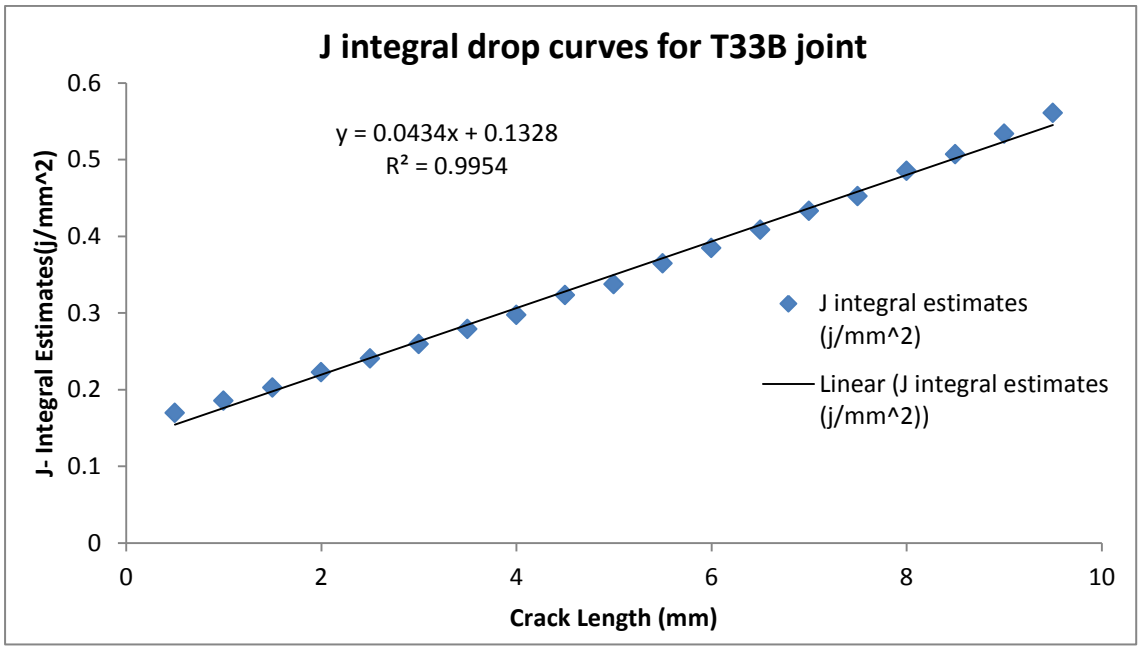

Figure 6.13: Energy release rate curve of T33B joint

6.3.5.2 CALCULATION OF FATIGUE CRACK PROPAGATION RATES FOR T33B JOINTS

In both of the curves, the cubic polynomial fit and linear fit was employed in order to get the best fit. The following equations were obtained by curve fitting:

$$y = -0.0043x^3 + 0.1724x^2 - 2.6046x + 15.843$$

$$R^2 = 0.9987$$

Where, y = Crack Length (mm) and x= Stiffness (kN/mm).

And,

y = 0.0434x + 0.1328

R^2 = 0.9954

Where, y= Energy release rate (J/mm^2) and x= Crack Length (mm).

The crack lengths and energy release rates for each precracked T33B joints were calculated by making use of the equations given above. Taking the successive differences of the crack lengths and cycles to failure, the fatigue crack propagation rates were calculated for every T33B precracked joint. The variation of crack length and energy release rates with respect to number of cycles was also plotted and is given in appendix 2 of this thesis.

6.3.5.3 FATIGUE CRACK PROPAGATION CURVE FOR T33B JOINTS

The fatigue crack propagation curves were obtained for T33B joints by plotting crack propagation rates against energy release rates using log-log scale (*see figure 6.14*). To reduce the scatter in fatigue test data, a moving average method was used. Also, to reduce the numbers of data points in the CGR curve, logical operation have also been used in the test data of these joints. Such a logical operation used in 3mm precrack T33B joint is given below.

*IF (ABS (V4) <ABS (0.9*V3), V4,"")*

IF (OR (X4<>"", Y4<>""), IF (ISERROR (V4), NA (), V4), NA ()).

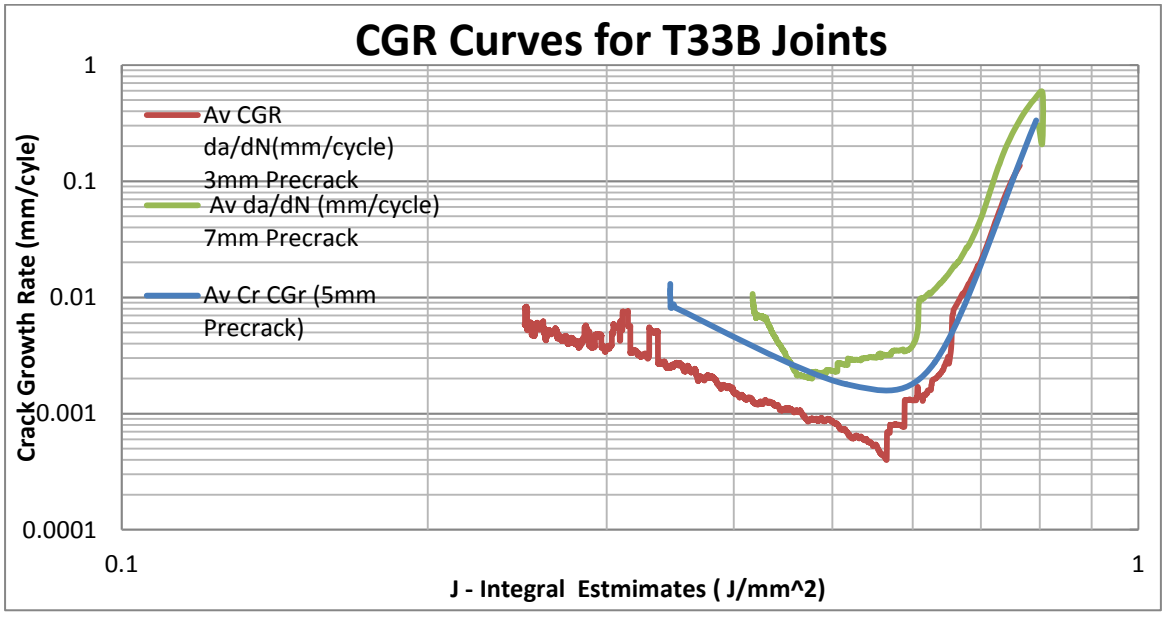

Figure 6.14: Crack growth rates curves for T33B joints

Summary: It can be noted from the shape of the above curves that they are similar to Paris law curve. A sharp drop in the crack propagation rates were noted in these curves. A very steep drop was noted for 3.0mm precracked T33B joint. Due to the higher order polynomial fit in the stiffness drop curve of T33B joints, large inflexion points were observed in fatigue test data while calculating the fatigue crack growth rates. Strain gauge on the adherends surface picked up high frequency vibrations during the start of fatigue test, which resulted in high peaks in CGR curve. The problem of inflexion points was overcome by taking the absolute values of crack propagation rates and then using them in plotting CGR curves.

6.4 ANALYSIS OF SINGLE LAP SHEAR BONDED JOINTS

6.4.1 TEST DESCRIPTION

The single lap shear bonded joints tested in this work were tested without any precracks. The sheet thickness employed in this joint are 2.0mm and 3.0mm. In order to compare the effect of PAA pretreatment on aluminium bonded joints, aluminium adherends for single lap shear joints were pretreated with PT2 silica pretreatment.

LS22B joints were tested at a load of 8kN and LS33B joints were tested at a load level of 9.0kN. Since two joints of LS22B were tested, hence these two joints were denoted as LS22B1 and LS22B2 joints. The crack propagation were recorded and monitored by using a high resolution USB microscope. Due to mixed mode loading in these joints, the failure noted was interfacial across the top sheet of these joints.

6.4.2 FINITE ELEMENT MODELLING OF LAP SHEAR BONDED JOINTS

The finite element models of single lap shear bonded joints were prepared by using sub-modelling approach as in case of T-peel bonded joints. The same material properties and boundary conditions used to model T-peel bonded joints were also used in lap shear models. The constant plastic strain element CPS4 was used to model these joints from abaqus element library.

However, it was noticed that while post processing the LS33B joints, the mesh was not fine in the adhesive bonded region. Due to this, there was variation in the

energy release rate values for crack lengths upto 3.5mm. Hence, the analysis of LS33B joints is not discussed here. It was also noted in the sub-modelling of lap shear joints that there were some errors in the stress intensity factor values and J-Integral values due to mismatched meshes. Also, the mesh requires more refinement in the bonded line area. Hence, all of the single lap shear bonded joints were re-modelled manually by placing the elements one by one in the bonded region. Since it was a time consuming process, the models were modelled upto a crack length of 3.5mm. Manually created models are known as bespoke models.

6.4.3 ANALYSIS OF LS22B1 JOINT

The analysis of LS22B1 joint by using the stiffness method is explained in the following steps:

6.4.3.1 STIFFNESS CALCULATION OF FE MODELS AND FATIGUE TEST DATA

The output results of damage model of LS22B joint was post processed by using Hyperview**.** The displacements from the model were measured along the y axis and the stiffness at each crack length was then calculated using these displacements. Since the joint failure was interfacial along the top sheet, hence energy release rates values were extracted for the interface 1 modelled using FEA. Stiffness and energy release rate curves were plotted for this joint as shown in figure.6.15 and 6.16.

Using fatigue test data of LS22B joints, the stiffness values were calculated by using the values of displacement range and load range. The variations of stiffness drop and load range were then plotted against the number of cycles (see appendix 2).

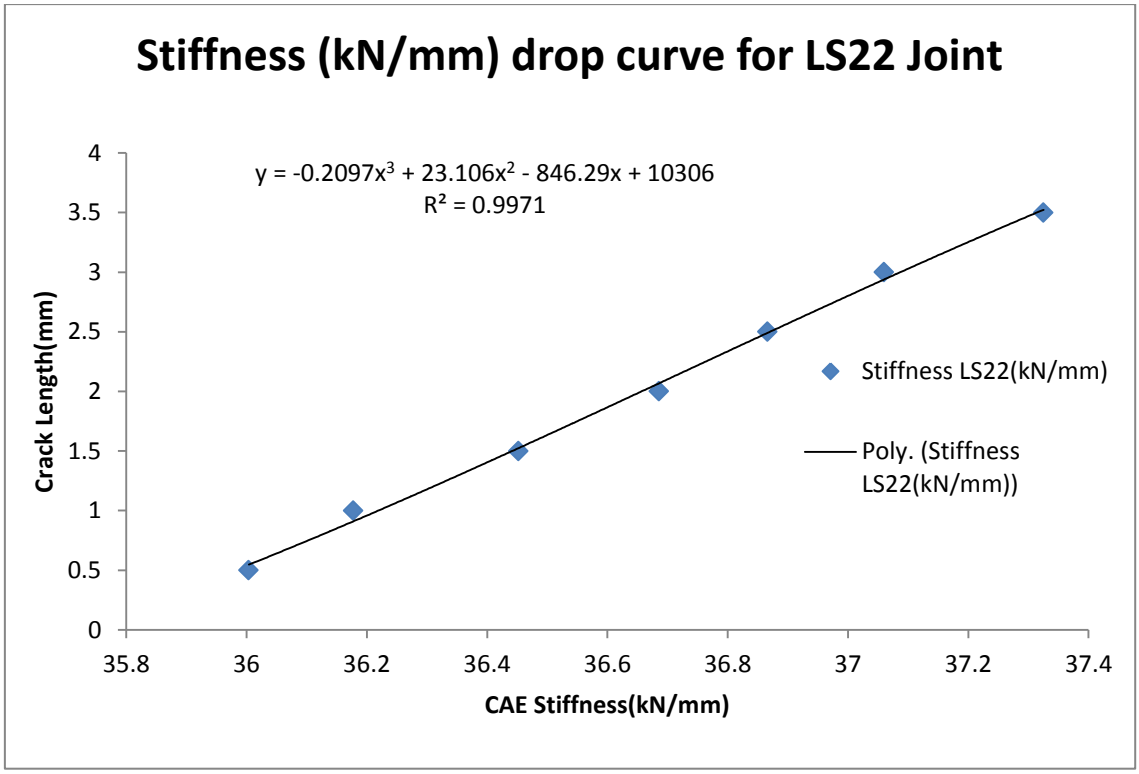

Figure 6.15: Stiffness drop curve of FE model of LS22B joint

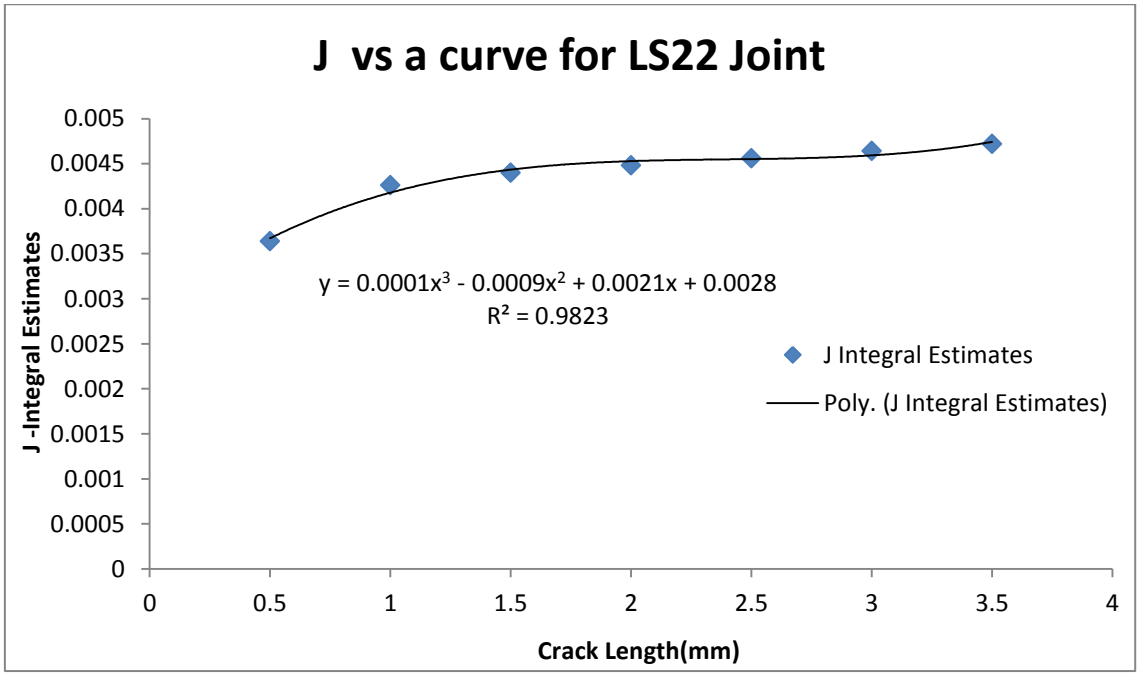

Figure 6.16: Energy release rate curve of LS22B joint

6.4.3.2 CURVE FITTING IN FE MODEL OF LS22B JOINT

A cubic polynomial fit was used to obtain the relations between the crack length vs. stiffness and energy release rate vs. crack length as shown in figure.6.15 and 6.16.

From the crack length (mm) vs. stiffness curve (kN/mm), the following equation was obtained.

$$y = -0.2097x^3 + 23.106x^2 - 846.29x + 10306$$

$$R^2 = 0.9971$$

Where, y = crack length (mm) and x = stiffness (kN/mm).

Similarly using the energy release rate curve, the following equation was obtained.

$$y = 0.0001x^3 - 0.0009x^2 + 0.0021x + 0.0028$$

$$R^2 = 0.9823$$

Where, y = energy release rate (j/mm^2) and x= crack length (mm).

The above equations were used to calculate the crack lengths and energy release rate in the fatigue test data of this joint. The fatigue crack propagation rates were calculated using the successive differences of crack lengths and number of cycles in the fatigue test data.

6.4.3.3 FATIGUE CRACK PROPAGATION CURVE OF LS22B JOINTS

After calculating the fatigue crack propagation rates, the moving averages was applied to the crack growth rates and energy release rates and were plotted on a double log-log scale to get the CGR curve of this joint. The CGR curve plotted is shown in figure 6.17.

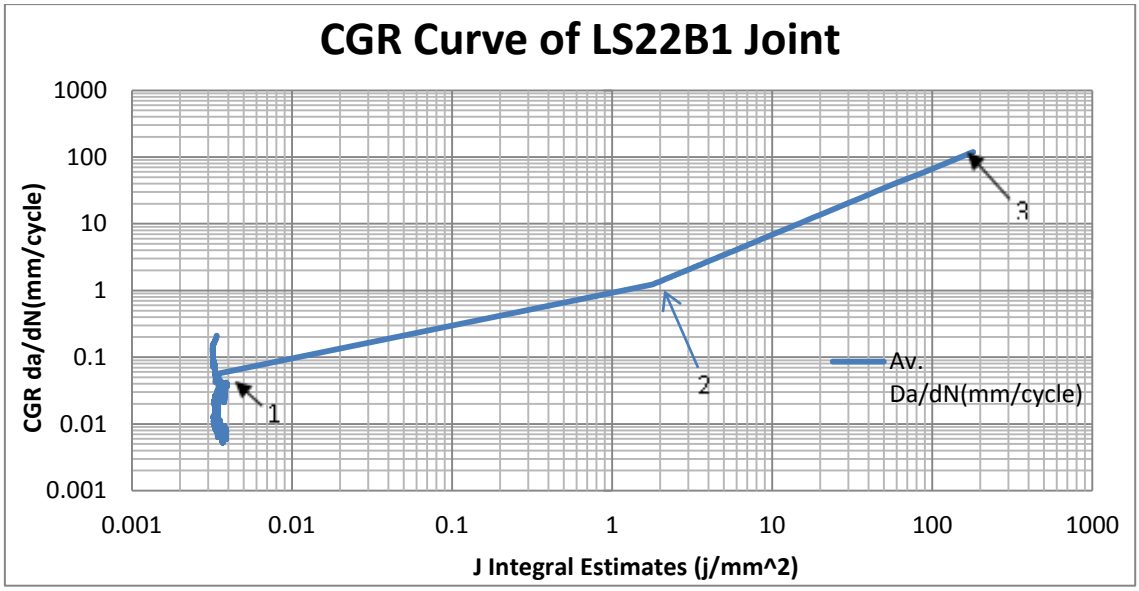

Figure 6.17: Crack growth rate curve of LS22B1 joint

In the similar manner, using the same CAE results the analysis of LS22B2 joints was carried out and crack propagation rates and energy release rates were calculated for this joint. The CGR curve obtained for this joint is shown in figure. 6.18.

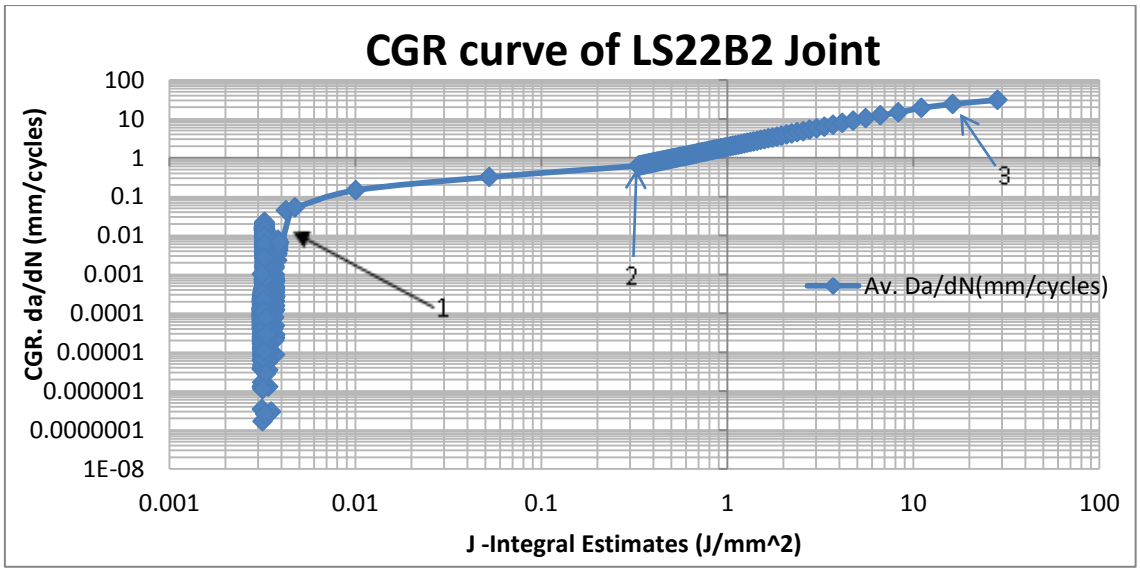

Figure 6.18: Crack growth curve of LS22B2 joint

SUMMARY: From the CGR curve of LS22B1 joint, it is evident that there is a rapid crack growth uptill point 1. As soon as the crack propagation reaches point 2, the crack growth stabilises and become slow. They almost follow a linear trend uptill point 2. As soon the crack reaches point 2, the crack propagation rate

increases and finally the joint finally separated out at point 3. The same trend was noticed while testing the same joint.

The same pattern of crack propagation was noticed from the crack growth curve of LS22B2 joint. There is a rapid crack propagation noticed upto point 1. In a similar fashion, the crack growth then stabilises and follows almost a linear pattern uptill point 2. The crack again began to propagate very fast after crossing point 2 and finally failed at reaching point 3. The nature and the shape of the curve resemble the Paris law curve except that there is rapid crack propagation within the point 1(threshold values).

6.5 VALIDATION OF THE STIFFNESS METHOD

The investigated method was applied to different bonded joint geometries and has been validated against the crack propagation videos recorded for T-peel and single lap shear bonded joints. The crack propagation in bonded joints were recorded for T33B joint with no precrack, 3.0mm precrack, 5.0mm precrack, T23B joint for 5.0mm and 7.0mm precrack and for LS22B and LS22B joints.

The method was validated in two stages.

- In the first stage, the crack lengths were measured by using the crack propagation videos from the point of crack propagation until the point of final failure at subsequent intervals. The respective time was noted and the number of cycles was calculated for each measured crack length.
- In the second stage, the crack lengths were taken from the fatigue test data at the same number of cycles calculated above. A variation of crack lengths with respect to number of cycles were plotted to compare the measure crack lengths from videos and calculated cracks lengths using curve fitting techniques in fatigue test data of bonded joints.

6.5.1 VALIDATION OF THE METHOD FOR T33B JOINT WITH NO PRECRACK

To validate the method for this joint, a scale factor was calculated to measure the crack length from the videos. A ruler was used in the test set up to measure how long the crack grows into the adhesive. The scale factor calculated is given below.

3mm (Sheet Thickness) = 82mm (Thickness Measured from Video)

1mm = 3/82 mm = 0.0365mm

Where, 3mm is the actual sheet thickness and 82 is the sheet thickness measured from the crack propagation videos. The scale factor was multiplied by the measured crack length from the videos at subsequent intervals of time.

The cycles rate used was 10 cycles/sec.

The measured results and the calculated results are given in table 6.1-6.2.

A quantitative comparison was made between the measured and calculated results of crack length are presented in the curve given in figure.6.19.

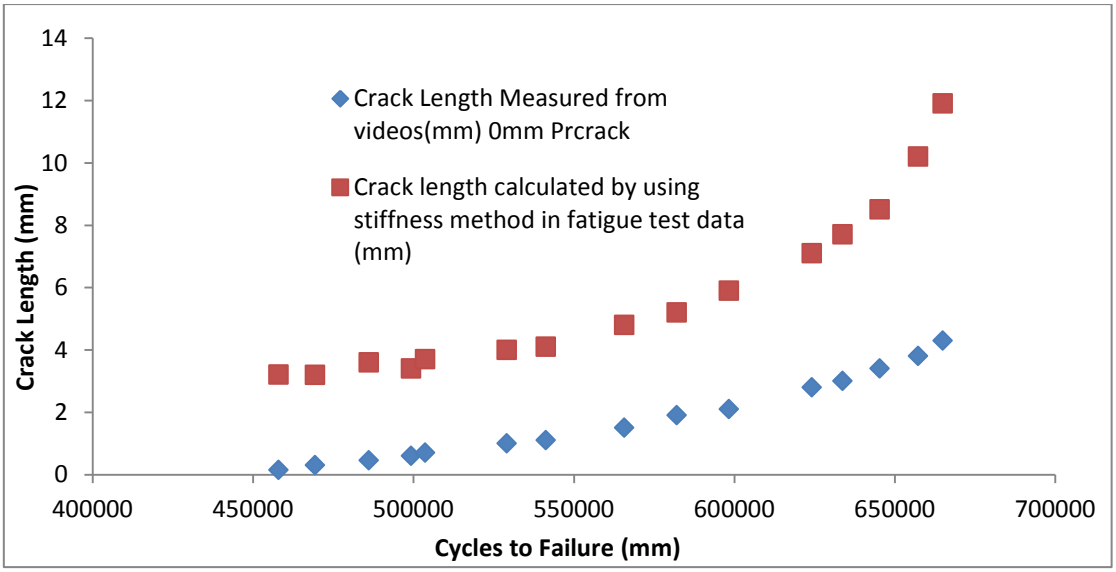

Figure 6.19: Crack length vs. cycles to failure curve for T33B joint with no precrack

It was noted from above curve that although both of the curves shows an increasing trend with number of cycles, the error between the two is 63% which shows a poor correlation between the measured crack lengths and calculated crack lengths in fatigue test data. Hence, the methodology didn't seems to work for T33B joint with no precrack.

6.5.2 VALIDATION OF METHOD FOR T33B JOINT WITH 3.0MM PRECRACK

To validate the method for this joint, the same scale factor was use to calculate the crack lengths along with cycle rate due to the same sheet thickness.

The crack length was measured from the point of crack initiation up till the point where joint completely separates out. The crack starts propagating at 54610 seconds and point of final failure was noted at 74522 seconds.

The results for this joint are given in table 6.3-6.4.

The variation of measured crack lengths from videos and calculated crack length in fatigue test is shown in figure.6.20.

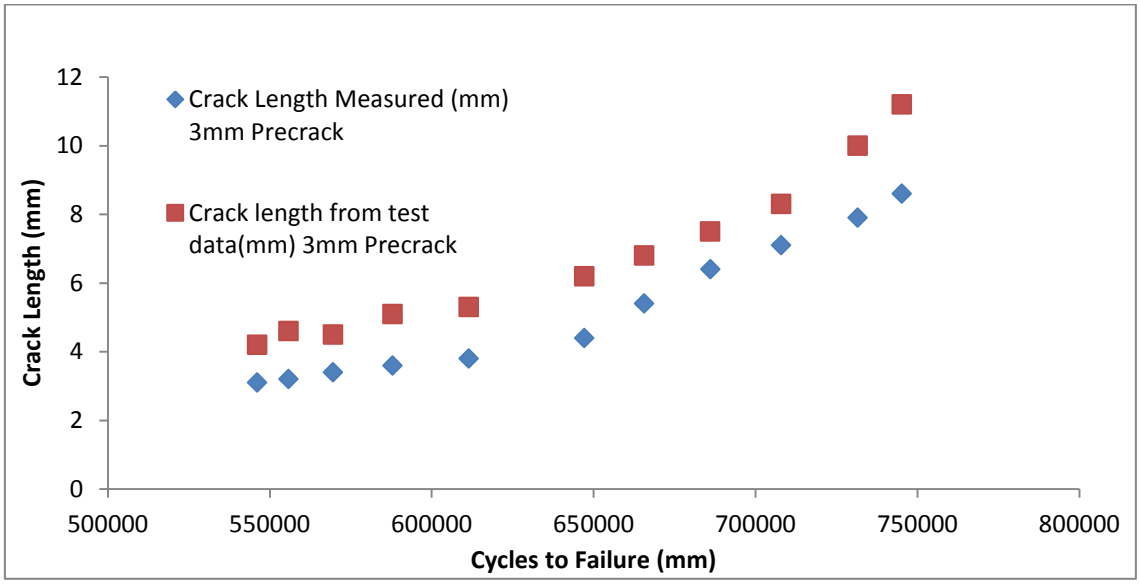

Figure 6.20: Crack length vs. cycles to failure curve for T33B 3mm precrack joint

From the above curve, it was noted that as soon as a precrack is introduced into the joint, the variation becomes less. The error between the two crack lengths (measured and calculated) was 37%. A good correlation was noted between the two curves as both are lying very close to each other and also, follows an increasing trend with the number of cycles. Hence, the methodology seems to work satisfactorily for this joint.

6.5.3 VALIDATION OF METHOD FOR T33B JOINT WITH 5.0MM PRECRACK

The validation of the method for this joint was done in the same way as done for the above joints. The same scale factor was used due to same sheet thickness along with cycle rate of 10 cycle/sec.

The results of this validation are given in table 6.5-6.6.

The variations of measured crack lengths from video and calculated crack length from fatigue test for 5mm precrack is shown in figure.6.21.

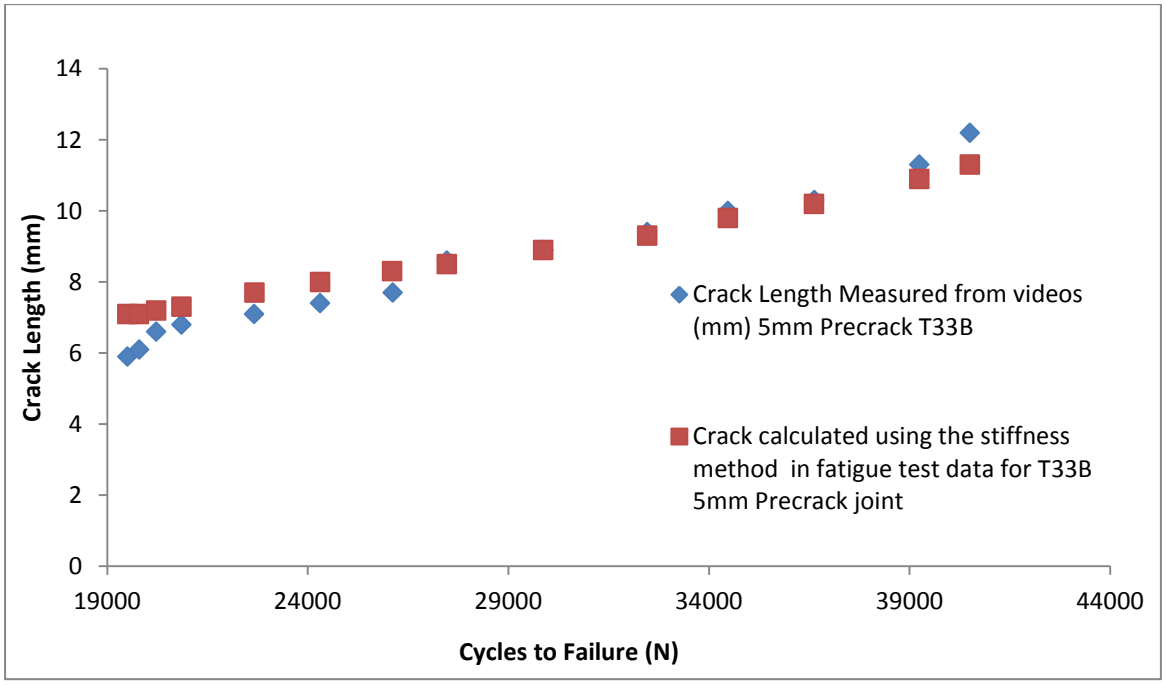

Figure 6.21: Crack Length vs. Cycles Curve for T33B 5mm Precrack Joint

A very good correlation was observed between the measured crack length and calculated crack length (mm) from fatigue test data for this joint. The error calculated was 3.2%. Hence, the results and correlation can be improved by increasing in precrack length of the joint. Also, the cubic polynomial curve fitting method proposed by Davies et al. (K. B. Davies 1973) proves the validity of this method in calculating crack lengths and fatigue crack propagation rates.

6.5.4 VALIDATION OF THE METHOD FOR T33B JOINT WITH 7.0MM PRECRACK

Using the same scale ratio and cycle rate, the crack length was measured from the 7mm precrack video and has been validated against the calculated results from the fatigue test data.

The results for T33B joint with 7.0mm precrack are given in table 6.7-6.8.

The variation of measured crack lengths and calculated crack lengths using the stiffness method in fatigue test data is given in figure.6.22. The measured crack lengths using 7mm precrack video matches well with the calculated crack lengths in the 7mm precrack fatigue test data. A very good correlation was observed as both of the curves are lying very near to each other (with 1.7% error) thus proving the validity of the used method for this joint.

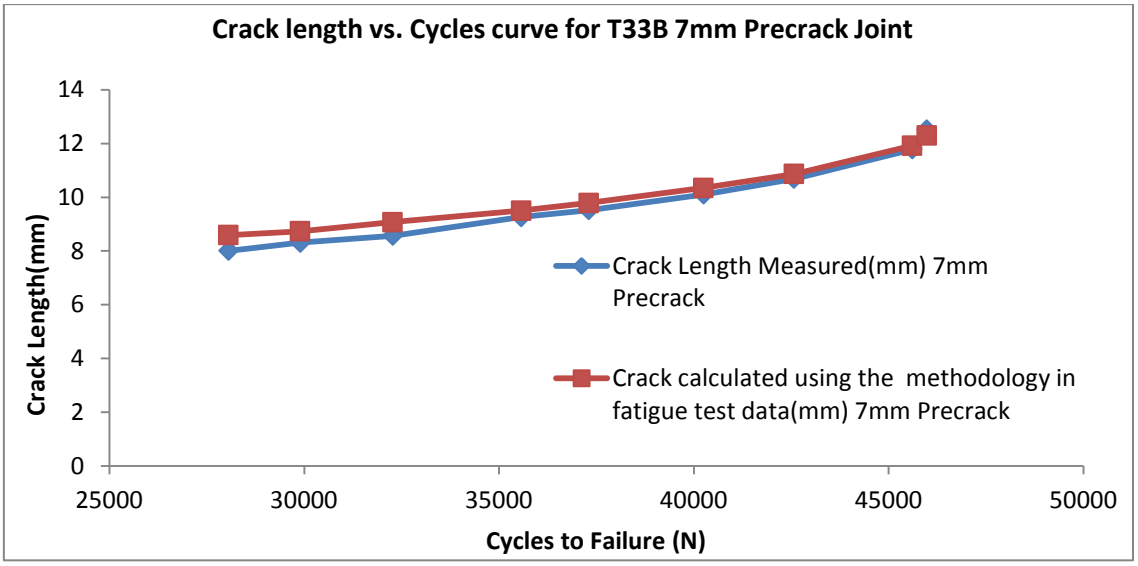

Figure 6.22: Crack length vs. Cycles curve for T33B 7mm Precrack Joint

6.5.5 VALIDATION OF THE METHOD FOR LS22B JOINT

The methodology used in the analysis was also investigated and validated for lap shear bonded joints. Two videos were recorded to monitor the growth of crack in these joints. The scale factor used for lap bonded joints was calculated in the same way as that of T peel joints.

Scale factor –

2mm (Sheet Thickness) = 59mm (Measured by using ruler from the LS22 B Video)

1mm = 0.0340mm

Thus, scale factor of 0.0340mm was used to find the crack length measured from the LS22B videos. The cycle rates used was 10 cycles/sec.

The results of the measured crack length from LS22B joint video and calculated crack length in the fatigue tests are shown in table 6.9-6.10. Similarly, variation of measured crack length (videos) and calculates crack length is shown in figure.6.23.

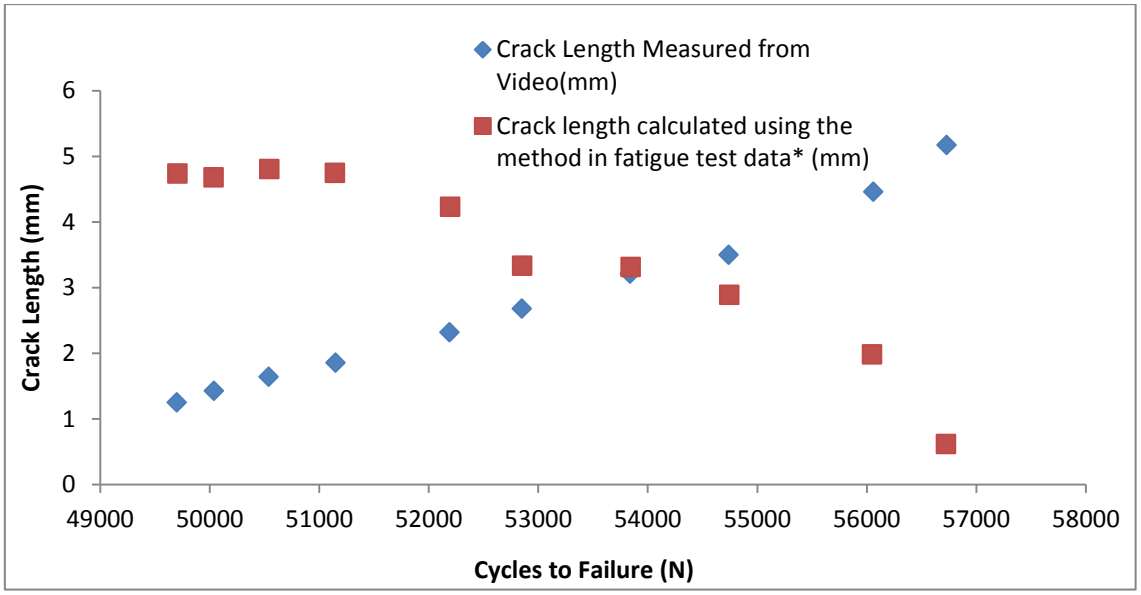

Figure 6.23: Crack length vs. Cycles curve for LS22B Joint

*The crack length's calculated in fatigue test data was done by using the method explained in the beginning of this chapter.

From the above curve, a poor correlation was observed between the measured crack length from LS22B video and calculated crack length using the methodology explained in the fatigue test data of the same joint. The failure noticed in these joints was interfacial failure on the top sheet due to mixed mode opening of cracks. Since the method was only valid upto Mode I failure and failure observed in lap joints were interfacial failure due to mix mode loading, the methodology didn't work satisfactorily for this joint.

6.6 CHAPTER SUMMARY

This chapter outlined the methodology which combines the finite element based stiffness data and fatigue test data of bonded joints to calculate the fatigue crack growth rates and obtain the fatigue crack propagation curves for T-peel and lap shear bonded joints. The analysis was conducted on fatigue test data of T peel bonded joints and lap shear bonded joints. It was noted down from the analysis that shape of obtained fatigue crack propagation curves resembles the shape of Paris law curve. The methodology was a validated for T33B and LS22B joints against the measured crack lengths and calculated crack lengths using the stiffness method in fatigue test of bonded joints. A good correlation was observed between the measured crack lengths from crack propagation videos and the

crack lengths calculated in the fatigue test data using the stiffness method for precracked joints. The method becomes more stable if a large precrack is introduced into the joints. The main limitation of this method was that it was only valid for Mode I loading, not for interfacial failure due to mixed mode loading, such as in single lap shear bonded joint.

6.7 RESULTS USED IN THE VALIDATION OF STIFFNESS METHOD

Time (sec)	Cycles to Failure(N)	Crack Length Measured from videos for T33B with no Precrack(mm)
45802	458020	0.15
46935.5	469355	0.3
48614.7	486147	0.45
49934.5	499345	0.6
50372.7	503727	0.7
52910.5	529105	1
54134.5	541345	1.1
56576.7	565767	1.5
58210.2	582102	1.9
59840.6	598406	2.1
62423.3	624233	2.8
63378.4	633784	3
64540.8	645408	3.4
65729	657290	3.8
66498.9	664989	4.3

Table 6-1: Crack length results measured from crack propagation video of T33B joint without precrack.

Time(sec)	Cycles to Failure(N)	Crack length calculated by using stiffness method in fatigue test data (mm)
45802.5	458025	3.1
46935	469350	3.2
48615	486150	3.6
49935	499350	3.4
50372.5	503725	3.7
52910	529100	4
54135	541350	4.1
56577.5	565775	4.8
58210	582100	5.2
59840	598400	5.9
62422.5	624225	7.1
63377.5	633775	7.7
64540	645400	8.5
65730	657300	10.2
66498.2	664982	11.9

Table 6-2: Crack length results from fatigue test data of T33B joint with no precrack

Time (sec)	Cycles to Failure(N)	Crack length measurement from crack propagation video of T33B joint with 3mm Precrack(mm)
54610	546100	3.1
55581	555810	3.2
56959	569590	3.4
58796	587960	3.6
61144	611440	3.8
64716	647160	4.4
66561	665610	5.4
68606	686060	6.4
70798	707980	7.1
73159	731590	7.9
74522	745220	8.6

Table 6-3: Crack lengths results measured for T33B 3mm precrack from crack propagation video

Time (Sec)	Cycles to Failure(N)	Crack length calculated from fatigue test data of T33B joint with 3mm Precrack (mm)
54610	546100	4.2
55580	555800	4.6
56960	569600	4.5
58795	587950	5.1
61145	611450	5.3
64715	647150	6.2
66560	665600	6.8
68605	686050	7.5
70797	707970	8.3
73160	731600	10
74522.5	745225	11.2

Table 6-4: Crack length results from fatigue test data of T33B joint with 3mm precrack

Time(sec)	Cycles to Failure(N)	Crack Length Measured (mm) 5mm Precrack T33B
1951	19510	5.9
1980	19800	6.1
2023	20230	6.6
2086	20860	6.8
2267	22670	7.1
2431	24310	7.4
2612	26120	7.7
2747	27470	8.6
2988	29880	8.9
3247	32470	9.4
3448	34480	10.0
3663	36630	10.3
3925	39250	11.3
4051	40510	12.3

Table 6-5: Crack length measurement from crack propagation video of T33B joint with 5mm precrack

Time(sec)	Cycles to Failure(N)	Crack length calculated using stiffness method in fatigue test data of T33B joint with 5mm precrack(mm)
1951	19510	7.0
1979.5	19795	7.1
2023	20230	7.2
2086	20860	7.3
2267	22670	7.7
2431	24310	8.0
2611	26110	8.3
2747	27470	8.5
2987	29870	8.9
3247	32470	9.4
3448	34480	9.8
3662.5	36625	10.3
3925	39250	10.9
4051	40510	11.3

Table 6-6: Crack length results from fatigue test data of T33B 5mm

Time(sec)	Cycles(N)	Crack length measured from crack propagation video of T33B joint with 7mm precrack(mm)
2818	28068	8.1
3003	29909	8.3
3241	32280	8.6
3558	35580	9.3
3746	37310	9.5
4042	40258	10.1
4275	42579	10.7
4580	45616	11.8
4617	45985	12.5

Table 6-7: Crack length results measured from crack propagation video of T33B joint with 7mm precrack

Time (sec)	Cycles (N)	Crack length from fatigue test data of T33B joint with 7mm precrack(mm)
2817	28170	8.6
3002	30020	8.8
3240	32400	9.1
3571	35710	9.5
3746	37460	9.8
4041	40410	10.4
4275	42750	10.9
4579	45790	11.9
4616	46160	12.3

Table 6-8: Crack length results using stiffness method in fatigue test of T33B joint with 7mm precrack

Time (sec)	Cycles (N)	Crack length measurements from LS22B joint video(mm)
4970	49700	1.3
5004	50040	1.5
5054	50540	1.6
5115	51150	1.9
5219	52190	2.3
5285	52850	2.7
5384	53840	3.2
5474	54740	3.5
5606	56060	4.5
5673	56730	5.2

Table 6-9: Crack length measurements from LS22B joint crack propagation video

Time(sec)	Cycles(N)	Crack length calculated using stiffness method in fatigue test data of LS22B joint (mm)
4970	49700	4.7
5003	50030	4.7
5054	50540	4.8
5114	51140	4.7
5219	52190	4.2
5285	52850	3.3
5384	53840	3.3
5474	54740	2.9
5605	56050	2.0
5672	56720	0.6

Table 6-10: Crack length results from fatigue test data of LS22B joint

CHAPTER 7
DISCUSSION

7.1 INTRODUCTION

This section attempts to combine and explain all of the observations and conclusions made within the previous chapters. It was clear from the experiments that the failure mode of the joints is dependent on the method of pretreatment. A discussion on the finite element modelling carried out for T-peel and single lap shear bonded joints along with a discussion on experimental results is presented in this chapter. Also, the methodology to calculate the fatigue crack propagation rates and curves is discussed in this chapter. Various modelling issues faced have also addressed in this chapter.

7.2 GENERAL OBSERVATIONS OF FATIGUE TEST RESULTS

This section presents a discussion on the observation noted during the fatigue testing of T-peel and single lap shear bonded joints. With the results, the effect of surface pretreatments on the failure of adhesively bonded joints has been investigated. The fatigue test on T-peel bonded joints and single lap shear bonded joints were conducted to obtain test data to combine it with finite element results of the same joints to calculate crack propagation rates.

To combine and correlate the finite elements models results, it was decided to prepare the joints having initial crack lengths. A minimum of three cracks lengths were tested in order to get a good curve fit on crack propagation curves. The stiffness method was investigated only for Mode I loading in this research.

In this research, the fracture mechanics approach was chosen as a method for testing and analysis of bonded joints because fracture tests display a more controlled failure mode than maximum strength based tests which usually failed catastrophically. As a result not only these tests provides a more detailed test data but also provides a more fundamental understanding of the failure mechanisms of the adhesively bonded joints. Fracture mechanics based tests applied the concept of strain energy release rates (SERR) to analyse and describe the crack propagation phenomena. In adhesive systems, the critical SERR can be a function of variables such as adherend materials, surface

pretreatment, adhesive layer thickness, etc. The total energy released via crack propagation in a bonded joint can be decomposed into three major components corresponding to the modes by which debonding can occur: opening (mode I), shearing (mode II), and tearing (mode III) as described in chapter no 3.

The artificial precracks were introduced in the adhesive bonded joints to conduct the fatigue tests based on fracture mechanics based method. The precrack was introduced by using PTFE film during adhesive joints preparations. The other reason for introducing precracks in the adhesive joints was record the crack propagation in these joints. The precracks length employed in bonded joints were 3.0mm, 5.0mm, 7.0mm and 9.5mm.

The fatigue tests were conducted for T-peel and lap shear bonded joints using different sheet thickness. The thicknesses used in the adherends are 2.0mm, 3.0mm and combination of these two sheet thicknesses. The T-peel joints were tested at different load levels of 0.5kN, 0.75kN for T22B joints, 1.1kN to 1.2kN for T33 bonded joints and 0.51kN to 0.6kN for T23 bonded joints. All these loads for peel joints have chosen in such a manner that the load levels remains below the threshold levels of adhesive. Whereas single lap shear joints were tested at a load levels of 8kN for LS22 bonded joints and 9kN for LS33 bonded joint.

The first thing we have noticed while testing the T-peel bonded joints was the consistency of the fatigue test data of these joints. This consistency was noted from the stiffness and displacement drop off curves of these joints for every precrack length as given in appendix 2. This is probable due to the fact that adherends used in these joints were pretreated by using PAA pretreateatment, which is considered to be the best treatment for aluminium adherends (Redux 2002).

The first peel joints tested in this research was T22B joints. These joints were tested with precrack lengths of 3.0mm, 5.5mm, 7.0mm and 9.5mm. The testing was conducted in two stages. In the first stage, a load of 0.5kN was applied and the joints were rran for 3000 or 4000 cycles at this load to open the precrack without growing the crack into the adhesive. These values were useful in calculating the stiffness of the joint for different precrack lengths. In the next stage, the load level was increased to 0.75kN, the crack propagates within the adhesive and the joint finally separated out. The failures observed in all these

joints were purely cohesive since the crack propagated within the adhesive layer. From the fatigue test results of T22B joints, the low cycle fatigue failure was observed.

Unfortunately,It was noted during the stiffness calculations of T22B joints that the calculated stiffness values in fatigue test data of these doesn't correlated well with stiffness values calculated in FE data of these joints. This was due to the method of measuring displacements of the coupon measured in FE model and in fatigue testing, i.e. the displacement in FE model of T22B joint were measured on the coupon itself while in fatigue testing, the displacements were measured across the frame of the machine. Measuring displacement across the frame of the machine includes the displacement of the coupon itself and displacement of the crosshead. A CAE analysis was then conducted on Jaguar Land Rover premises to investigate this difference. It was found from this analysis that the best stiffness correlations can be achieved (within 10%) if the effects of poisons ratio was neglected in FE models. Also, the displacement should be measured across the coupon itself by using strain gauge.

One of the observations noted from the testing of T22B joints that the test data was not refined and detailed in terms of threshold values. To get more consistent and detailed fatigue test data, the T23B and T33B joints were tested at the low load levels. The levels were chosen in such a way that it lies below the threshold of adhesive. Strain gauge was used for measuring the displacements of T23B and T33B precracked coupons. The crack propagation was also recorded for T33B joints and T23B 5.0mm precracked joints. During the testing of T23B joints, it was noticed that strain gauge some time picked up high frequency vibrations due to which it got detached during the test and the test was restarted again. The failures noted in all of these joints were purely cohesive, i.e. the precrack grows into the adhesive film. A high cycle fatigue failure was observed from the test results of the T23B and T33B joints.

Single lap shear bonded joint was other configuration investigated in this research. As the name indicates, these joints were made by overlapping one sheet over the other. These joints were tested without having any precracks in them. The aluminium substrates used in single lap shear bonded joints were pretreated by using silica pretreatment. These joints were tested at the load

levels of 8kN for LS22B joints and 9kN for LS33B joint. During testing, the joints were subjected to mixed mode loading due to the shear loading across the bondline thickness. The failure observed in these joints was interfacial failure across the top sheet. In LS22B joint, it was observed that the crack propagated from the front side of the joint and in other LS22B joint, the crack was propagated from the rear side of the joints as a result of which the crack propagation was not recorded for this joint. The same trend was noted for LS33B joint too.

It was observed from the testing of the single lap shear joints that they have the poor fatigue performance as compared to PAA pretreated peeled joints. As soon as the crack initiated into the joint, it propagated very quickly and failed the joint immediately. In case of PAA pretreated joints, the crack propagates cohesively through the adhesive and this was the reason for superior fatigue performance over single lap shear joint. What was important to note from these fatigue tests is the superior performance of PAA pretreatment over other treatment methods in enhancing the fatigue life of bonded joints.

As mentioned earlier, the surface preparation of adherends for adhesive bonding has been realized to be a dominating factor in the performance and durability of adhesively bonded components. These pretreatment were used to develop an adherends surface that optimizes the bonding at the adhesive-adherend interface. Surface pretreatments may also modify the topography of the adherend which may increase the mechanical interlocking between the adhesive and the adherend (Minford 93). PAA pretreatment falls under the category of anodising treatments. The main purpose of anodising treatments is to form a porous oxide layer on top of the oxide layer formed after etching. The porous oxide layer enables adhesive to penetrate the pores to form a strong bond (Minford 93). The layer thickness formed with various surface treatments for aluminium is shown in table.7.1. The superior bond durability of PAA over other commonly used pretreatments is shown in figure 7.1.

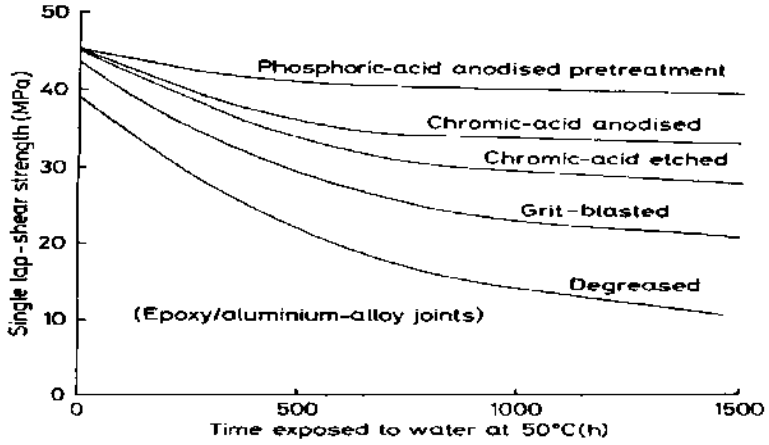

Figure 7.1: The superior bond durability of PAA over the other commonly used pretreatment methods (A.J. Kinloch 1983).

The oxide layer formed by PAA is relatively thin, extending to around 800nm, with much larger and more open process. Such a thin and highly porous oxide doesn't provide good corrosion resistance on surfaces directly exposed to environment (Bishopp 88 and Minford 93). Though the adhesive is able to penetrate and partially fill the open PAA pores. This action provides more surface area over adsorption bonding can take place, and enables a significant amount interlocking to occur (Albericci 1983 and Bishopp 1988). Venables et al. (J.D. Venables 1979) showed that when the oxide structure on PAA treated aluminium interlocks mechanically with the adhesive, it forms a much stronger bond than possible with a smooth oxide. In addition to the microporous cell structure, the protruding oxide whiskers are thought to make a valuable additional contribution to the bond strength. Thus, Boeing's PAA process is widely regarded as the best pretreatment available for producing durable adhesive bonds made from aluminium alloys. This method of pretreatment is more suitable for aluminium alloy 5754 since heat treatment of magnesium-containing alloys increases both the oxide layer's thickness and its magnesium content (Sapa 2003). Anodizing in phosphoric acid gives a thin and magnesium-poor boundary layer with very good durability. Table.7.2 gives an idea of how various surface treatment methods effect magnesium content in the oxide and the durability of the bonded joint made from aluminium alloy 5754.

Table 7-1: Layer thickness with various surface treatments for aluminium (Redux 2002)

Surface treatment	Thickness, approx.
Chromic/sulphuric acid pickling	40 nm
Phosphoric acid anodizing	400 nm
Chromic acid anodizing	1,500 nm
Sulphuric acid anodizing	15,000 nm

Table 7-2: Magnesium content in the surface in relation to the long term strength of bonded joint (Sapa 2003).

Surface treatment	Al:Mg ratio	Joint's long-term strength
Degreasing	6:1	Very poor
Sand blasting	15:1	Moderate
Chromic acid pickling	57:1	Good
Phosphoric acid anodized	110:1	Very Good

7.3 DISCUSSION ON ANALYSIS OF BONDED JOINTS AND VALIDATION OF THE STIFFNESS METHOD

The fatigue test data obtained by the testing of T-peel and single lap shear joints were combined with the stiffness results of FE model data to calculate fatigue crack propagation rates and obtain the fatigue crack growth curves. The analysis was done by using the stiffness method explained in chapter 6.

The method proposed here is based upon the stiffness drop approach. From the FE damage models, the stiffness and energy release rates were calculated for T-peel and single lap shear bonded joints. Curves were plotted for stiffness and energy release rates of bonded joint FE models with respect to crack length. The method then makes the use of standard curve fitting techniques to obtain the equations of stiffness and energy release rates in FE models. These equations from the FE models were used in fatigue test data of bonded joints to calculate

the crack propagation rates. The crack growth rates curves were obtained by plotting crack propagation rates and energy release rates on log-log scale.

This method mainly depends upon the selection of proper curve fitting method by which accurate crack propagation rates can be obtained. The determination of fatigue crack growth rates from fatigue test data is certainly a tedious job. There are numerous curve fitting models proposed to calculate the crack propagation rates and reduce the scattering in fatigue test data including the standard ASTM methods as well. We know that, fatigue crack propagation is a continuous physical process of material damage which is characterised by the rate of change of crack length (a) vs. number of cycle's data from the measurements of various specimens. Unlike monotonic tests, fatigue test results contain a large amount of scatter.

In recent years, many crack growth rate models have been proposed and used to predict the fatigue life under various conditions which primarily deals with the relationships between the fatigue crack growth rates and the crack drive forces, which are often expressed in terms of stress intensity factors. In majority of instances, the method of crack growth rates from fatigue test data is not explicitly mentioned. The most widely used techniques used in determination of crack growth rates are:

- By calculating the finite differences between successive data points in fatigue test data and making a linear interpolation to estimate the gradient at the midpoint (Mukherjee 1972).
- Fitting the best smooth curve in the a-N data and then taking the gradients of the slope (Smith 1973).
- Fitting an analytical curve (i.e. Polynomial fit, Power law fit) through all or part of the data (K. B. Davies 1973). This is the approach we have used by fitting a curve in the FE models to get the line of best fit and then used the same equation to calculate the crack growth rates and energy release rates of bonded joints.
- Using orthogonal cubic polynomial method for fitting cubic expressions to equidistantly spaced crack length measurements (Munro 1973).

- By using spline technique both for interpolation and data smoothening (Polak 1975).
- By using moving averages method.
- By incremental polynomial method fitting a second order polynomial to a set of 2n+1 points, where n = 1, 2, 3, ...successive data points (ASTM 647-308).

Each method described above has got its own merits and demerits. The crack growth rate obtained for bonded joints in this research contains a large amount of scatter due to large number of data points and also, some negative terms in fatigue crack growth rates. Hence, it was necessary to use some means of data smoothening. The most simple and attractive technique is to fit a polynomial curve through the data and then use the same equations to calculate the fatigue crack propagation rates.

When the crack growth rates and energy release rates from fatigue tests were plotted on log-log scale, a heavy scatter was observed in the crack growth rates curves of T-peel bonded joints. This was due to negative terms which were noted in the fatigue test data while calculating the crack propagation rates (figure. 7.2).

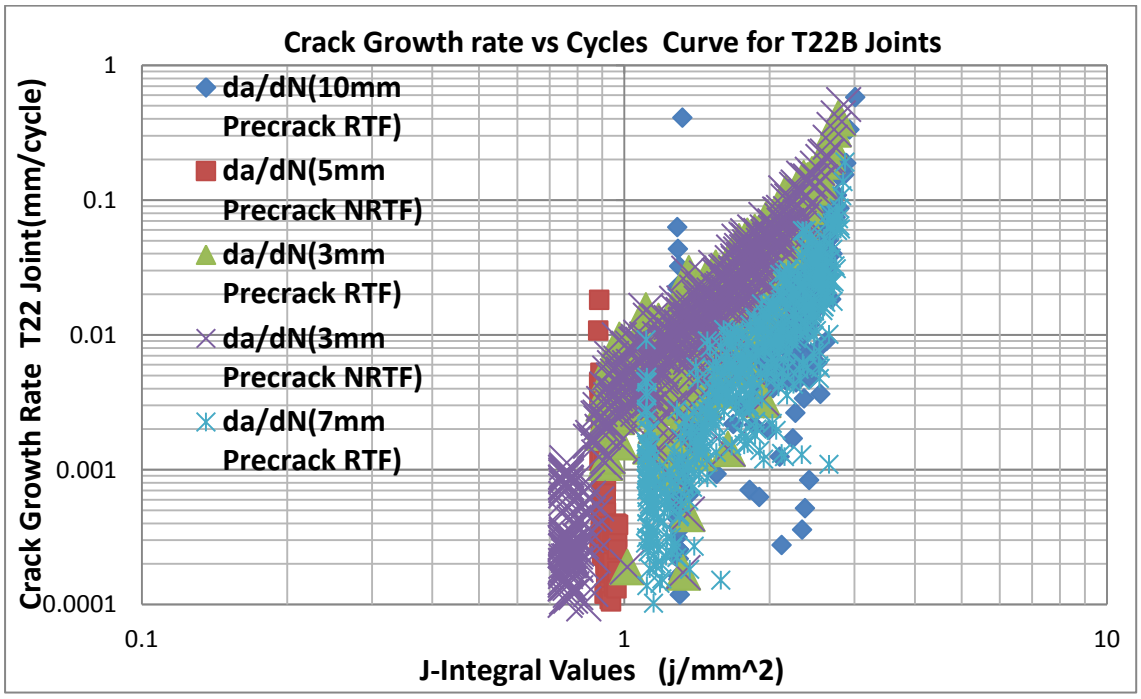

Figure 7.2: Scattering observed in crack growth rate curve of T22B joints

A cubic polynomial was used to calculate the crack propagation rates in fatigue test data of T-peel bonded joints as the use of cubic polynomial curve in FE models correlates well with the fatigue test data of peel joints. However, the applicability of this method was first questioned by Davies and Feddersen (K.A. Davies 1973) because of the requirement of a higher order polynomial curve for entire data range which suffers from various inflexions like negative terms in the crack growth rate observed in fatigue tests data of T-peel joints. Although the higher order polynomials gives a better value of regression coefficient (R^2 value), the value of standard error of estimates increases due to the presence of negative terms in fatigue test data. This problem was overcome by taking the absolute values of fatigue crack growth rates and taking the moving averages of crack growth rates and energy release rates, a very smooth fatigue crack growth curves can be obtained. One of such curve was obtained for T22B joints is shown in figure.7.3 Due to this reason, the polynomial curve fitting was used to calculate fatigue crack propagation rates of T-peel bonded joints.

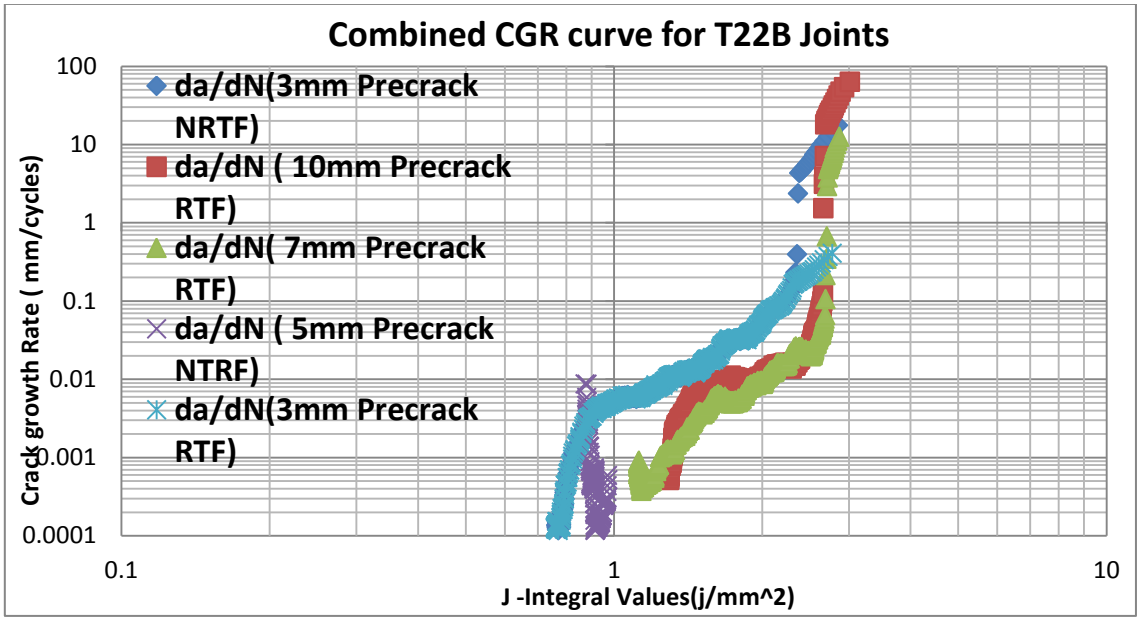

Figure 7.3: Crack growth curve of T22B joints obtained after taking the absolute values and applying moving average methods.

Same cubic polynomial curve fit was used in fatigue test data of single lap shear bonded joints. Some issues were noted in submodelling of single lap shear

bonded joints. To overcome this problem, the bespoke models were prepared for single lap shear joints by modelling the crack lengths upto 3.5mm. During the analysis of these joints, it was noted that curve fitting used doesn't correlate well with stiffness results of fatigue test data of lap shear joints. Though the curve obtained by using this method resembles the shape of Paris law shape and nature as discussed in chapter no 6. In case of T- peel bonded joints, 19 cracks were plotted which gives the higher value of coefficient of regression whereas for lap shear joints, 7 cracks values were plotted which gives a poor value of coefficient of regression. Hence, better results can be obtained by modelling large number of cracks in lap shear joints.

From the shapes of fatigue crack curve obtained for T-peel bonded joints, it is clear that the curves of all precracked joints are lying very close to each other and behaves in a similar way as of standard Paris law curve. The shapes of all curves are sigmoidal in shape thus proving the effectiveness of the stiffness method for this joint. The same nature and shape of Paris law curve was observed for single lap shear bonded joints as well. Hence, the stiffness method investigated in this research work can effectively predict the fatigue crack propagation rates and obtain the fatigue crack propagation curves of similar nature and shape as that of Paris law curve. The major limitation of this method as mentioned earlier is that it was investigated for Mode I loading. As the name of joint T-peel indicates, this type of geometry only experiences Mode I loading and peel (normal) stresses are more dominant in fatigue crack propagation. Hence, this method can be effectively used for T-peel bonded joints within the mentioned limitation.

The stiffness method was also validated against the recorded crack propagation videos. The crack propagation videos were recorded during the test by using a high resolution microscope with a rate of 15 frames per second. The crack propagation was recorded for T33B. T23B with 5.5mm precrack and for LS22B and LS33B joints. The method was validated for T33B and LS22B joints. The cycle rate per second used was calculated from fatigue test data and a scale factor was used in the crack propagation videos to measure the crack length at subsequent time intervals. These cracks were measured from the point of crack

propagation uptill the time the joint finally separated out. Using the similar number of cycles from the fatigue test data of these joints, the crack lengths calculated by using the stiffness method were taken and plotted against the measured crack lengths from crack propagation videos.

The first joint tested for validation was T33B joint with no precrack in it. A very poor correlation was observed between the measured crack lengths and calculated crack length from the fatigue test data for T33B joint with no precrack. Since the tests conducted was based upto fracture mechanics approach, which assumed the presence of pre-existing cracks in the body itself. A better correlation was then observed as soon as the artificial precracks were introduced in the bonded joints. The best correlation was obtained for the joints having large precrack length. Hence, from the validation in case of T-peel joints, it was clear that the stiffness method is most suitable for joints having precracks in them since a larger value of crack length when put in cubic polynomial expression gives a value of stiffness comparable with the stiffness of FE models. But there should be a limitation on the use of crack length along with the degree of polynomial used to calculate the fatigue crack propagation rates. Though, the use of higher order polynomial slightly improves the accuracy but increases the complexity in the calculation of fatigue crack propagation rates.

The stiffness method was also validated for single lap shear bonded joints as well. The failure observed in these joints was interfacial failure across the top sheet. The interfacial failure was probably due to the weak adhesive adherend bonding. During testing of this joint, it was observed that the joint was subjected to mix mode loading (Mode I + Mode II) across the overlap ends. An opposite trend was noticed between the measured crack length in the crack propagation videos and crack lengths calculated using stiffness method. Hence, the methodology was not validated for single lap shear joints.

7.4 FINITE ELEMENT MODELLING ISSUES IN T-PEEL AND LAP SHEAR BONDED JOINTS

This section summarizes the modelling work conducted on T-peel and single lap shear bonded joints for this research work. The two dimensional models were prepared for T-peel and single lap shear bonded joints. These damage models

were based on fracture mechanics based tools in abaqus. The damage models were modelled upto elastic limit and are linear in nature. The linearity in FEA models was proved by plotting the extracted stress intensity factors (K1) against the applied loads used in FEA models. Table 7.3 below shoes the extracted stress intensity factor values using Perl scripting against applied loads in FEA models of bonded joints.

Table 7-3: Stress intensity factor data extracted out for FE models using PERL scripting

Load Applied(N)	Crack Length	SIF K1						
1000	CRACK_5	K1:	60.81	60.22	60.53	60.73	60.82	60.622
1200	CRACK_5	K1:	72.95	72.24	72.62	72.86	72.96	72.726
2000	CRACK_5	K1:	121.6	120.4	121.1	121.5	121.6	121.24
3000	CRACK_5	K1:	182.4	180.7	181.6	182.2	182.5	181.88

The stress intensity factors were plotted against the applied loads as shown in figure.7.4 Only one set of values are plotted in the given curve to show the linearity.

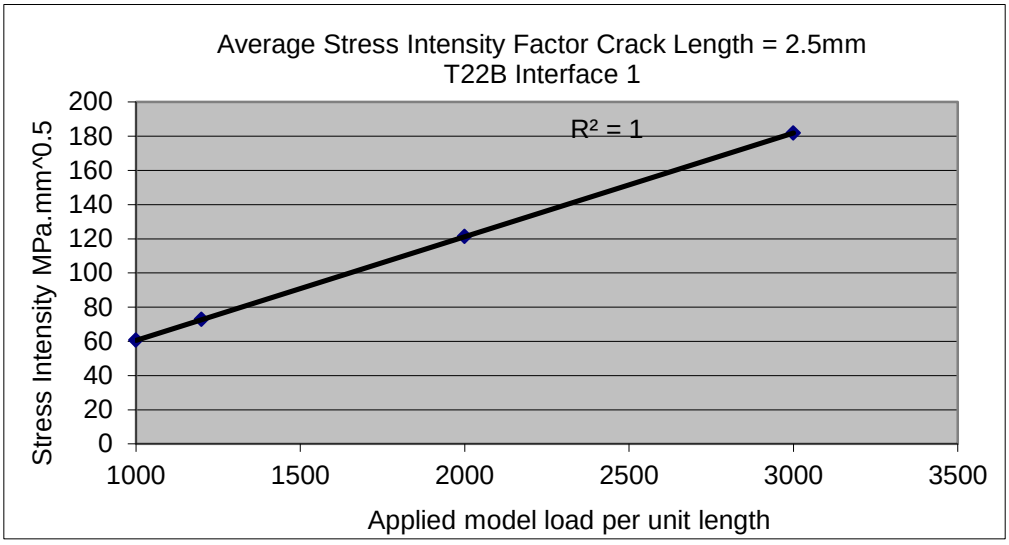

Figure 7.4: Linear checks for FEA damage models of bonded joints

It is evident from the above curve that stress intensity factors follows a linear pattern with the applied loads thus proving that all the damage models modelled are purely linearly in nature, i.e. the stiffness of the FE models decreases linearly with increase in crack length. Plasticity effects are not included in these damage models.

Adhesive bonding in the damage models were modelled by using sub-modelling approach in abaqus. This approach was first used by Crocombe et al. (A.D. Crocombe 1994) and Bogdanovich et al. (Bogdanovich 1999) to model the composites with adhesive joints. The damage models were modelled in two parts - global model and sub model. These damage models were run by using node displacement method and elements from the bondline region were deleted at each and every incremental time step representing the opening and closing of cracks.

In the damage models, there were 19 steps in the analysis and each time step a crack growth of 0.5mm were simulated. The maximum crack length modelled in damage models was 9.5mm. The sub-models developed using driven nodes of global models were used to extract out the energy release rates associated with each simulated crack length. The strain energy release rates were extracted in form of stress intensity factors and J-Integrals. The J-integral values were then used in bonded joints analysis due to their ease of calculation and excellent numerical approximation as it gives the more accurate values. The submodelling technique is used to study a local part of the model with a refined mesh based on interpolation of the solution from a relatively coarse, global model. This technique is most useful when it is necessary to obtain an accurate, detailed solution in a local region. It can also be used to drive a local part of the model by using nodal results, such as displacement, or by the element stress results from the global mesh. The submodelling based on nodal results is known as node based submodelling and those based on elements results is known as surface based submodelling.

Three crack regions were modelled in the damage models of T-peel and single lap shear bonded joints (*sec 5.5 of chapter 5*). The locations modelled are:

- Interface 1 along the top sheet.
- Interface 2 along the bottom sheet.
- In the adhesive bonded region.

7.4.1 SUBMODELLING ISSUES IN T-PEEL AND LAP SHEAR BONDED JOINTS

The sub-modelling approach seems to work quite well for T-peel bonded joints. It was noted during the analysis that there were some negative terms of stress intensity factors in LEFM sheet of T-peel bonded joints. It was found that refining of the mesh in the adhesive bonded region can overcome this problem. When the same models were simulated again after the mesh refinement, the negative stress intensity factors were then removed from the LEFM sheets of T-peel bonded joints. The differences in the deflection of T-peel joints were also noted as shown in figure.7.5. This was observed due to the fact that the driven nodes were not restrained enough in the global model as a result of which the sub-model was free to move.

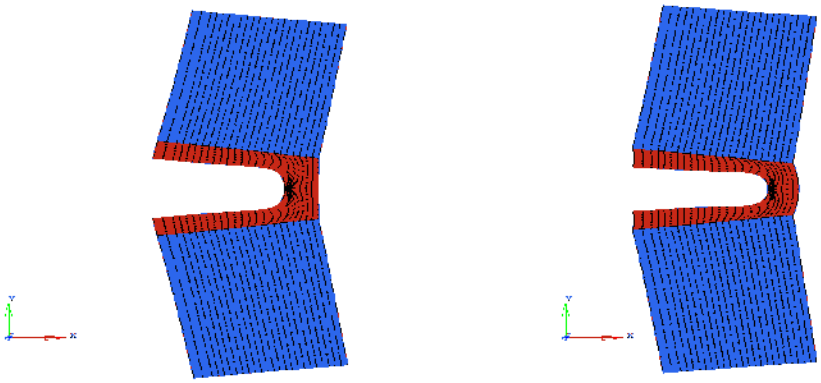

Figure 7.5: Differences in the deflection of sub-model and global model of T-peel bonded joints

Same modelling issues were noted for single lap shear bonded joints. It was noted in the damage models of lap shear joints that due to shear action across the bondline thickness, the lap shear joint was subjected to mixed mode crack opening across the top sheet as shown in figure.7.6. The difference in the deflection mode for lap shear bonded joints was also noted and is shown in figure. 7.7. This was due to the driven nodes which are not restrained enough in the global model. To overcome this problem for lap shear joints, and also, due to time constraint, the bespoke models for single lap shear joints were modelled upto a crack length of 3.5mm. These models were modelled without using the

submodelling approach and a very fine mesh was used in the adhesive bond region to extract out the energy release rates.

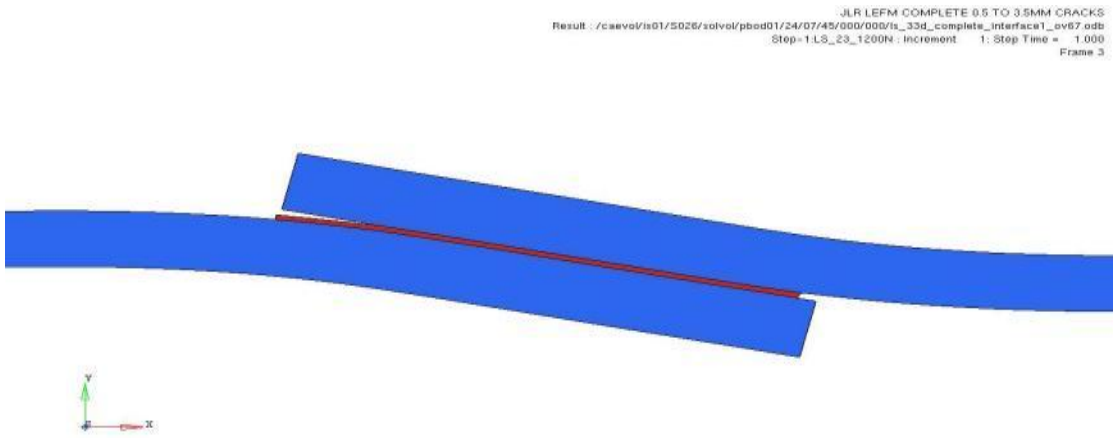

Figure 7.6: Lap shear simulation Mode I and Mode II crack opening

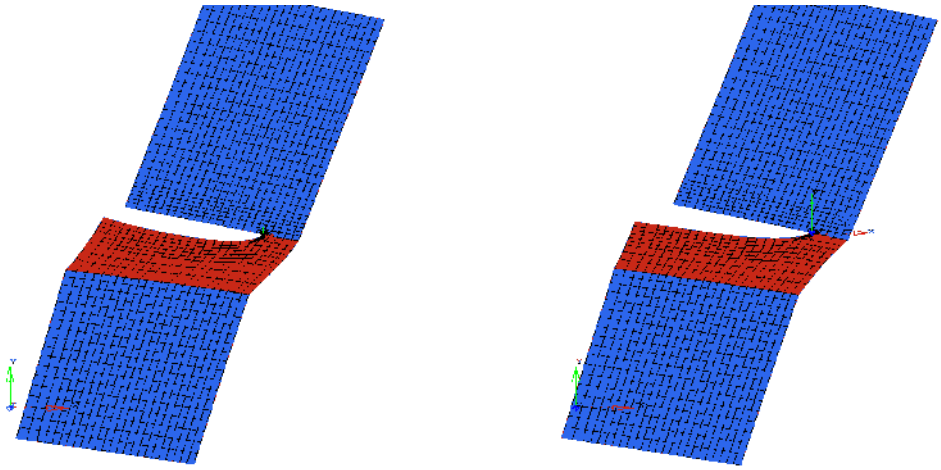

Figure 7.7: Difference in deformation mode of global model and sub-model of single lap shear bonded joint

As mentioned earlier that in damage models the failure of the joints was modelled for top sheet interfacial failure1, at the adhesive bondline thickness and interfacial failure on the bottom sheet 2. The failure noted in single lap joint testing was purely interfacial failure on the top sheet, hence to combine the stiffness drop of fatigue test data with the stiffness drop of FE model of single lap shear joints, the energy release extracted for the interfacial failure across the top sheet has been used in the analysis.

Hence, it can be concluded that the small differences in driven boundary nodes gives a big error in the submodelling approach used for lap shear bonded joints. It is likely that the global model requires more mesh refinement in the adhesive bond region to match better with the focused mesh of the sub model. More refined mesh in the global model can give the same deformation mode as sub model.

CHAPTER 8

CONCLUSIONS ANS FUTURE WORKS

8.1 INTRODUCTION

The main hypothesis of this research was to investigate a mathematical method of calculating fatigue crack propagation rates and obtaining the fatigue crack growth curves by combining the stiffness data of FE models of bonded joints with the stiffness in the fatigue test data of the same. The hypothesis was investigated by; (1) by developing the two dimensional damage models of T peel and single lap shear bonded joints (2) by fatigue testing of the same joints using different precrack lengths. The main conclusions of this research work and future recommendations are presented in this chapter.

8.2 CONCLUSIONS

The conclusions of this research work are as follows-

- The stiffness method investigated in this research work can effectively predict the fatigue crack propagation rates and obtain the fatigue crack propagation curves of similar nature and shape as that of Paris law curve.
- From the analysis of T-Peel and single lap shear bonded joints, it is shown that the method can be effectively used for T-Peel bonded joints subjected to Mode I loading but is not suitable for single lap shear bonded joints due to the mixed mode loading in these joints.
- The stiffness method is only valid and applicable for Mode I loading and joints having precracks in them since it is based on the principles of fracture mechanics. This method does not work for joints subjected to interfacial failure due to mixed mode loading.
- The method gives a very good correlation with the precracked bonded joints since it is based upon fracture mechanics based method.
- The submodelling approach used in damage bonded joint models works well for T-peel bonded joints with little modification in mesh across adhesive bond but it does not work for the single lap shear bonded joints due to the difference in the deformation modes of single lap shear joints, thereby, required more detailed focused mesh in the sub model.

8.3 RECOMMENDATION FOR FUTURE WORK

The stiffness method investigated for adhesively bonded joints can be further enhanced and improved by using proper curve fitting techniques to calculate the fatigue crack propagation rates. More investigation is required in understanding the curve fitting techniques to reduce the scatter in fatigue test data and to calculate the fatigue crack propagation rates.

The submodelling approach used in the damage models can further be improved by using very fine mesh in the sub-models. More detailed modelling methods based on fracture mechanics tools like cohesive zone modelling; Low cycle fatigue analysis should be investigated in detail to model the adhesively bonded joints using different failure criteria in abaqus. Practically, most of the adhesive bonded joints are subjected to plasticity; hence, plasticity effects may be included to study the failure of adhesively bonded joints. The inclusion of plasticity can provide more realistic prediction of stresses in the adhesively bonded joints. The effect of non-linearity should also be studied in the finite element models of adhesively bonded joints.

The stiffness method needs more investigation in case of lap shear joints since they are subjected to interfacial failure frequently. The method also needs investigation for joints without having any precracks in them. The influence of surface pretreatments and moisture effects should also be included in this investigation.

REFERENCES

Abaqus HTML Documentation. *Stress Analysis - Fracture Mechanics.* Rhode Island, USA: Dassault Systems, Oct, 2009.

Adams, R. D., Comyn, J. and Wake, W. C. *Structural Adhesive Joints in Engineering, 2nd Edition.* London, UK : Chapman and Hall, 1997.

Adams, R.D. *Adhesive Bonding: Science, Technology and Applications .* Cambridge, England: Woodhead Publishing House, 2005.

—. *Adhesive Bonding: Science, Technology and Applications.* Cambridge, England: Woodhead Publishing House, 2005.

Adams, R.D. and Crocombe, A.D. “Peel analysis using finite element method.” *Journal of Adhesives and Adhesion*, 1981: 127.

Adams, R.D. and Mallick, V. “A method for the stress analysis of single lap joints.” *Journal of Adhesives and Adhesion*, 1984: 65.

Adams, R.D. and Peppiat, N.A. “Effect of poissons ratio strain in adherends on stresses of an idealized lap joints.” *International Journal of Adhesives and Adhesion*, 1973: 134.

Adams, R.D. and Peppiat, N.A. “Effect of poissons ratio strain in adherends on stresses of an idealized lap joints.” *International Journal of Adhesives and Adhesion*, 1973: 134.

Adams, R.D. and Peppiat, N.A. “Stress analysis of adhesive-bonded lap joints.” *Journal of Strain Analysis:9*, 1974: 185.

Adams, R.D., Coppendale, J. and Peppiat, N.A. “Stress analysis of axisymmetric butt joints loaded in tension and torsion .” *Journal of Strain Analyses*, 1978.

Adams, R.D., Coppendale, J., Mallick, V. and Al-Hamdan, H. “The effect of temperature on strength of adhesive joints.” *International Journal of Adhesives and Adhesion.,12* , 1992: 185.

Adamson, M.J. “Thermal expansion and swelling of cured epoxy resin used in graphite/epoxy composite materials.” *J. Mat. Sci., 15*, 1980: 1736-1745.

Albericci, P. *Durablity of structural adhesives (edited by A.J Kinloch).* Applied Science Publishers,, 1983.

Aminopour, M.A. and Holsapple, K.A. “Near-field solutions for propagating cracks at the interface of dissimilar anisotropic elastic materials.” *Journal of Engineering Fracture Mechanics: 36*, 1991: 93-103.

Andruet, Raul H. *Special 2-D and 3-D Geometrically Nonlinear Finite Elements for Analysis of Adhesively Bonded Joints.* Virginia, USA: Virginia polytechnique Institute , 1998.

Armao, F.G. *Design and Fabrication of Aluminium Automobiles.* Corporate Report, Cleveland, Ohio: The Welding Technology Center, The Lincoln Electric Company, 2002.

Ashcroft, I.A., Critchlow,G.W., Crocombe, A.D. and Shenoy, V. “Unified methodology for the prediction of the fatigue behaviour of adhesively bonded joints .” *International Journal of Fatigue:32*, 2010: 1277-1288.

Audi . *www.audi.com spaceframe technology .* n.d.

Badari Narayana, K., Dattaguru, B., Ramamurthy, T.S. amd Vijayakumar, K. “A general procedure for modified crack closure integral in 3D problems with cracks.” *Journal of Engineering Fracture Mechanics*, 1994: 167-176.

Bahram, F. and Kamran, N. “Predicting fracture and fatigue crack growth properties using tensile properties.” *Journal of Engineering Fracture Mechanics: 75*, 2008: 2144-2155.

Barbero, E.J. and Reddy,J.N. “The jacobian derivative method for three dimensional fracture mechanics.” *Communication in Applied Numerical Methods .* 1992. 507-518.

Barosoum, R.S. “On the use of isoparametric finite elements in linear fracture mechanics.” *International Journal of Numerical Methods in Engineering*, 1976: 25-37.

Barsoum, W. and Carpenter, R. “Two finite elements for modelling of adhesive in bonded configurations.” *Journal of Adhesives and Adhesion* , 1989: 25-26.

Beer, G. “An isoparametric joint/interface elements for the finite element analysis .” *International Journal of Numerical Methods* , 1985: 30.

BIS. “BS EN 28510-1: 1993 Adhesives - Peel test for a flexible-bonded-to-rigid test.” 1993.

BIS. “Determination of the mode I adhesive fracture energy G of structure adhesives using double cantilever and tapered double cantilever beam specimens.” 2001.

Bishopp, J.A., Sim, E., Thompson, G., and Wood, G. “The adhesively bonded aluminium joint: The effect of pretreatment of joint durablity .” *Journal of Adhesives and Adhesion, Vol 26*, 1988: 237-263.

Board, National Materials Advisory. *Structural Adhesives with emphasis on Aerospace Applications .* Marcal Dekker Inc, 1976.

Bogdanovich, A.E. and Kizhakkethara, I. “Three dimensional finite element analysis of double lap composite adhesive joint using submodelling approach.” *Journal of Composites, 30(6)*, 1999: 537-551.

Brewis, D.M., J. Comyn, A.K. Raval, and A.J. Kinloch. “The effect of humidity on the durability of aluminium-epoxide joints.” *International Journal of Adhesives and Adhesion, 10(4)*, 1990: 247-253.

Brewis, D.M., J. Comyn, R.J.A. Shalash, and J.L. Tegg. “Interaction of water with some epoxide adhesives.” *Polymer, 21*, 1980: 357-360.

Briskham, P. and Boomer, D. “Joining Processes for Low-Carbon Automotive Applications.” *Material Congress, Institute of Materials .* 2006.

Briskham, P. and Mehta, M. *Bonded joint manufacturing process.* MTARG, Coventry University, UK , 2010.

British Standard Institute. “BS 5350-C13: 1990 Adhesives - Part C13: Climbing drum peel test.” 1990.

Brussat, T.R., Chiu, S.T. and Mostovoy, S. *Fracture Mechanics for structural adhesive bonds final report .* AFML-TR-77-163, Ohio, USA: Air Force Materials Laboratory, 1977, 1977.

Budzik, Micheal K. *Fracture in Asymmetri Bonded Joints.* PhD thesis , GDANSK University of Technology , 2010.

Byskov, E. “The calculation of stress intensity factors using finite element method with cracked elements.” *International Journal of Fracture Mechanics*, 1970: 159-167.

Callister, W.D. *Material Science and Engineering: An Introduction .* NewDelhi, India: TataMcgraw Hill, 2007.

Chai, H. “Observation of deformation and damage at the tip of cracks in adhesive bonds loaded in shear and assessment of a criterion for fracture.” *Znt. J. Fract., 60*, 1993: 311.

Chen, D. and Cheng, S. “An analysis of adhesive bonded single lap joint.” *Journal of Applied Mechanics*, 109: 1983.

Chen, D., Cheng, S. and Yupu, S. “Analysis of adhesive bonded joints with non-identical adherends .” *Journal of Applied Mechanics* , 1991: 605.

Clark, J.D. and McGregor,I.J. “Ultimate tensile stress over a zone: a new failure criteria for adhesive joints.” *International Journal of Adhesives and Adhesion: 40*, 1992: 1.

Cole, G. S. and Sherman, A. M. “Lightweight Materials for Automotive Applications:.” *Materials Characterization, 35*, 1995: 3-9.

Combyn, J. *Adesion Science .* The Royal Society of Chemistry, 1997.

—. *Durability of Structural Adhesive (Edited by A.J. Kinloch).* New York: Applied Science Publishers, 1983.

Comrie, R. *Dielectric Studies of the Durability of Aluminium/Epoxy Bonded Systems.* PhD Thesis, University of Strathclyde, 1998.

Cook, R.D. *Finte Element Modelling for stress analysis.* John Wiley and Sons , 1995.

Cook, T.S. and Tracey, D.M. “Analysis of power type singularities using finite elements.” *International Journal of Numerical Methods in Engineering*, 1977: 1225-1235.

Coppendale, J. *The stress and failure analysis of structural adhesive joints.* PhD Thesis, Bristol, UK: University of Bristol, 1997.

Corporation, Hexcel. “Redux Bonding Technology .” 2002.

Critchlow, G.M. and Brewis, D.M. “Review of surface pretreatments for aluminium alloys.” *International Journal of Adhesives and Adhesion, 16*, 1996: 255-275.

Critchlow, G.W. *Private communication .* Insitution of Surface Science, Louborough University, UK, 1997.

Crocombe, A.D. and Adams, R.D. “Influence of spew fillet and other parameters on the stress distribution in single lap joint.” *Journal of Adhesives and Adhesion*, 1981: 127.

Crocombe, A.D. and Goefong, Wu. “Simplified finite element modelling of structural adhesive joints .” *International Journal of Numerical Methods in Engineering*, 1994.

Crocombe, A.D., Bigwood, D.A. and Richardson, G. “Analysising structural adhesive joints for failure.” *International Journal of Adhesives and Adhesion*, 1990: 167.

Crocombe, A.D., Richardson, G. and Smith, P.A. “A unified approach for predicting the strength of cracked and noncracked adhesive joints.” *International Journal of Adhesives and Adhesion:49*, 1995: 211.

Dattaguru, B., Everett Jr. R.A., Whotcomb, J.D. and Johnson, W.S. “Geometrically non-linear analysis of adhesively bonded joints .” *Journal of Engineering Materials and Technology 106*, 1984: 59-65.

Davidson, B.D., Hu, H. and Schapery, R.A. “An analytical crack-tip element for layered elastic structures.” *Transactions of ASME 62.* 1995. 294-305.

Davies, K.B. and Feddersen, C.E. “Evaluation of fatigue crack growth rate by polynomial curve fitting.” *International Journal of Fracture, vol 9*, 1973: 116-118.

Davies, R.G.H. and Adams, R.D. “Strength of joints involving composites.” *Journal of Adhesives and Adhesion*, 1996: 59.

Davis, G.D. and Shaffer, D.K. *Handbook of Adhesive Technology (Edt by K.L. Mittal).* New York: Marcel Dekker Inc, 1994.

Dillard, D.A. and A.V. Pocius. *The mechanics of adhesion. Adhesion Science and Engineering .* Amsterdam: Elsevier Science, 2002.

Dow Automotive . “BETAMATE Epoxy 4601 Structural Adhesive .” Technical datasheet , Michigan , 2008.

Doyle, G. and R.A. Pethrick. “Environmental effects on the ageing of epoxy adhesive joints .” *International J. of Adhesion and Adhesives; 29(1)*, 2009: 77-90.

Fernlund, G., Papini,M., Mccammond, D. and Spelt, J.K. “Fracture load predictions for adhesive joints.” *Journal of Composites Materials Technology: 51*, 1994: 587.

Gettens, R.J. and Stout, G.L. *Painting Materials.* New York: Van Nostrand Reinhold, 1942.

Gledhill, R.A., Kinloch, A.J. and Shaw, S.J. “Effect of moisture on bonded joints durability.” *Journal of Adhesives and Adhesion, 11* , 1980: 3.

Goland, M. and Reissner, E. “The stresses in cemented joints .” *Journal of Applied Mechanics* , 1944: A-17-A-27.

Gradin, P.A. and Groth, H.L. *A fracture criteria for adhesive joints in tens of material inducced singularities.* Report No. 83-12, Stockholm : The Royal Institute of Technology , 1984.

Greenwood, L., Boag, T.G. and Mclaren,A.S. *Stress distribution in single lap joints in Adhesion: Fundamentals and Practice.* London, Uk : Mclaren, 1969.

Group, Material Technology Applied Research. *Lap joint analysis report.* Coventry, UK : Faculty of Engineering and Computing, Coventry University , 2010.

Gunawardana, Suranga. *Prediction of failure initiation of adhesively bonded joints using mixed-mode fracture data.* Wichita State University , Dec 2005.

Haber, R.B. and Koch, H.M. “Explicit expressions for energy release rates using virtual crack extension method .” *International Journal of Numerical Methods in Engineering : 21*, 1985: 301-315.

Hand, H.M., C.O. Arah, D.K. McNamara, and M.F. Mecklenburg. “Effects of environmental exposure on adhesively bonded joints.” *Int. J. Adhesion and Adhesives; 11(1)*, 1991: 15-23.

Harris, J.A. and Adams, R.D. “Strength prediction of bonbed single lap joints by non-linear finite element methods.” *Journal of Adhesives and Adhesion*, 1984: 65.

Harris, J.A. and Adams, R.D. “Strength prediction of bonded single lap joints by non-linear finite element methods.” *Journal of Adhesives and Adhesion* , 1984: 65.

Harris, J.A. and Adams, R.D. “The influence of local geometry on the strength of adhesive joints.” *Journal of Adhesives and Adhesion*, 1987: 69.

Hart-Smith, L.J. *Adhesive bonded single lap joints.* NASA CR-112236 , 1973.

Hellen, T.K. “On the method of virtual crack extensions .” *International Journal of Numerical Methods in Engineering: 9*, 1975: 185-207.

Hellen, T.K. “Virtual crack extension method for non-linear materials.” *International Journal of Numerical Methods in Engineering: 28*, 1989: 929-942.

Henshell, R.D. and Shaw, K.G. “Crack tip elements are unnecessary.” *International Journal of Numerical Methods in Engineering:28*, 1989: 929-942.

Hu, G.K. “Non-linear fracture mechanics for adhesive joints.” *International Journal of Adhesives and Adhesion: 37*, 1992: 261.

Ikegami, M., Kishimoto, W., Okita,K., Nakayama, H. and Shirato,M. “Strength of adhesively bonded scarf joint between glass fibre reinforced plastics and metals.” *Proceedings of Structural Adhesives in Engineering: Institute of Materials.* London, UK , 1969.

Instituion, British Standard. “Adhesives- Determination of tensile lap shear strength of rigid to rigid bonded assemblies.” 2003.

Institute, British Standard. “BS ISO 4587: Adhesives - Determination of tensile lap-shear strength of rigid to rigid bonded assemblies.” (British) 2003.

ISO. *Adhesives- Peel test for a flexible bonded to rigid test specimen assembly-part1.* ISO, 1990.

J. D. Venables, D. K. McNamara, J. Chen, T. S. Sun, and R. L. Hopping. “Characterisation of aluminium surfaces prepared for adhesive bonding,” .” *Structural Adhesive Bonding Conference.* California : Technol. Conferences Assoc., El Segundo, 1979b. 11-23.

J.D. Venables, D.K.McNamara, J.Chen, T.S.Sun and R.L Hopping. “Oxide morphologies on adhesively bonded aluminium structures.” *Journal of Applie Surface Sciences, 3-88*, 1979.

Karachalios, V.F. *Stress and failure analysis of adhesively bonded single lap joints.* Bristol, UK : PhD thesis University of Bristol, 1999.

Kinloch, A. J. “Adhesives in Engineering.” *Proceedings of the Institution of Mechanical Engineers Part G, 211.* 1997. 307-335.

Kinloch, A.J. *Adhesion and Adhesives.* London, UK : Chapman and Hall, 1987.

Kinloch, A.J. and Osiyemi, S.O. “Predicting the fatigue life of adhesively bonded joints .” *Journal of Adhesives and Adhesion 43*, 1993: 79-90.

Kinloch, A.J. and Shaw, S.J. “The fracture resistance of a toughened epoxy adhesive .” *International Journal of Adhesives and Adhesion: 12*, 1981: 59.

Kinloch, A.J. and Williams, J.G. “Crack blunting mechanisms in polymers.” *Journal of Material Sciences: 15*, 1980: 987.

Krueger, R. *The virtual crack closure technique - History, Approach and Applications .* Virginia, USA: NASA Inc. , 2002.

Lee, S.J. and Lee, G.L. “Similarity concepts in the fatigue fracture of adhesively bonded joints.” *Journal of Adhesives and Adhesion: 21*, 1987: 1-21.

Liljedahl, C.D.M., A.D. Crocombe, M.A. Wahab, and I.A. Ashcroft. “Modelling the environmental degradation of adhesively bonded aluminium and composite joints using a CZM approach.” *Int. J. Adhesion and Adhesives; 27*, 2007: 505-518.

Lin, C. and Liechti, K.M. “Similarity concepts in the fatigue fracture of adhesively bonded joints .” *Journal of Adhesives and Adhesion 21*, 1987: 1-24.

Loh, W.K., A.D. Crocombe, M.A. Wahab, and I.A. Ashcroft. “Modelling anomalous moisture uptake, swelling and thermal characteristics of a rubber toughened epoxy adhesive.” *Int. J. Adhesion and Adhesives, 25*, 2005: 1-12.

Lyrner, T. and Marklund, P.E. *Finite element analyses of adhesive joints with bondline flaws.* Stockholm: Royal Insitute of Technology , 1984.

Meguid, S.A. *Engineering Fracture Mechanics.* London, UK : Elsevier Science Publishers, 1989.

Minford, J.D. *Handbook of aluminium bonding technology and data.* ISBN 0-8247-8817-6, Marcal Dekkar inc., 1993.

Mnich, J. and Schoneman, C. “Sulphuric/Boric acid anodising status report: First 22 months of operation .” *38th Int. SAMPE symp.* May 10-13 1993.

Mostovoy, S. and Ripling, E.J. *In Adhesion Science and Technology .* NewYork , USA : Plenum Press , 1975.

MTARG. *Lap Joints Analysis Report.* Coventry : Faculty of Engineering and Computing, Coventry University, 2010.

Mubashar, Aamir. *Modelling Degradation in Adhesive Joints Subjected to Fluctuating Loading Conditions.* UK : Wolfson School of Mechanical and Manufacturing Engineering, Loughborough Universiy, Jan 2010.

Mukherjee, B. “A note on the analysis of fatigue test data.” *International Journal of Fracture, Vol 8*, 1972: 449-51.

Munro, H.G. “The determination of crack growth rates by data smoothening technique.” *International Journal of Fracture, Vol 9*, 1973: 366-368.

Mushkhelishvili, N.I. *Some basic problems of the mathematical theory of elasticity (2nd ed.translated 1962).* Noordhoff, Groningen, The Netherlands: J.R.M Radog from 4th russian edition, 1963.

Nabousli, S. and Mall, S. “Thermal effects on adhesively bonded composite repair of cracked aluminium panels.” *Theoritical and Applied Fracture Mechanics 26*, 1997: 1-12.

Nikishkov, G.P. and Atluri, S.N. “Calculation of fracture mechanics parameters for an arbitary three dimensional crack, by thr equivalent domain integral method.” *International Journal of Numerical Methods in Engineering* , 1987: 1801-1821.

Owens, D.R.J. and Fawkes, A.J. *Engineering Fracture Mechanics: Numerical Methods and Applications .* Swansea, UK : Pineridge Press Ltd, 2001.

Packham, D.E.,. *Handbook of adhesion.* Chichester: John Wiley & Sons, 2005.

Parks, D.M. “The virtual crack extension method for nonlinear material behaviour.” *Computer Methods in Applied Mechanics and Engineering. vol 12*, 1977: 353-364.

Pocius, D.A. Dillard and A.V. *The Mechanics of Adhesion.* Elsiever Science , 2002.

Polak, J. and Knesl, Z. “On the fatigue crack growth rate evaluation from experimental data.” *International Journal of Fracture, Vol 11*, 1975: 693-696.

Rao, A.K., Raju, L.S. and Krishna Murty, A.V. “A powerful hybrid method in finite element analysis.” *International Journal of Numerical Methods in Engineering*, 1971: 389-403.

Richardson, G. *An investigation of interfacial failure of adhesive joints.* Surrey, UK: PhD Thesis, University of Surrey , 1993.

Rider, A.N. and Arnott, D.R. “SIA.” *Surf. Interface Anal., 24*, 1996: 583.

Saunders, D. *Preparing for adhesive bonding .* TWI Bulletin 460/3 , 1994.

Schmit, F. and Fraisse, P. “Fracture mechanics analysis of strength of bonded joints .” *Journals of Materials Technology* , 1992: 4-5.

Shih, C.F, B.Moran,and T.Nakamura. “Energy release rate across a three dimensional crack front in thermally stressed body.” *International Journal of Fracture, vol 30*, 1986: 79-102.

Shivakumar, K.N., Tan, P.W. and Newman, J.C. “A virtual crack-closure technique for calculating stress intensity factors for cracked three dimensional bodies.” *International Journal of Fracture Mechanics: 56*, 1988: R43-R50.

Smith, R.A. “The determination of fatigue crack growth rates from experimental data.” *International Journal of Fracture, Vol9*, 1973: 352-355.

Sneddon, I. *Adhesion. The distribution of stress in adhesive joints.* Oxford, UK : Oxford University Press., 1961.

Spaggiari, Andrea. *EFFICIENT MODELLING OF COMPLEX ADHESIVELY BONDED STRUCTURES BY STANDARD FINITE ELEMENT TECHNIQUES.* Portugal: Doctoral school in High Mechanics and

Automotive Design & Technology - Advanced Methods for Mechanical Design, 2003.

Taylor, R.L. and Zienkiewicz, O.C. *The Finite Element Method .* NewYork: McGraw Hill , 2002 .

Tong, P., Pian, T.H.H. and Lary, S.J. “An hybrid-element approach to crack problems in plane elasticity.” *International Journal of Numerical Methods in Engineering: 7*, 1973: 297-308.

Toya, M. “Fracture mechanics of interfaces.” *JSME Int. J. Sel: I: Solid Mech.,33*, 1990: 413.

Tracey, D.M. “Finite elements for determination of crack tip elastic stress intensity factors .” *Engineering Fracture Mechanics* , 1971: 255-256.

Trantina, G.C. “Fracture mechanics approach to adhesive joints .” *Journal of Composite Materials: 6*, 1972: 192.

Tsai, M.Y. and Morton, J. “Mechanics of laminated composite single lap joints.” *Mechanics of Composites*, 1993.

Tsai, M.Y., Morton, J. and Matthews, F.L. “Experimental and numerical studies of a laminated composite single lap adhesive joint.” *Journal of Composite Materials*, 1995: 1154.

Volkerson, O. “Die nietkraftverteilung in zugbenspruchten nietverbindungen mit konstant laschenquerschitten.” *Luftfahrtforschung*, 1938: 41.

Weitsman, Y. “An investigation of non-linear visoelastic effects on load transfer in a symmetric double lap joint.” *Journal of Ahesives and Adhesion :11*, 1981: 279.

Wheeler, M. J., Sheasby, P. G. and Kewley, D. “Aluminium Structured Vehicle Technology - A Comprehensive Approach to Vehicle Design and Manufacturing in Aluminium.” *SAE Technical Paper Series No. 870146*, 1987.

Wu, Z.A., Romeijn, A. and Wardenier, J. “Stress expressions of single lap adhesive bonded joints with disimilar adherends.” *Composite Structures* , 1997: 273.

Yang, C. and Pang, S.S. “Stress-strain analysis of single lap composite joints under tension.” *Journal of Engineering Materials and Technology:118*, 1996: 247.

Zhao, X. *Stree and failure of adhesively bonded lap joint .* Bristol: PhD thesis, Bristol University, UK , 1991.

APPENDIX 1

PERL SCRIPT USED TO EXTRACT OUT THE ENERGY RELEASE RATES FROM DAMAGE MODELS

```
#!/usr/bin/perl
#
# Check to see if user wants a non-standard search
# Read the abaqus data file
#
#Read from the command prompt tha master surface name this will be the second user input the first being the file name
$node_set_name = $ARGV[1];
open (DATAFILE,"$ARGV[0].dat") or die "Can't open file $ARGV[0] $!\n Usage j_integral_grep.pl abaqus dat filename without .dat CRACK surface name \n";
print "Reading data file $ARGV[0]....\n";
```

```
while(<DATAFILE>) {
chomp;
#Create a list of all the lines in the data file
push(@abaqus_data_file,$_);
}
close(DATAFILE);
print "Completed Reading $ARGV[0]\n";
print "The crack string is $node_set_name\n";
$count=0;
$linenumber=0;
#Find the table start
while ($count < @abaqus_data_file) {
        if ($abaqus_data_file[$count] =~ /I N T E G R A L/ and
$abaqus_data_file[$count] =~ /J/ and $abaqus_data_file[$count] =~ /E S T I M A
T E S/ and $abaqus_data_file[$count+8] =~ /$node_set_name/  ){
        push(@lines_j,$count);
      $count++;}
        elsif ($abaqus_data_file[$count] =~ /F A C T O R/ and
$abaqus_data_file[$count] =~ /K/ and $abaqus_data_file[$count] =~ /E S T I M A
T E S/ and $abaqus_data_file[$count+8] =~ /$node_set_name/ ){
        push(@lines_k,$count);
      $count++;}
        elsif ($abaqus_data_file[$count] =~ /T - S T R E S S/ and
$abaqus_data_file[$count] =~ /E S T I M A T E S/ and
$abaqus_data_file[$count+8] =~ /$node_set_name/ ){
        push(@lines_t,$count);
      $count++;}
      $count++;
}
```

```
#
$number_of_tables_k = @lines_k;
$number_of_tables_t = @lines_t;
$number_of_tables_j = @lines_j;
print "There are $number_of_tables_k K occurrences of table $ARGV[1] \n";
print "There are $number_of_tables_t T occurrences of table $ARGV[1] \n";
print "There are $number_of_tables_j J occurrences of table $ARGV[1] \n";
#
#
#Below is the routine for extracting the lines from
open (OUTFILE,">$ARGV[0]_$ARGV[1]_$ARGV[2].csv");
#Get the table headings only for element sets
$a = substr($abaqus_data_file[$lines_j[0]+4],30,14);
$b = substr($abaqus_data_file[$lines_j[0]+4],44,14);
$c = substr($abaqus_data_file[$lines_j[0]+4],58,14);
$d = substr($abaqus_data_file[$lines_j[0]+4],72,14);
$e = substr($abaqus_data_file[$lines_j[0]+4],86,14);
$f = substr($abaqus_data_file[$lines_j[0]],28,45);#table title for j
#
$aa = substr($abaqus_data_file[$lines_k[0]+4],30,14);
$bb = substr($abaqus_data_file[$lines_k[0]+4],44,14);
$cc = substr($abaqus_data_file[$lines_k[0]+4],58,14);
$dd = substr($abaqus_data_file[$lines_k[0]+4],72,14);
$ee = substr($abaqus_data_file[$lines_k[0]+4],86,14);
$ff = substr($abaqus_data_file[$lines_k[0]],28,45);#table title for k1
#
$aaa = substr($abaqus_data_file[$lines_t[0]+4],30,14);
$bbb = substr($abaqus_data_file[$lines_t[0]+4],44,14);
```

```
$ccc = substr($abaqus_data_file[$lines_t[0]+4],58,14);
$ddd = substr($abaqus_data_file[$lines_t[0]+4],72,14);
$eee = substr($abaqus_data_file[$lines_t[0]+4],86,14);
$fff = substr($abaqus_data_file[$lines_t[0]],28,45);#table title for t

#Print a table
#print "@line[0]\n";
#print "@lines_end[0]\n";
#print OUTFILE "$e\n";
#print OUTFILE "$f\n";
print OUTFILE "$f\n";
print OUTFILE "TABLE LOCATION $a $b $c $d $e\n";
$count = @lines_j[0];
$counta = 0;
$countb = 0;
while ($counta != $number_of_tables_j){
$countb = $countb+8;
print OUTFILE "$abaqus_data_file[$lines_j[$counta]+8]\n";
$counta++;
}
print OUTFILE "$ff\n";
print OUTFILE "TABLE LOCATION $aa $bb $cc $dd $ee\n";
$count = @lines_k[0];
$counta = 0;
$countb = 0;
while ($counta != $number_of_tables_k){
```

```
$countb = $countb+5;
print OUTFILE "$abaqus_data_file[$lines_k[$counta]+8]\n";
print OUTFILE "$abaqus_data_file[$lines_k[$counta]+9]\n";
$counta++;
}
#print OUTFILE "$eee\n";
print OUTFILE "$fff\n";
print OUTFILE "TABLE LOCATION $aaa $bbb $ccc $ddd $eee\n";
$count = @lines_t[0];
$counta = 0;
$countb = 0;
while ($counta != $number_of_tables_t){
$countb = $countb+5;
print OUTFILE "$abaqus_data_file[$lines_t[$counta]+8]\n";
$counta++;
}
close (OUTFILE);
#end
```

APPENDIX 2

RESULTS OF THE ANALYSIS

1. T Peel 22B Curves

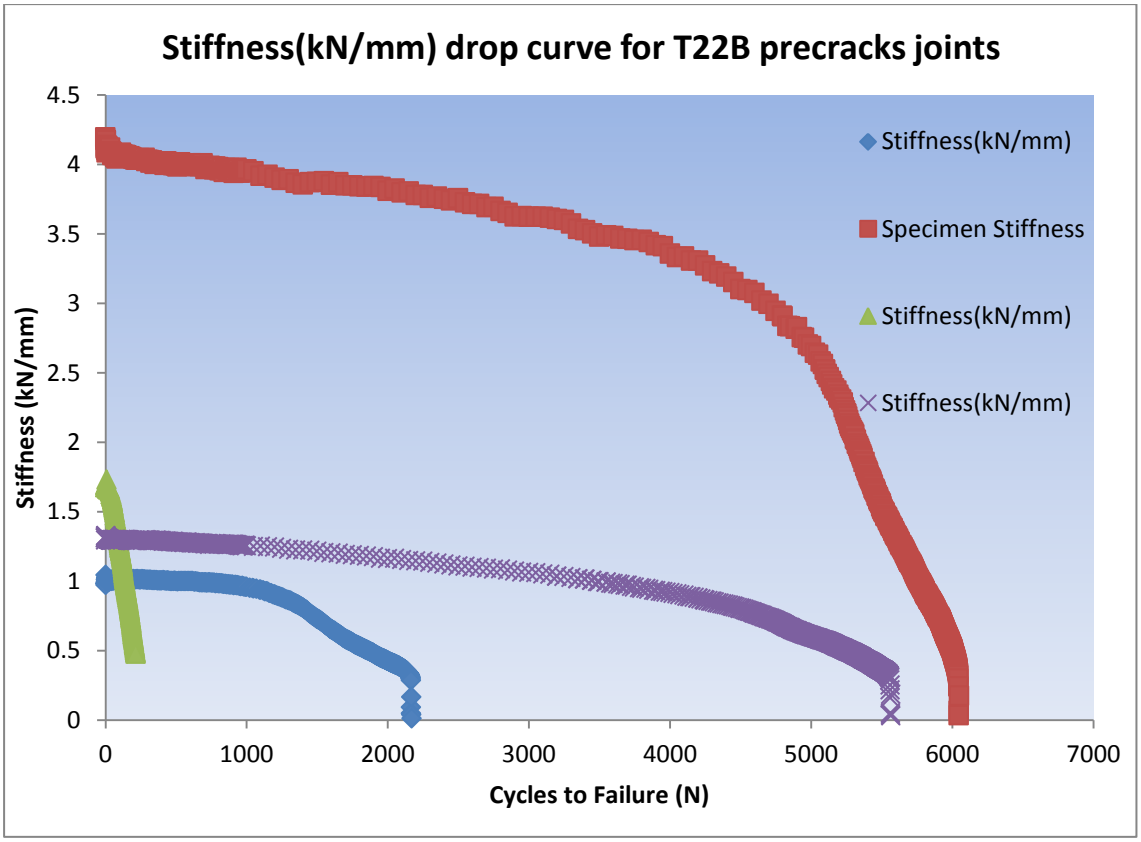

Crack Length vs. Cycles to failure curve

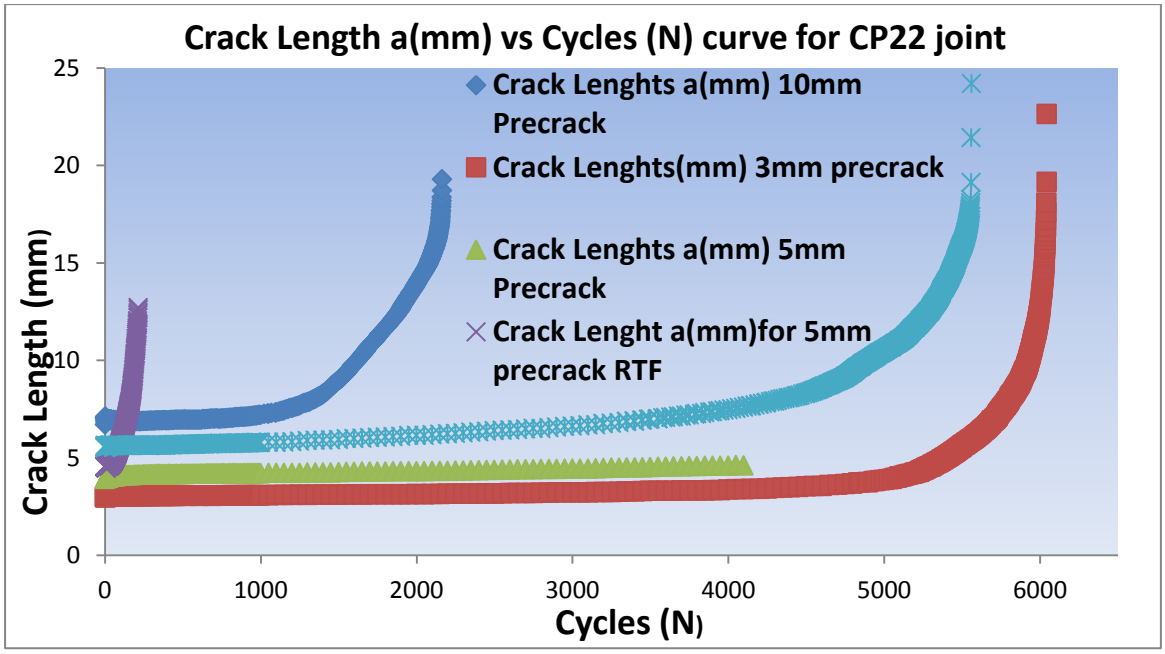

2. T23B Joint curves

a. T23B Joint with 3mm Precrack

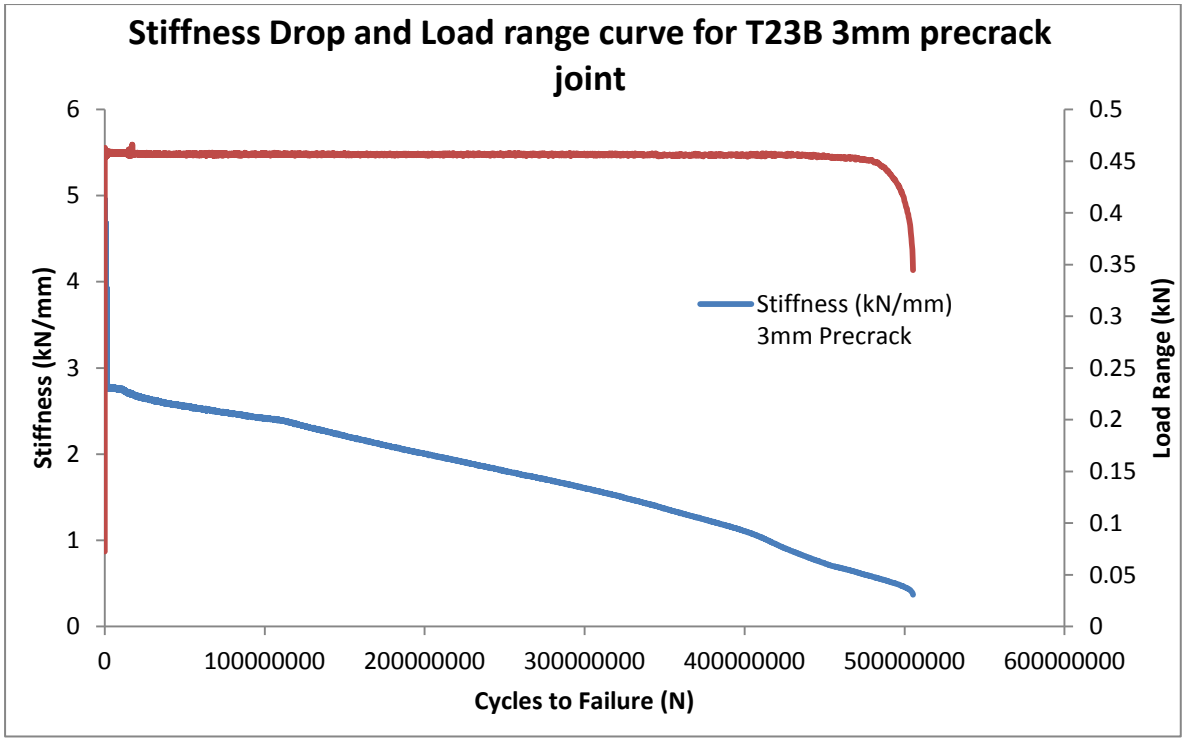

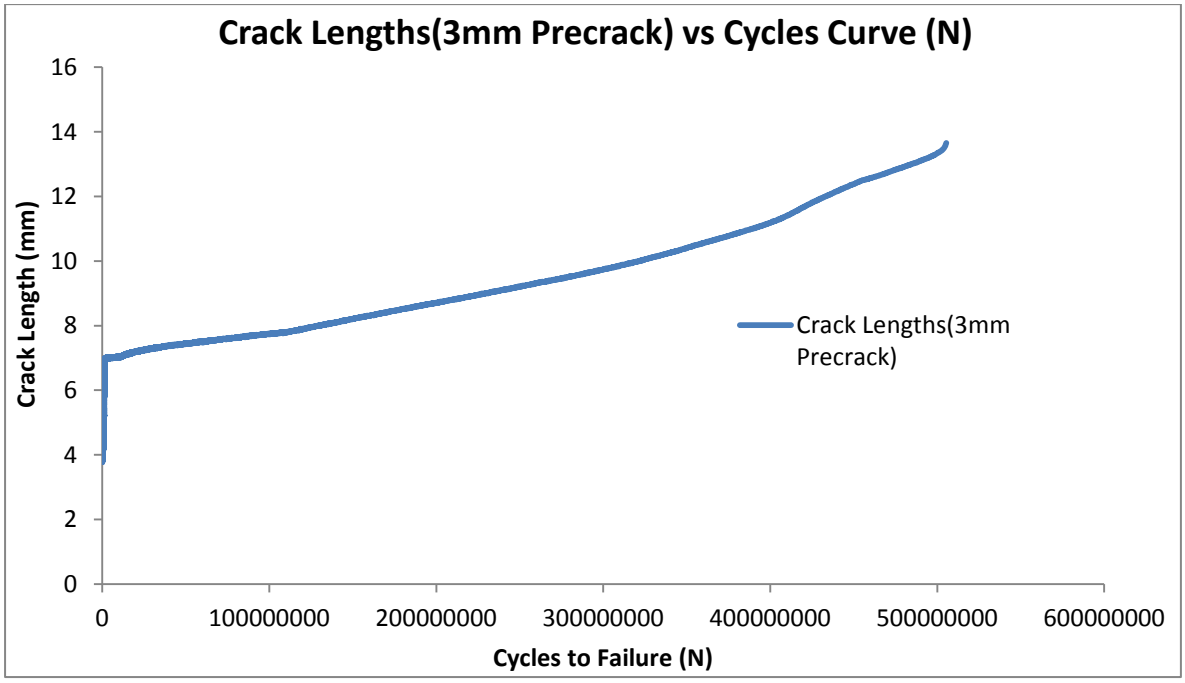
Crack Lengths(3mm Precrack) vs Cycles Curve (N)
Crack Length (mm)
16
14
12
10
8
6
4
2
0
0
100000000
200000000
300000000
400000000
500000000
600000000
Cycles to Failure (N)
Crack Lengths(3mm Precrack)

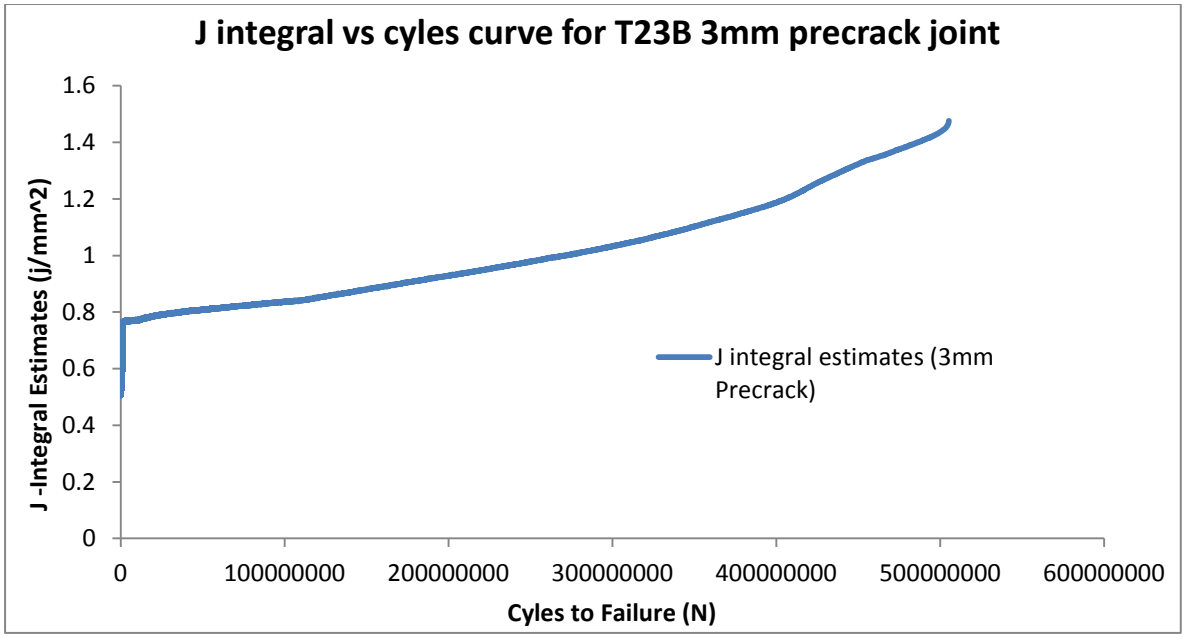
J integral vs cyles curve for T23B 3mm precrack joint
J -Integral Estimates (j/mm^2)
1.6
1.4
1.2
1
0.8
0.6
0.4
0.2
0
0
100000000
200000000
300000000
400000000
500000000
600000000
Cyles to Failure (N)
J integral estimates (3mm Precrack)

b. T23B 5mm Precrack Joint

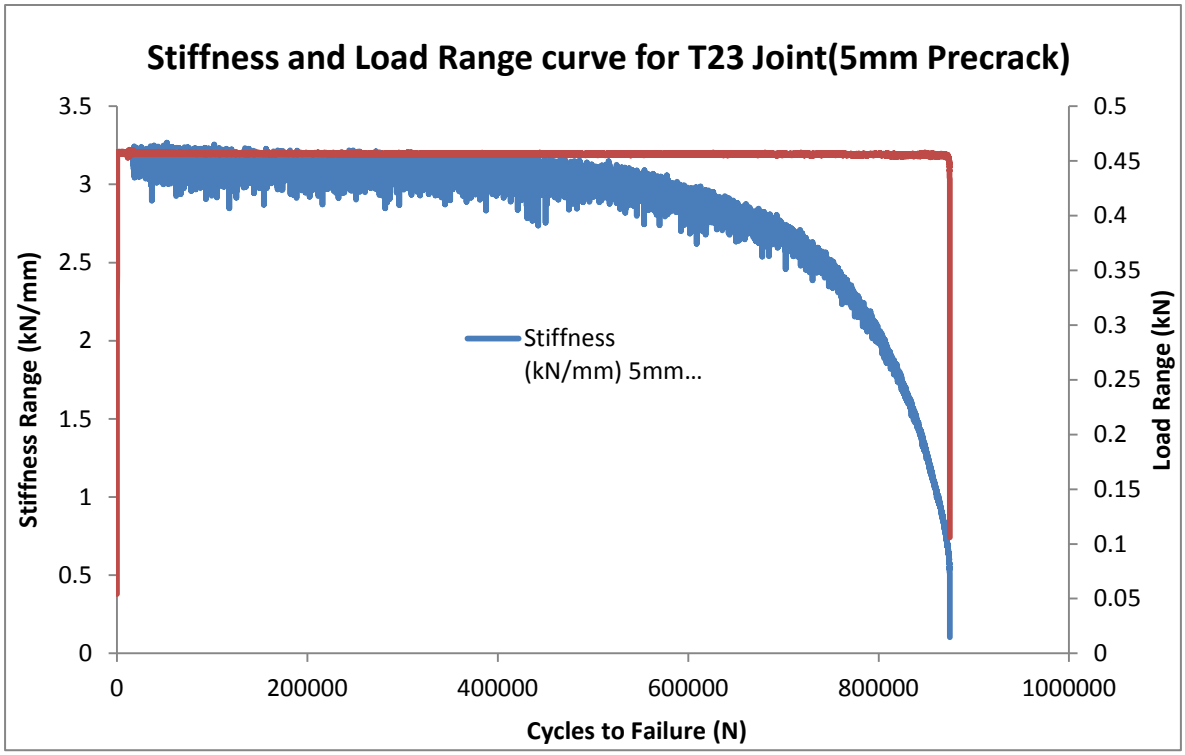

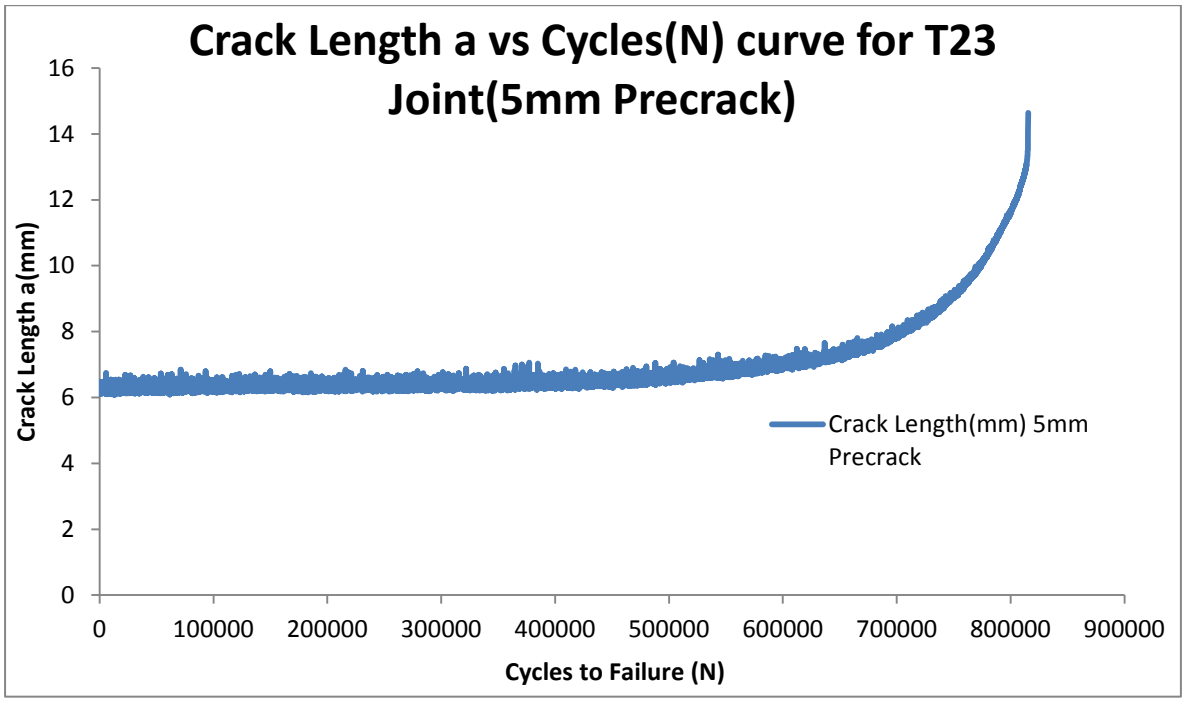

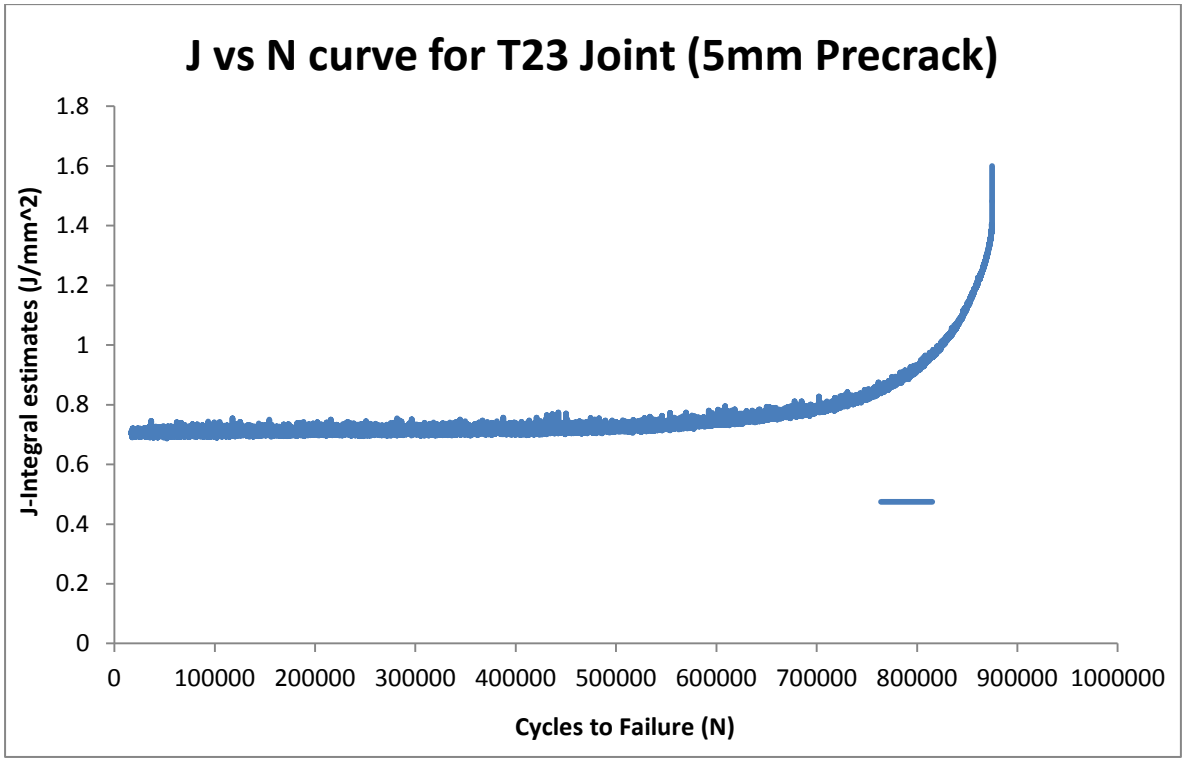

c. T23B 7mm Precrack Joint

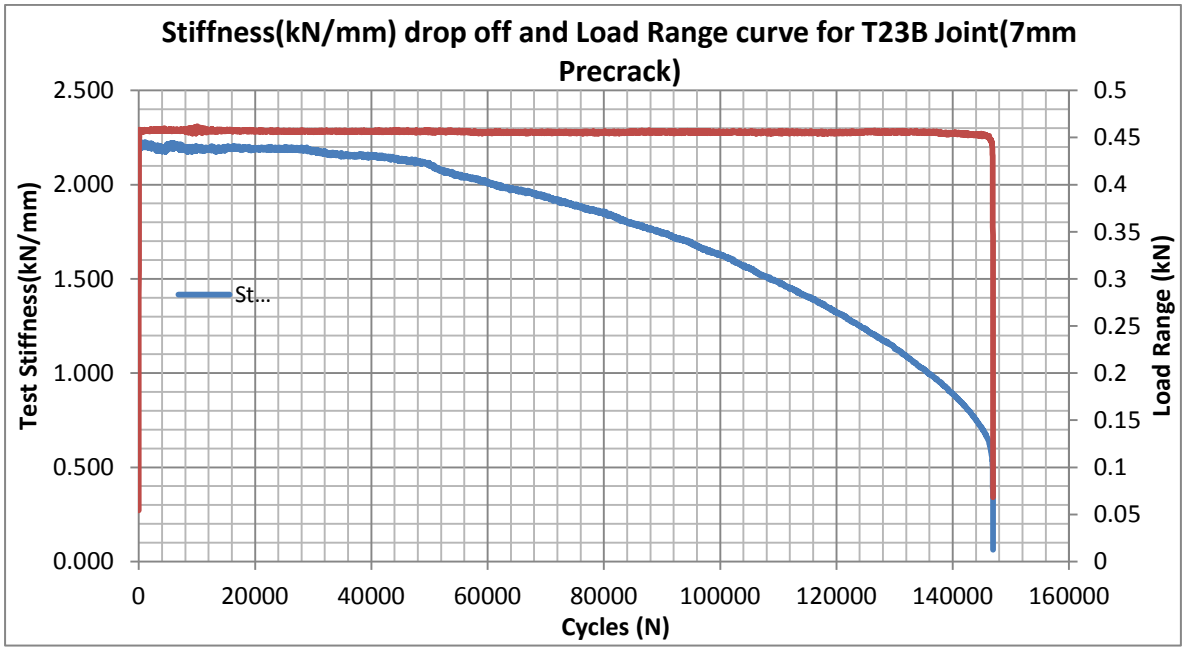

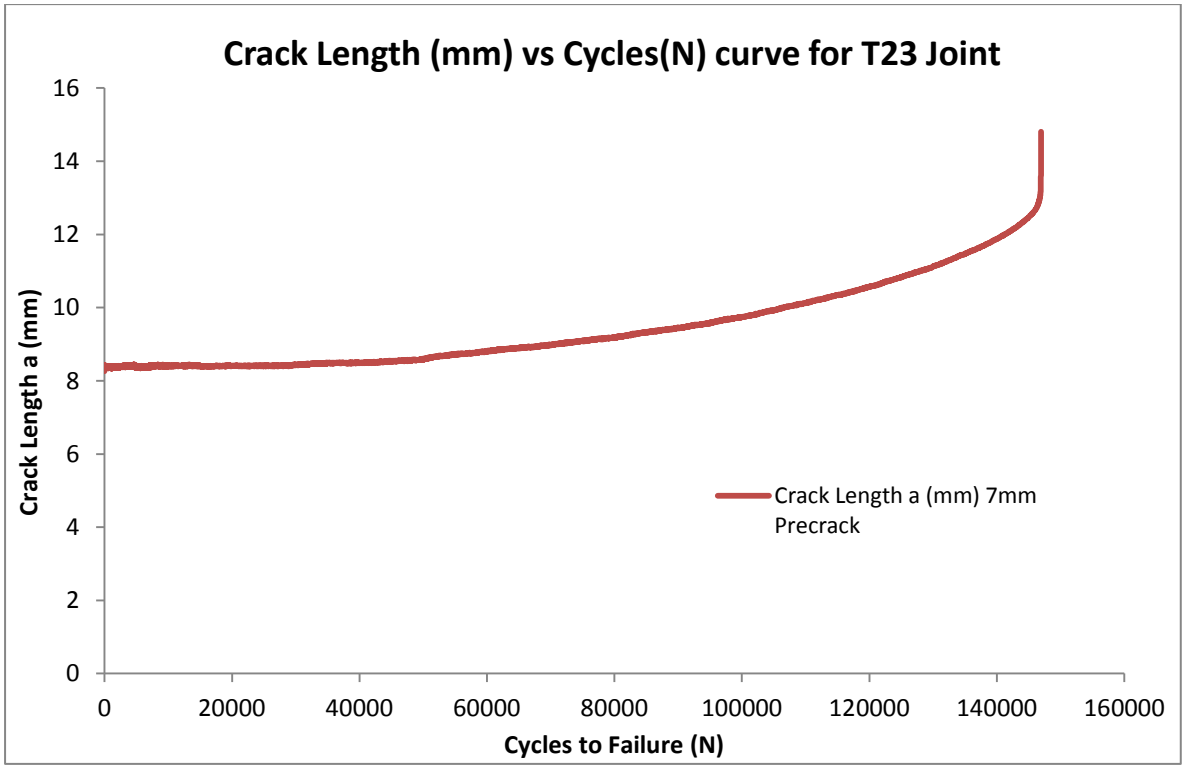
Crack Length (mm) vs Cycles(N) curve for T23 Joint
Crack Length a (mm)
16
14
12
10
8
6
4
2
0
0
20000
40000
60000
80000
100000
120000
140000
160000
Cycles to Failure (N)
Crack Length a (mm) 7mm Precrack

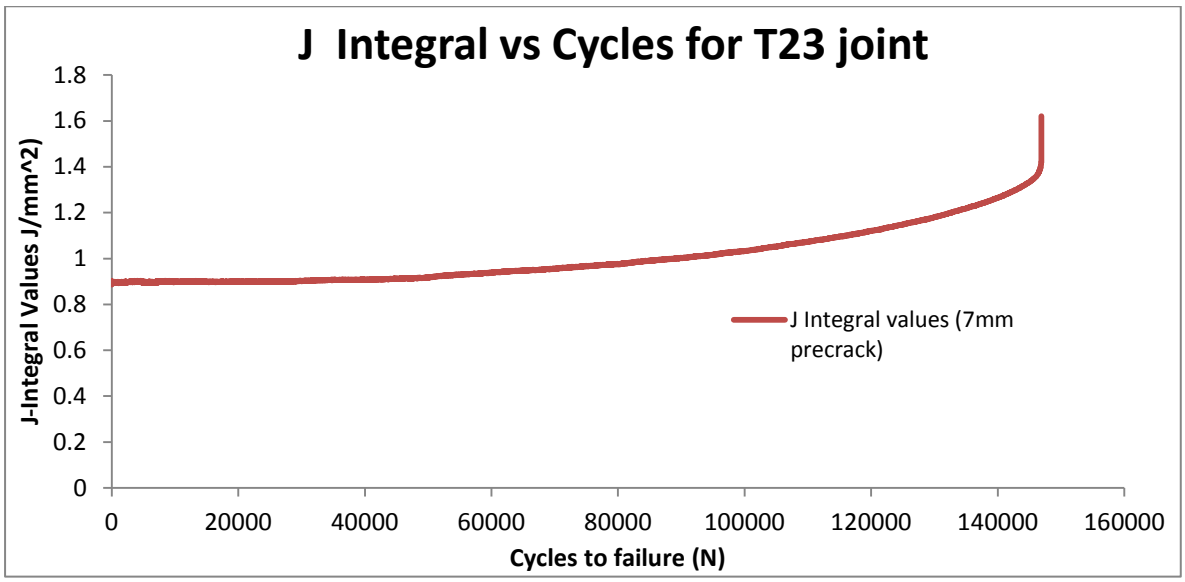
J Integral vs Cycles for T23 joint
J-Integral Values J/mm^2)
1.8
1.6
1.4
1.2
1
0.8
0.6
0.4
0.2
0
0
20000
40000
60000
80000
100000
120000
140000
160000
Cycles to failure (N)
J Integral values (7mm precrack)

3. T33B Joint

a. T33B joint with 3mm Precrack

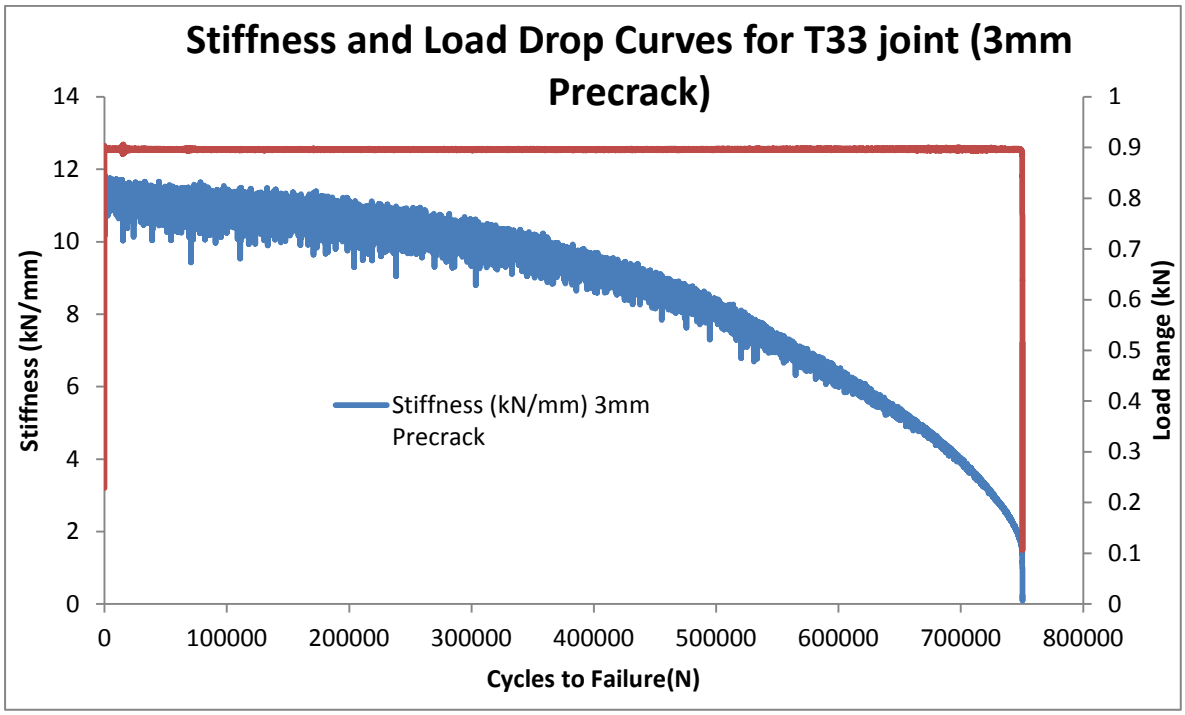

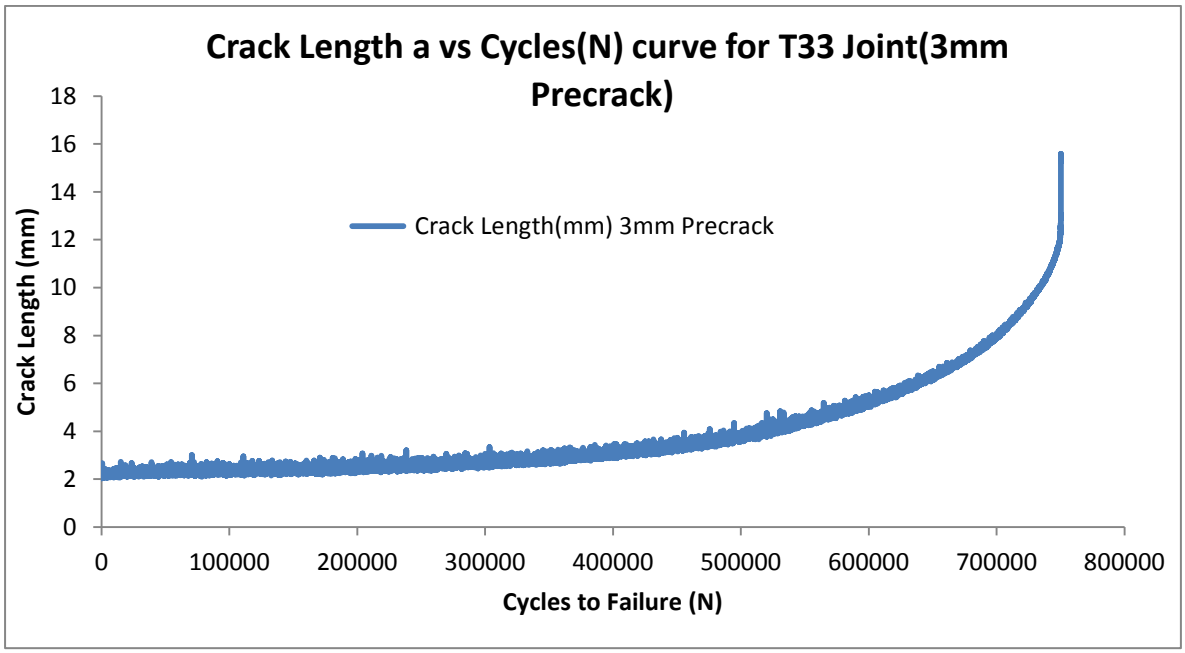

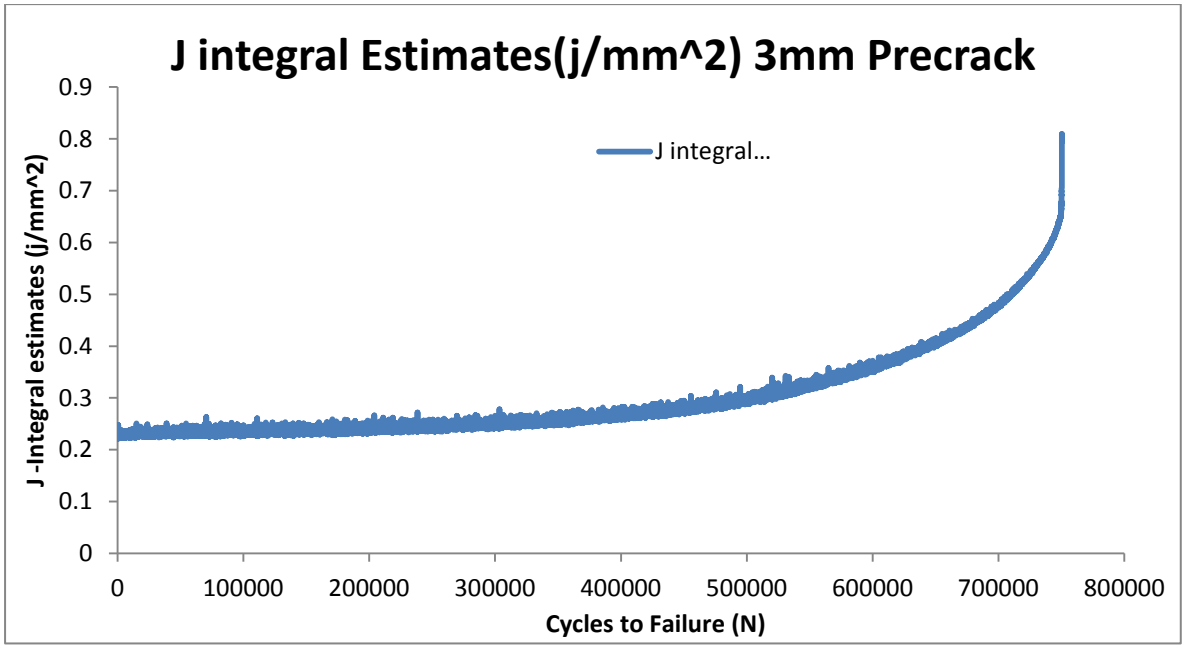

b. T33B joint with 5mm Precrack

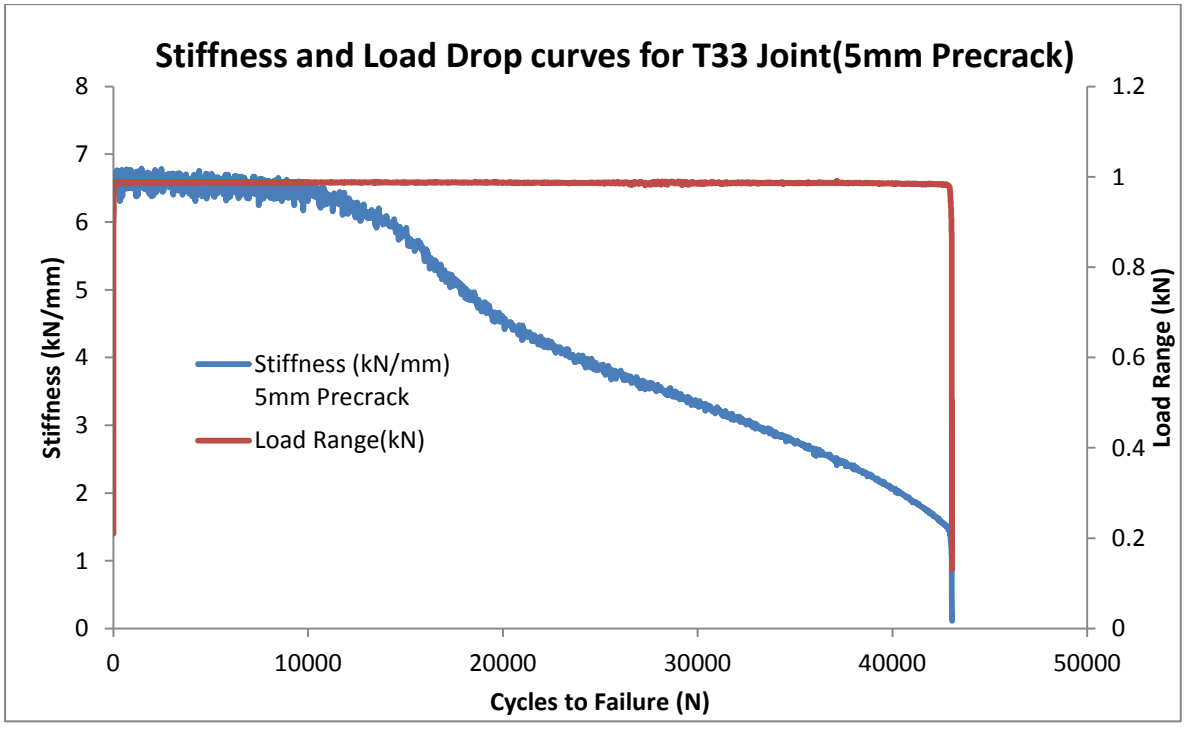

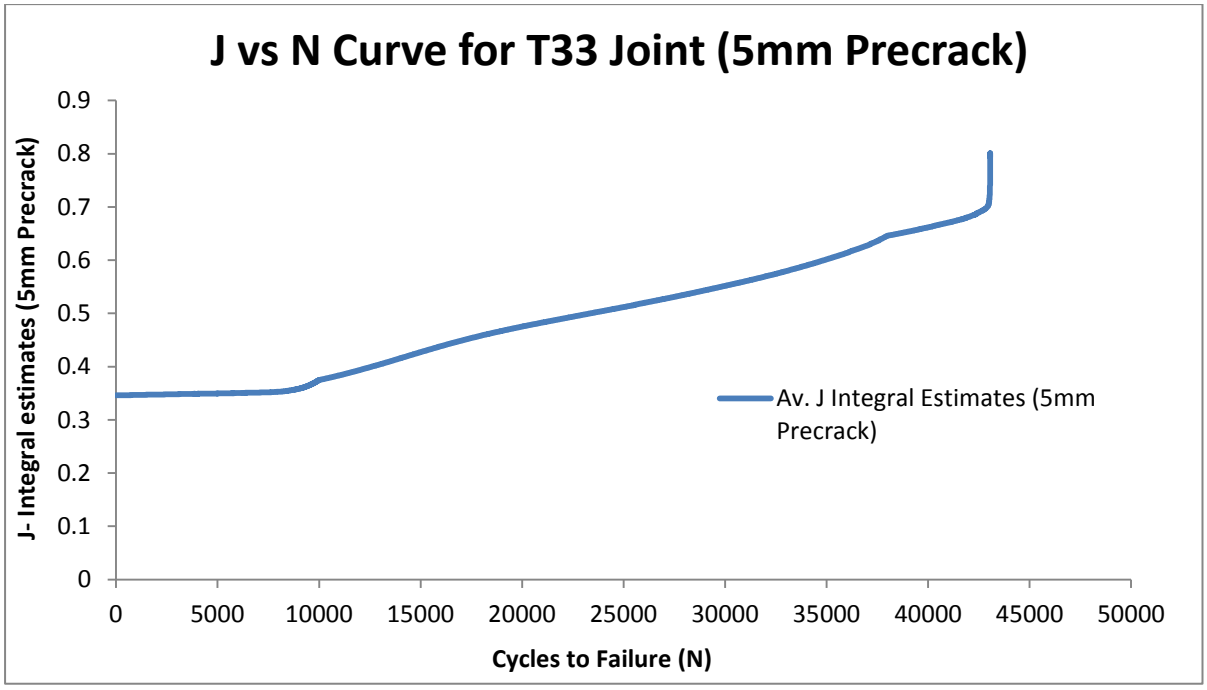
J vs N Curve for T33 Joint (5mm Precrack)
J- Integral estimates (5mm Precrack)
0.9
0.8
0.7
0.6
0.5
0.4
0.3
0.2
0.1
0
0
5000
10000
15000
20000
25000
30000
35000
40000
45000
50000
Cycles to Failure (N)
Av. J Integral Estimates (5mm Precrack)

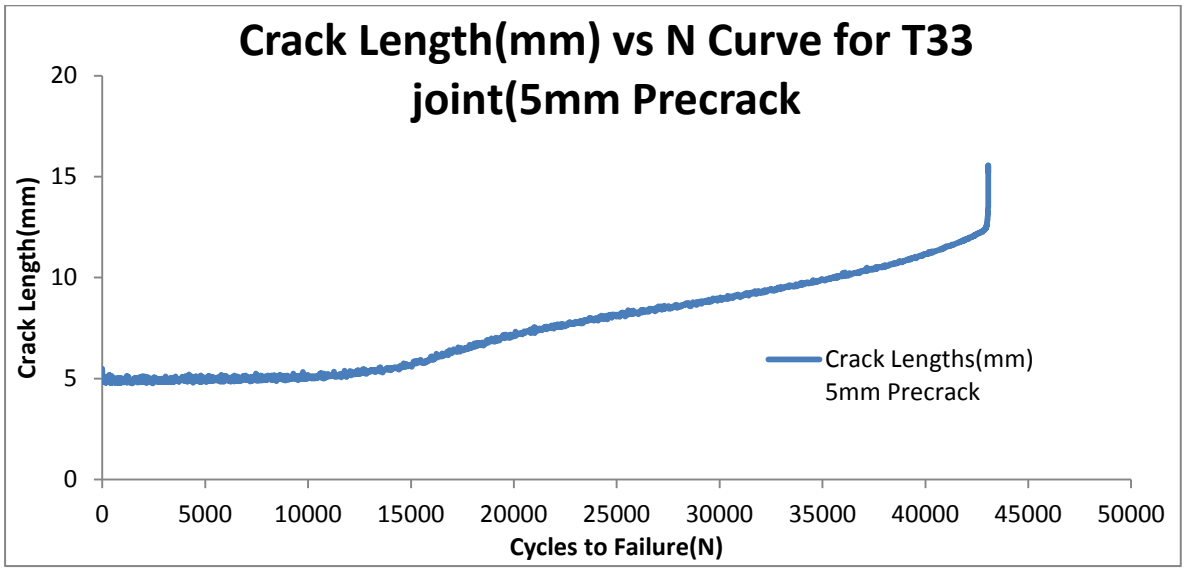
Crack Length(mm) vs N Curve for T33 joint(5mm Precrack
Crack Length(mm)
20
15
10
5
0
0
5000
10000
15000
20000
25000
30000
35000
40000
45000
50000
Cycles to Failure(N)
Crack Lengths(mm) 5mm Precrack

c. T23B Joint with 7mm Precrack

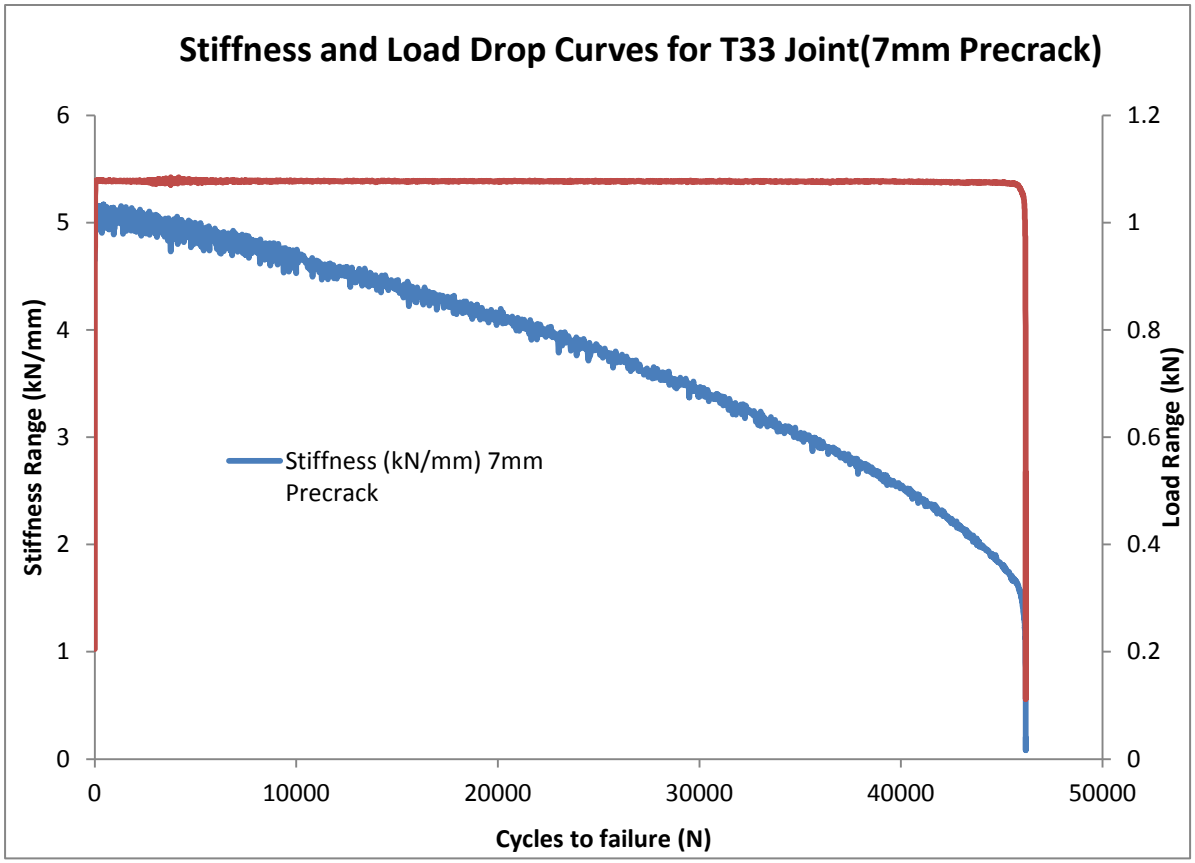

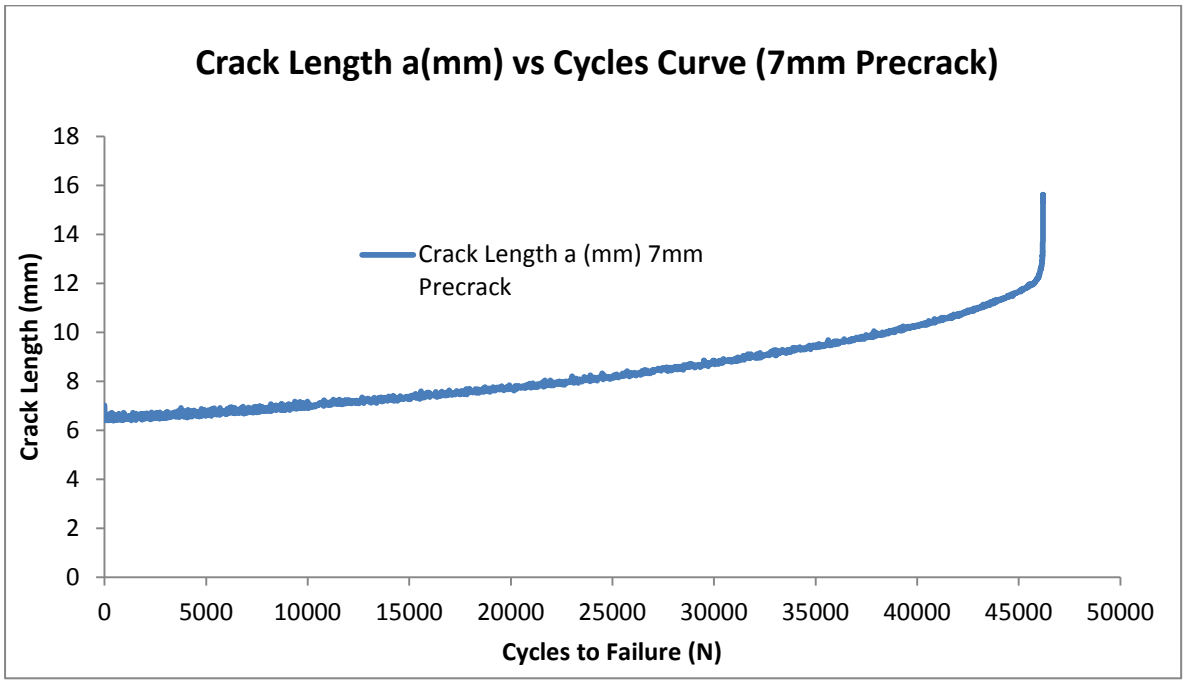

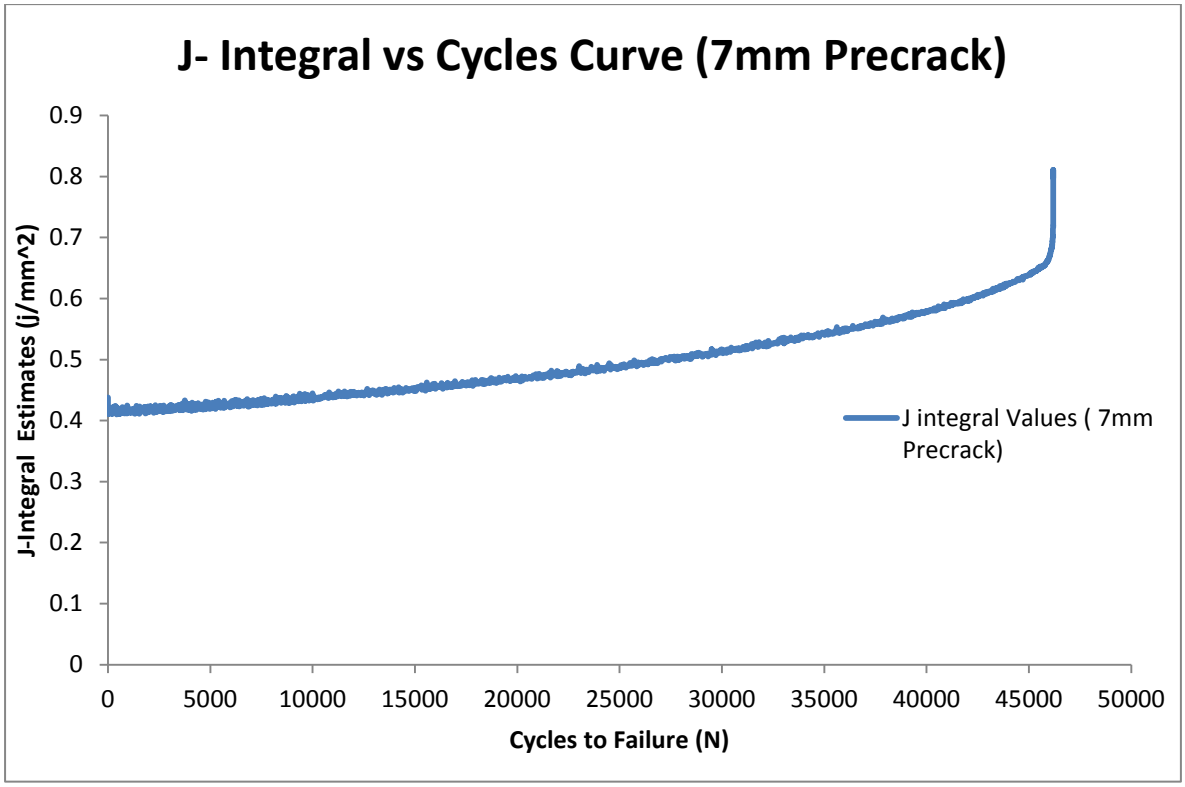

4. Lap Shear Joint

a. LS22B1 Joint

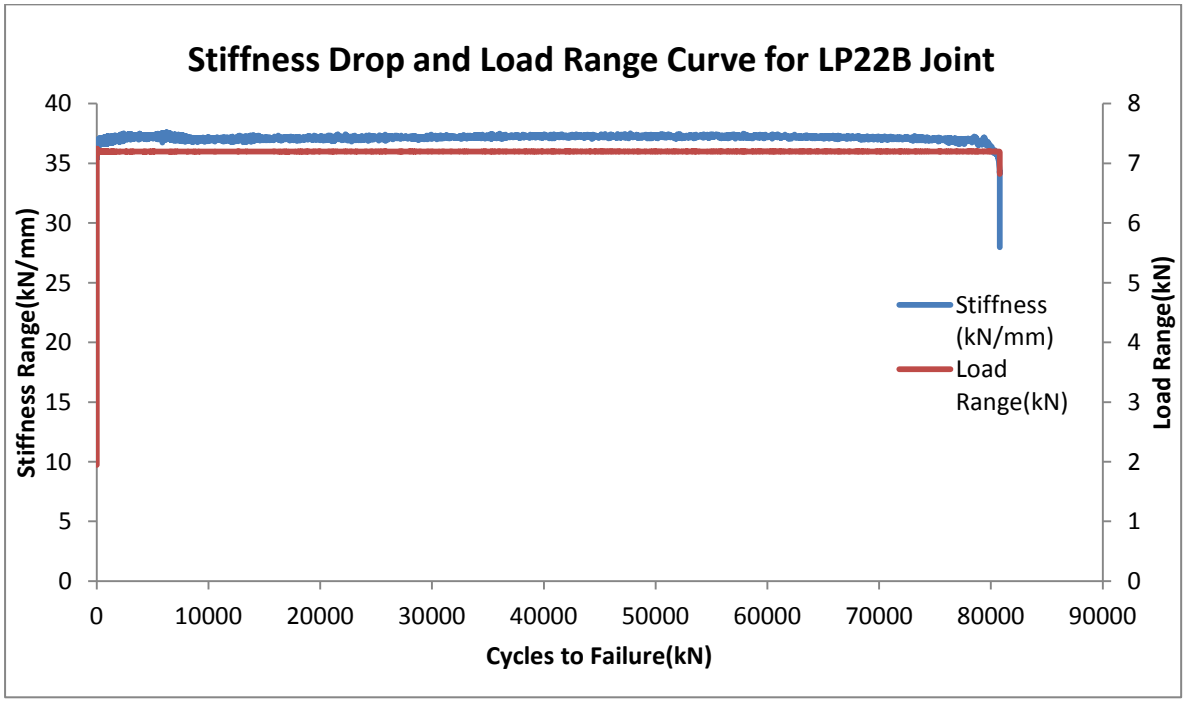

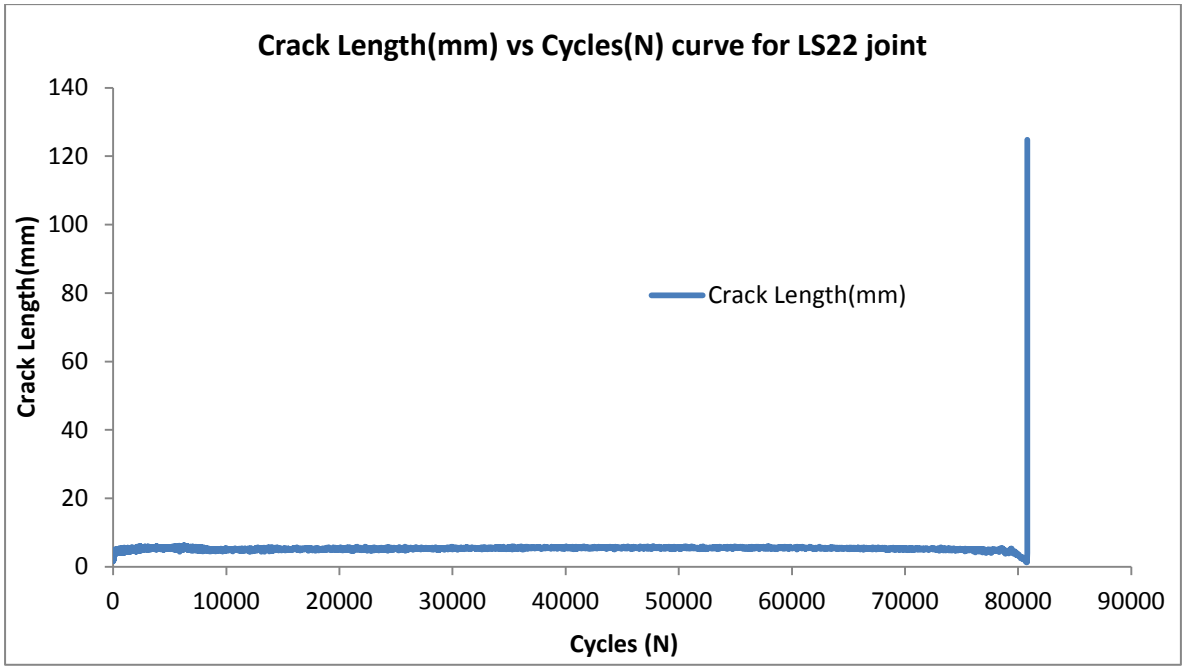
Crack Length(mm) vs Cycles(N) curve for LS22 joint
Crack Length(mm)
140
120
100
80
60
40
20
0
0
10000
20000
30000
40000
50000
60000
70000
80000
90000
Cycles (N)
Crack Length(mm)

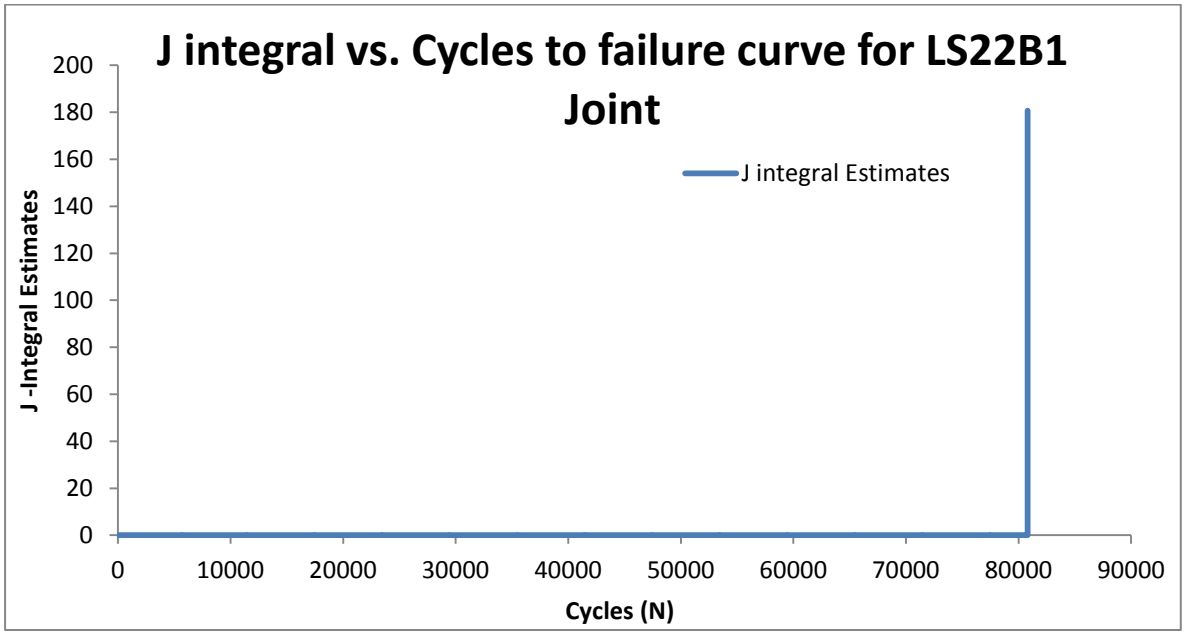
J integral vs. Cycles to failure curve for LS22B1 Joint
J integral Estimates
200
180
160
140
120
100
80
60
40
20
0
0
10000
20000
30000
40000
50000
60000
70000
80000
90000
Cycles (N)
J -Integral Estimates

b. LS22B2 Joint

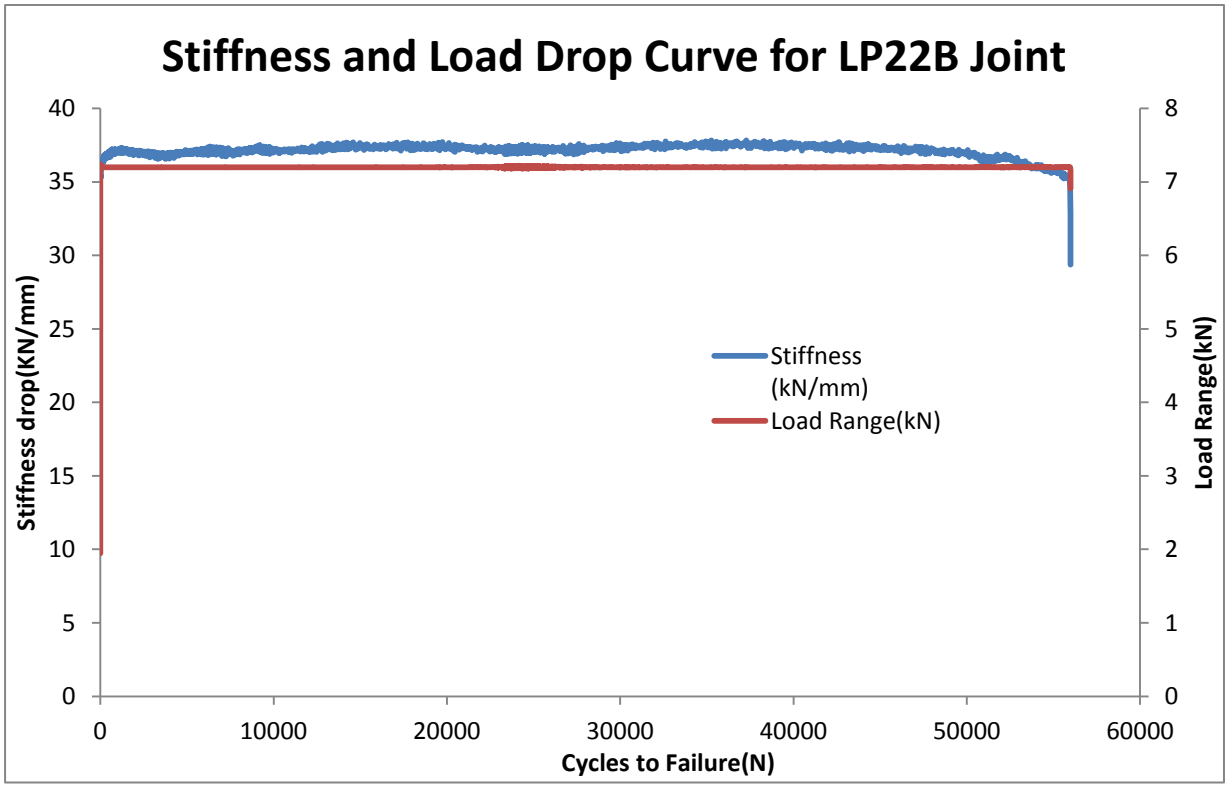

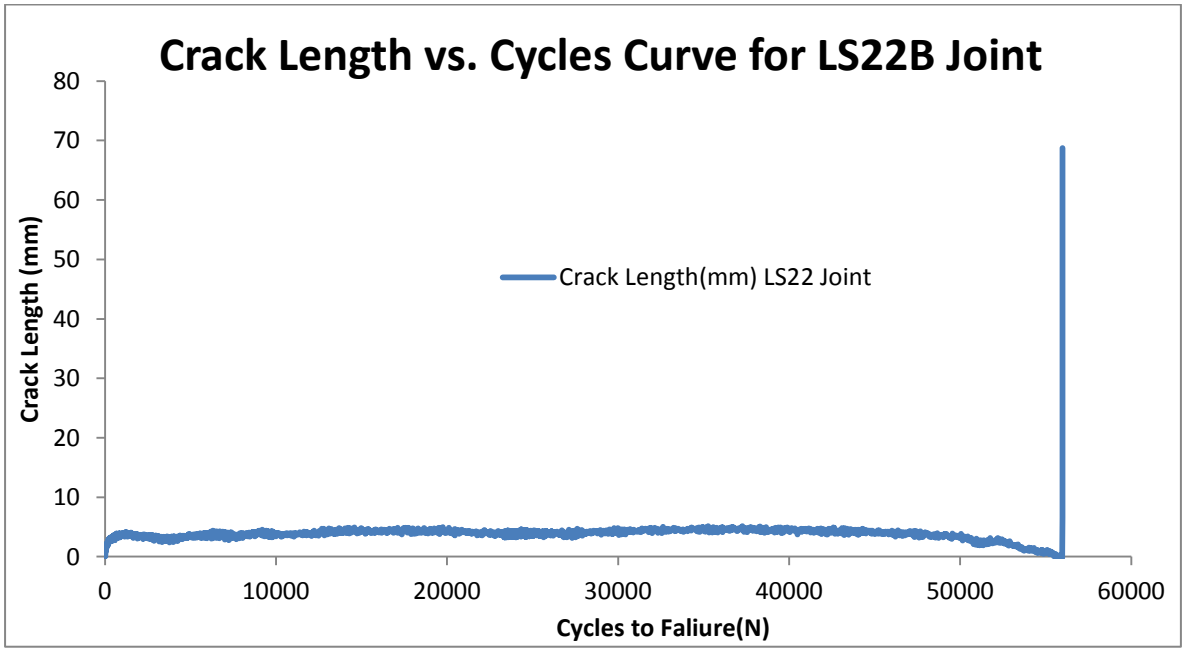

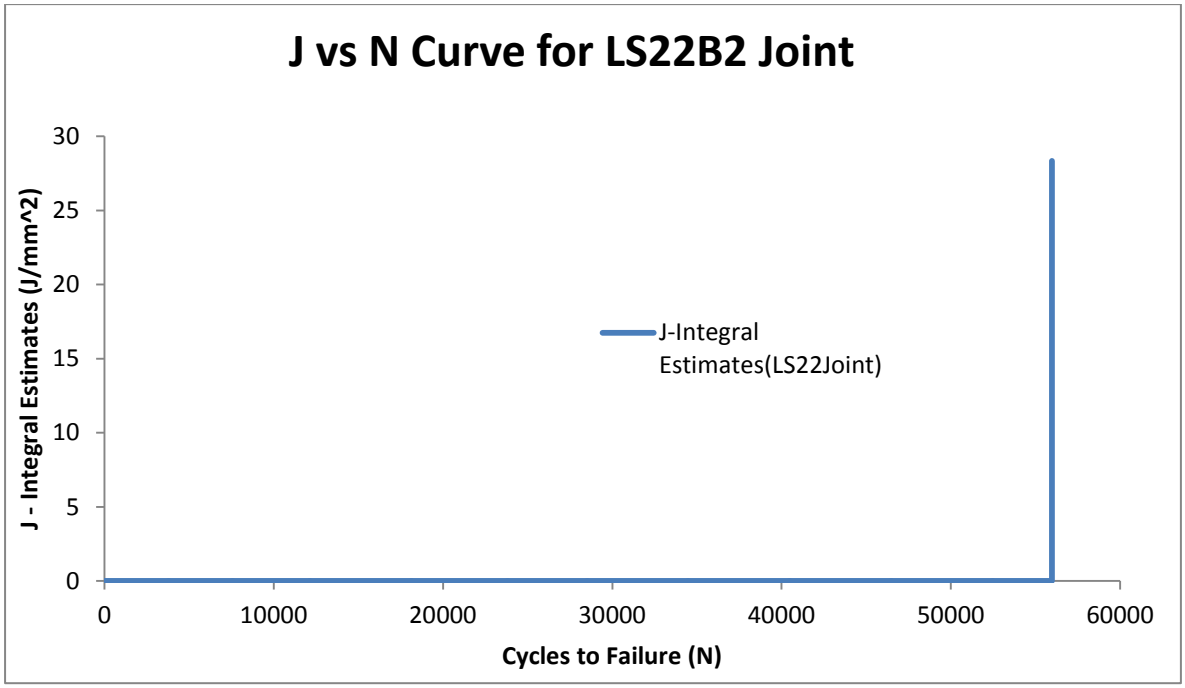
J vs N Curve for LS22B2 Joint
J - Integral Estimates (J/mm^2)
30
25
20
15
10
5
0
0
10000
20000
30000
40000
50000
60000
Cycles to Failure (N)
J-Integral Estimates(LS22Joint)